Synthesis and Characterization of ZIF-71/PDMS Membranes for Biofuel Separation

by

Huidan Yin

A Dissertation Presented in Partial Fulfillment
of the Requirements for the Degree
Doctor of Philosophy

Approved August 2017 by the
Graduate Supervisory Committee:

Mary Laura Lind, Chair
Bin Mu
David Nielsen
Don Seo
Jerry Lin

ARIZONA STATE UNIVERSITY

December 2017

ABSTRACT

Membranes are a key part of pervaporation processes, which is generally a more efficient process for selective removal of alcohol from water than distillation. It is necessary that the membranes have high alcohol permeabilities and selectivities. Polydimethylsiloxane (PDMS) based mixed matrix membranes (MMMs) have demonstrated very promising results. Zeolitic imidazolate framework-71 (ZIF-71) demonstrated promising alcohol separation abilities. In this dissertation, we present fundamental studies on the synthesis of ZIF-71/PDMS MMMs.

Free-standing ZIF-71/ PDMS membranes with 0, 5, 25 and 40 wt % ZIF-71 loadings were prepared and the pervaporation separation for ethanol and 1-butanol from water was measured. ZIF-71/PDMS MMMs were formed through addition cure and condensation cure methods. Addition cure method was not compatible with ZIF-71 resulting in membranes with poor mechanical properties, while the condensation cure method resulted in membranes with good mechanical properties. The 40 wt % ZIF-71 loading PDMS nanocomposite membranes achieved a maximum ethanol/water selectivity of 0.81 ± 0.04 selectivity and maximum 1-butnaol/water selectivity of 5.64 ± 0.15.

The effects of synthesis time, temperature, and reactant ratio on ZIF-71 particle size and the effect of particle size on membrane performance were studied. Temperature had the greatest effect on ZIF-71 particle size as the synthesis temperature varied from -20 to 35 ºC. The ZIF-71 synthesized had particle diameters ranging from 150 nm to 1 μm. ZIF-71 particle size is critical in ZIF-71/PDMS composite membrane performance for alcohol removal from water through pervaporation. The membranes made with

micron sized ZIF-71 particles showed higher alcohol/water selectivity than those with smaller particles. Both alcohol and water permeability increased when larger sized ZIF-71 particles were incorporated.

ZIF-71 particles were modified with four ligands through solvent assisted linker exchange (SALE) method: benzimidazole (BIM), 5-methylbenzimidazole (MBIM), 5,6-dimethylbenzimidazole (DMBIM) and 4-Phenylimidazole (PI). The morphology of ZIF-71 were maintained after the modification. ZIF-71/PDMS composite membranes with 25 wt% loading modified ZIF-71 particles were made for alcohol/water separation. Better particle dispersion in PDMS polymer matrix was observed with the ligand modified ZIFs. For both ethanol/water and 1-butanol/water separations, the alcohol permeability and alcohol/water selectivity were lowered after the ZIF-71 ligand exchange reaction.

DEDICATION

I would like to dedicate this dissertation to my dear husband Vick. I am so blessed to have you in my life. Thank you for your love, care, patience, encouragement and support at all times. My dissertation and my work could not have been possible without your support.

Next I would like to thank my parents for their unconditional love and support. Thank you, dad and mom, for always reminding me to work hard and be responsible for my PhD study. Without you two I can never get to this point.

ACKNOWLEDGMENTS

First, I would like to express my deepest gratitude to my advisor, Dr. Mary Laura Lind. It has been a great honor for me to work with such a wonderful professor. She gave me the opportunity to work in her lab and work on interesting research projects. Thank her for always being so supportive throughout my time at ASU. Many times I was frustrated with my research process, but I am so thankful that she always encouraged me and inspired me to move on. Thank her for her continuous guidance, assistance, advise and encouragement throughout my study. She has taught me so much not only about research but also about how to be a right person.

Next, I would like to thank my committee members, Dr. Bin Mu, Dr. David Nielsen, Dr. Don Seo and Dr. Jerry Lin, for their time and effort helping me with my research. I would like to express my deep appreciation for all their invaluable suggestions. I would also like to thank Dr. Matthew Green for all his guidance and assistance, it has been a great help to me. I want to thank Fred Pena for all his assistance in designing and setting up experimental equipment, fixing our equipment and keeping us safe in the lab. I would like to thank the National Science Foundation for the financial support of this work.

Finally, thank you so much to all the current and past lab members I has worked with in Dr. Lind's group: Dr. Tianmiao Lai, Dr. Afsaneh Khosravi, Pinar, Heather, Winnie, Chelsea, Michael, Yifei, Brandon, Kiah, Regina, Stew and Uyen; thank you all for making the past five years memorable to me.

TABLE OF CONTENTS

Page

LIST OF TABLES

Table Page

LIST OF FIGURES

1 INTRODUCTION

1.1 Biofuels

Biofuels are a very promising alternative to fossil fuels. Biofuels are solid, gaseous or liquid fuels produced from renewable resources. Three sources of biofuels are food crops (corn, sugar cane or soybeans), known as first generation biofuels; agricultural residues (stems, leaves, etc) or non-food crops, known as second generation biofuels; and algae, known as third generation biofuels.[1] A number of liquid biofuels such as methanol, ethanol, butanol, propanol and biodiesel can be produced from renewable biomass. Methane and hydrogen can also be produced as biogases.[2] The ethanol concentration contained in the bio-fermentation broth varies from 1 to 15 wt%.[3] According to the Renewable Fuel Standard (RFS) established by the US Congress in 2005, 36 billion gallons of biofuels should be included in transportation fuel by 2022.[4] In the U.S., one commercial scale cellulosic ethanol plant was formally opened in 2014 in the Midwest.[5] Additional biofuel plants will be built in Brazil and elsewhere.

Figure 1-1. POET-DSM Advanced Biofuels cellulosic ethanol plant which was opened on September 3, 2014 in Emmetsburg, Iowa. (Source: http://poet-dsm.com/liberty)

Biofuels are attractive because they can be partially substituted for conventional transportation fuel without affecting car performances. Up to 15-20% volume percent of bioethanol can be blended with gasoline without any issues.[6] According to the U.S. Department of Energy, up to 12.5% of bio-butanol can also be blended with gasoline in order to make sure that the oxygen content limit is 3.7% when it is blended with ethanol/gasoline mixtures.[7]

The production of biofuels includes several steps: preprocessing (e.g. milling), fermentation, distillation and dehydration.[8, 9] The existence of the ethanol-water azeotrope (with a composition of 95.63 wt% ethanol and 4.37 wt% of water) means that standard distillation purification yields a product ethanol concentration of approximately 95 wt%.[10] However, in the production of fuel grade ethanol, the maximum allowable water content is 0.3 wt% according to European standard.[11] Therefore, in order to meet the standard, the excess water that is not removed through standard distillation is further

removed through molecular sieve adsorption processes. In addition, while distillation has been widely used to separate biofuels due to its simplicity and reliability, it is an energy intensive process.[12] Motivated by this, separation processes that consume less energy have been extensively pursued. Pervaporation has emerged as a potential energy efficient alternative to distillation.

1.2 Pervaporation

Membrane technology is one of the promising low energy alternatives to separation processes such as distillation. Pervaporation membrane processes for separating biofuels are an attractive option because of their energy efficiency compared to distillation.[13] Pervaporation is used to separate liquid mixtures through dense, non-porous or microporous membranes. The permeate side of the membrane is usually maintained under vacuum. The driving force of the process is the chemical potential gradient across the membrane.[14] Figure 1-2 shows a schematic diagram of the pervaporation process. A hot feed liquid contacts the feed side of the membrane, then different feed components permeate through the membrane at different rates and evaporate into vapor phase. Unlike processes such as membrane distillation, the pervaporation membrane has selectivity towards the individual components of the feed. The vapor is then condensed and collected as permeate. In laboratory environment, the vacuum is usually created on the downstream side by a vacuum pump. The condensation of the permeate enables continuous removal of the components through the membrane. The difference in affinities and diffusion rate enables the separation of different species.[15] In distillation, the phase change consumes a significant amount of energy

because of the volume of material that undergoes the phase change is large. Conversely, in pervaporation only a relatively small amount of liquid feed solution is heated and as a result the energy consumption is much less than distillation.[16] Additionally, different from normal distillation, pervaporation can separate azeotrope mixtures.[17] Another advantage of pervaporation is the operation temperature is much lower than distillation, therefore it can be used to separate heat sensitive mixtures.[18]

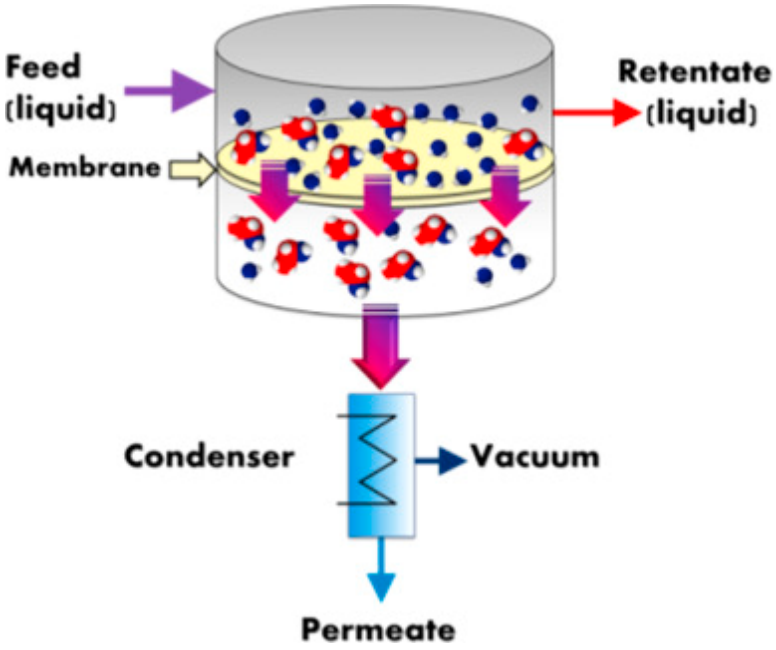

Figure 1-2. Schematic diagram of pervaporation process.[19]

For pervaporation, two parameters are directly calculated: flux and separation factor. Two additional parameters are calculated which describe the intrinsic membrane separation performances: selectivity and permeability. Permeability is determined by the sorption coefficient and diffusion coefficient. Sorption coefficient is governed by the chemistry of membrane materials while diffusion is related to the permeants' mobility.[20] Permeability is calculated by normalizing flux (as is shown in equation

(1.1)) with driving force and membrane thickness. The equation describing separation factor is shown in equation (1.2). Selectivity is defined by the ratio of permeability of different components. Selectivity, as is shown in equation (1.3) indicates the separation capacity of different components through the membrane.

$$J_i = \frac{M_i}{At} \tag{1.1}$$

where M_i (grams) is the mass of permeate component i, A (m^2) is the effective membrane area and t (h) is the operating time.

$$\beta = \frac{\left(Y_{Alcohol} \middle/ Y_{Water} \right)}{\left(X_{Alcohol} \middle/ X_{Water} \right)} \tag{1.2}$$

where β is alcohol/water separation factor, Y and X represents the component weight fractions in the permeate and feed side, respectively.

$$P_i = j_i \frac{l}{\gamma_{io} x_{io} p_{io}^{sat} - p_{il}} \tag{1.3}$$

where j_i (cm^3 s^{-1} cm^{-2})(STP) is the molar flux of component *i*; *l* (cm) is membrane thickness; the subscript *o* represents the feed solution, the subscript *l* represents the permeate; γ_{io} is the activity coefficient of component *i* in feed solution (unitless); x_{io} is the mole fraction of component *i* in the feed solution (unitless); P_{io}^{sat} (cmHg) is the saturated vapor pressure of component *i* in the feed; and p_{il} (cmHg) is the partial pressure of component *i* on the permeate side of the membrane. The activity coefficients γ was calculated with the UNIFAC model through Aspen Plus simulation software and the

Dortmund Data Bank (DDB) website.[21] The Antoine equation was used to determine the saturated pressure p^{sat}.

Sometimes permeance is used when the membrane thickness is unknown. It is defined as flux normalized by driving force.

$$\frac{P_i}{l} = \frac{j_i}{\gamma_{io} x_{io} p_{io}^{sat} - p_{il}} \tag{1.4}$$

Selectivity is the ratio of permeabilities.

$$\alpha_{ij} = \frac{P_i}{P_J} \tag{1.5}$$

where α_{ij} is the selectivity of component i over j. P_j is the permeability of component j.

According to Baker et al., analysis based on permeability and selectivity is more reliable and yields results with decreased dependence on operating conditions compared with flux and separation factor.[20] In this thesis we primarily report our pervaporation data in permeability and selectivity.

The most developed application of pervaporation is the separation of water from organic solvents (e.g. ethanol, isopropanol).[16] The first commercialized ethanol dehydration plant was built by GFT Membrane Systems in 1982. The pervaporation process reduces water concentration in ethanol from 10% to less than 1%.[18] Another application of pervaporation is the separation of a small quantity of volatile organic compounds (VOCs) from aqueous solutions. Pervaporation can be applied to remove alcohols from biofuel fermentation broths to eliminate the inhibitory effect on bacterial metabolism, which occurs when the alcohol concentration is greater than 20 g/L.[22] Pervaporation can also be used for organic-organic mixture separations, which is the

most challenging application for this membrane process as the components have similar sorption properties in general.[16] Swelling of membranes in organic mixtures is also an important topic. Therefore, the development of membrane materials that have better selectivity as well as limited swelling is needed. The pervaporation unit can be used alone or can be integrated with other liquid separation processes to reduce energy consumption.[23-25]

1.3 Pervaporation membranes

1.3.1 Solution-diffusion theory

The solution-diffusion model is used to describe the transport mechanism through the membrane in pervaporation. The mechanism describes the transport in three steps (as Figure 1-3 depicts): (1) the permeant molecule dissolves in the membrane material; (2) diffusion of the dissolved molecules through the membrane under chemical potential gradient; (3) evaporation of the molecule from the membrane into the downstream side of the membrane.[26]

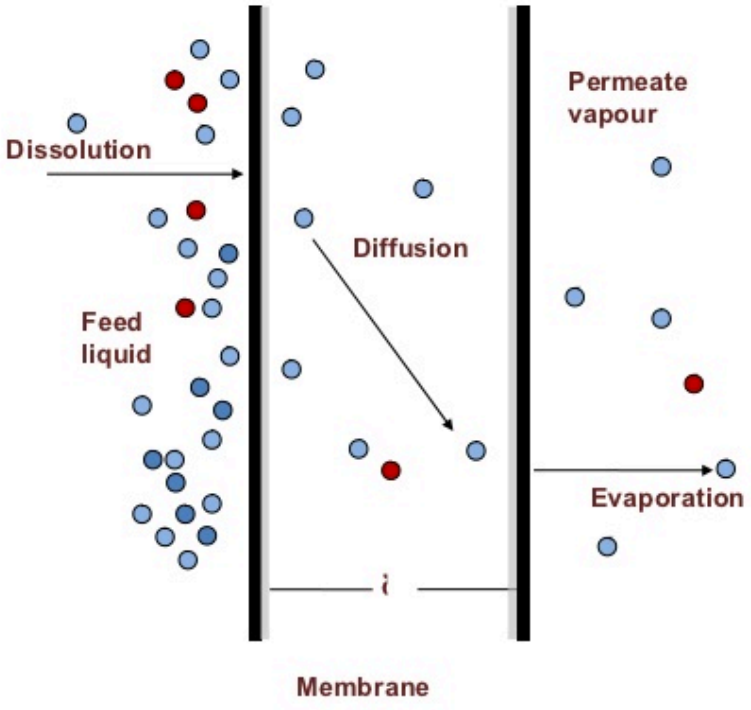

Figure 1-3. The schematic diagram of solution-diffusion mechanism in pervaporation. (https://www.slideshare.net/EngineersAustralia/1345-sule.)

1.3.2 Pervaporation membrane materials

To be competitive with distillation separation, the membrane material is critical. Membrane affects the entire pervaporation separation performances. Three major types of pervaporation membranes have been studied over the years including polymeric membranes, crystalline inorganic or metal-organic microporous membranes and mixed matrix membranes (MMMs).

1.3.2.1 Polymeric membranes

Polymeric membranes are the most commonly used materials in membrane technology because of the many advantages they possess such as low capital cost, easy to fabricate and scale up.[27] Polymeric membranes are formed through the cross-linking of

polymer chains and the tiny spaces between polymer chains enable the diffusion of molecules. However, polymeric membranes suffer the trade-off between permeability and selectivity, which is known as the "upper bound" limit.[28]

Polymeric membranes are widely used for solvent dehydration pervaporation processes. Hydrophilic cross-linked polyvinyl alcohol (PVA) is one of the most commonly used commercialized polymer materials for dehydration applications. PVA exhibits excellent film formation ability, low cost, good flexibility and high tensile strength.[29, 30] Moreover, PVA has excellent water selective properties. Other commercial hydrophilic membranes includes Chitosan, polyimides, etc.[31]

Polydimethysiloxane (PDMS) is the benchmark hydrophobic membrane material for recovering organic compounds from water through pervaporation.[32] PDMS exhibits high chemical and thermal stability, as well as good separation ability for common VOCs (shown in Figure 1-4).[33]

Separation factor for VOC over water	Volatile organic compound (VOC)
200–1000	Benzene, toluene, ethylbenzene, xylenes, TCE, chloroform, vinyl chloride, ethylene dichloride, methylene chloride, perchlorofluorocarbons, hexane
20–200	Ethyl acetate, propanols, butanols, MEK, aniline, amyl alcohol
5–20	Methanol, ethanol, phenol, acetaldehyde
1–5	Acetic acid, ethylene glycol, DMF, DMAC

Figure 1-4. PDMS polymer separation performances of VOCs from water. Image reproduced from Baker et al.[33]

The ethanol/water selectivity of PDMS is about 0.6 indicating the polymer is still water-selective.[20] Membrane materials that possess higher selectivities have been explored, such as poly(1-trimethylsilyl-1-propyne) (PTMSP). PTMSP is hydrophobic,

has remarkably high free volume up to 25% and is one of the rare polymer materials that are ethanol and butanol permselective.[34-36] The key disadvantage preventing further application of PTMSP is physical aging, which results in a decline in transport properties over time. Several attempts have been made to improve the stability of PTMSP, for instance by adding elastomeric filler materials.[37] Overall, PDMS is still the state-of-art material for VOC/water separation applications.

1.3.2.2 Crystalline microporous membranes

The second type of pervaporation membranes is crystalline microporous membranes. Microporous materials are classified as materials with pore size less than 2 nm.[38] Microporous crystalline materials can be categorized into two groups: zeolites and metal-organic-frameworks (MOFs). Those crsytalline membranes have many advantages over polymeric membranes such as: high permeabilities, no swelling, high thermal and chemical stabilities.[39, 40] However, the cost to make the membranes is significantly higher than polymeric membranes and the scalability is limited.[41] Additionally, the appearance of intercrystalline pores is detrimental to membrane selectivities in most cases.[42]

Zeolitic membranes are microporous inorganic aluminosilicate crystalline materials that could separate liquid mixtures based on sorption and diffusion differences. Zeolites have well-defined molecular-size pores. The alumina to silica ratio varies with different types of zeolites and zeolites of higher Al/Si ratios are more hydrophilic.[43]

In general, zeolite membranes are prepared on porous support such as ceramic supports to provide mechanical strength. The synthesis of zeolite membranes involves

several steps: pretreatment of supports, synthesis of zeolite membranes on the support (e.g. in-situ hydrothermal synthesis, secondary growth method, microwave method, etc.) and defect elimination.[44-47]

Type A zeolites, with a Si/Al ratio of 1, are hydrophilic and exhibit higher organic dehydration properties than ZSM-5, X-type, Y-type and T-type zeolite membranes.[48] Type A zeolite membranes was firstly commercialized for solvent dehydration applications by Mitsui Engineering and Shipbuilding Co. Ltd.[49] However, the high capital cost remains the major disadvantage limiting the commercial use. The most promising hydrophobic zeolite membranes for removing ethanol from water are silicalite-1 membranes. The comparison of three different hydrophobic zeolite membranes for alcohol/water separations is shown in Figure 1-5. Silicalite-1 is aluminum-free and exhibited greater alcohol permeability and selectivity over hydrophobic ZSM-5 zeolite membranes. Silicalite-1 membranes synthesized via in-situ crystallization technique were reported to have maximum ethanol/water separation factor of 106.[50] A higher separation factor of 125 was achieved by coating silicalite-1 membranes with PDMS polymer, yet the ethanol flux was significantly lower.[51]

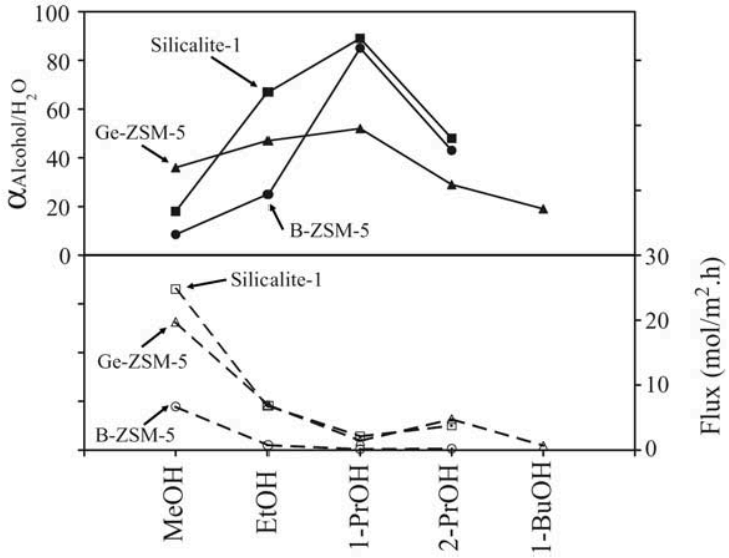

Figure 1-5. The separation performances for 1-5 wt% alcohol/water solutions through silicalite-1, Ge-ZSM-5 and B-ZSM-5 zeolite membranes at 30 °C.[48]

MOFs, including zeolitic imidazolate frameworks (ZIFs), are the second type of microporous crystalline materials that have been intensively studied. MOFs are crystalline nanoporous materials formed by metal ions or clusters connected with organic ligands. MOFs have notably high porosities, typically higher than 50% and up to 90%. MOFs also possess great surface areas ranging from 1000 to 10,000 m^2/g. More than 20,000 MOFs have been synthesized from the multitude of metal ions and organic ligands.[52, 53] MOFs are applied to a number of fields such as gas storage (e.g. hydrogen), carbon dioxide capture, catalysis as well as separations.[54-61] UiO-66 is one typical example used for organophilic pervaporation separations. Miyamoto reported the separation performances of UiO-66 membranes for separating methanol, ethanol and acetone from water.[62] The ethanol/water separation factors obtained ranges from 4.3 to 4.9 when testing temperature varies from 303 to 343K with 10 wt% ethanol/water feed

solution. For methanol/water separation with UiO-66 membranes, the separation factor is 5.0 at 323K when 10 wt% methanol/water is used as feed.

ZIFs are a subclass of MOFs, which are composed of transition metal ions (e.g. Zn, Co) that are connected by imidazole organic linkers.[63] ZIFs have zeolitic topologies because the metal-imidazole-metal angle of 145 ° is similar to the angle of the Si-O-Si bridges in zeolites (Figure 1-6). ZIFs have high surface areas, like MOFs, but notably improved thermal and chemical stabilities compared to most MOFs.[64] Generally, ZIFs possess small pore sizes of less than 5 Å (Table 1-1), which are in the range of the kinetic diameter of several important gas and liquid molecules. Therefore, ZIFs are attractive in many applications such as carbon dioxide capture, gas storage, gas and liquid separations. Two typical ZIFs studied for separation applications are ZIF-71 and ZIF-8.[65] ZnO supported organophilic ZIF-71 membranes were prepared by Dong et al. for solvent separation through pervaporation.[66] The membranes exhibited promising solvent separation properties: the methanol/water selectivity was 4.32, the ethanol/water selectivity obtained was 1.50 and the dimethyl carbonate/methanol selectivity was 8.08. Propane/propylene separation is one of the most important industrial separation processes. Crystalline ZIF-8 membranes have been synthesized and studied for this separation purpose. Pan et al. prepared ZIF-8 membranes via secondary growth method.[67] The membranes demonstrated propylene permeance in the order of 10^{-8} mol/m^2 s Pa and propylene/propane separation factors greater than 30. The separation performances obtained with ZIF-8 membranes successfully overcame the "upper bound" limit of both polymeric membranes and carbon membranes. Hara et al. synthesized ZIF-8

membranes for the same separation and their results showed that the separation of propylene/propane is governed by diffusion separation.[67]

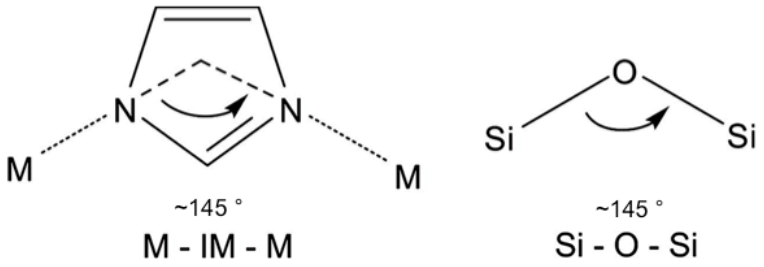

Figure 1-6. The similarity of bridging angles existed in ZIFs and zeolites. Image is reproduced from Park, et al.[64]

Table 1-1. Composition, topology and pore size of representative ZIFs.

ZIF type	Composition	Topology	Pore size/nm
ZIF-7	$Zn(benzimidazole)_2$	SOD	0.30
ZIF-8	$Zn(2\text{-}methylimidazole)_2$	SOD	0.34
ZIF-9	$Co(benzimidazole)_2$	SOD	< 0.30
ZIF-11	$Zn(benzimidazole)_2$	RHO	0.3
ZIF-71	$Zn(4,5\text{-}dichloroimidazole)_2$	RHO	0.48
ZIF-90	$Zn(imidazolate\text{-}2\text{-}carboxaldehyde)_2$	SOD	0.35

1.3.2.3 Mixed matrix membranes

Mixed matrix membranes (MMMs) are defined as the incorporation of a solid phase into a continuous polymer base. Ideal MMMs combine the good processability of polymers and the superior separation performance of molecular sieves.[68] The molecular sieves used in pervaporation MMMs are mostly zeolites and MOFs. Vane et al.

found there are three crucial parameters influence the overall MMMs performances: filler material particle size, particle loading and particle dispersion.[3] Particle size is important in making MMMs, because smaller particles allow the synthesis of thinner membranes for enhanced fluxes; yet smaller particles are more likely to aggregate than bigger particles because of the strong capillary force between particles. The aggregation of particles may create non-selective pathways for the feed components to diffuse through and thus reduce the membrane selectivity. Thus, the filler particle size needs to be optimized for the sake of maximum membrane separation performance. High filler particle loading (without particle agglomeration) is desirable in making MMMs in order to achieve higher selectivities and permeabilities. Particle dispersion within the polymer matrix is important to limit particle agglomeration that may result in defects in membranes, and ultimately may be detrimental to membrane separation performances. As a result, uniform particle dispersion is desired in membrane preparation.

Two primary approaches are reported to improve particle dispersion in polymer matrix. (1) sonication and (2) priming. (1) Sonication is an effective way to help disperse filler particles in the polymer matrix casting solution. Vane et al. compared the membranes prepared with sonication versus the membranes made merely by grinding the particles and shaking the membrane casting mixture.[3] They observed severe particle agglomeration as well as poor membrane separation performance with the membranes made without sonication. Moreover, they found ultrasonic probe-sonicators are more powerful than ultrasonic bath to disperse the particles. Usually during the membrane preparation, first the filler particles are well dispersed in the synthesis solvent using the

probe sonicator before combing the solvent/filler mixture with the polymer/solvent mixture. The mixture is then further sonicated with the probe sonicator before membrane casting. It is important to note that the probe sonicator can create significant heat during the mixing, this may increase the cross-linking of the polymers and reduce the sample preparation time. (2) "Priming" of the particles is the second primary method for dispersing particles within a polymer matrix. In "pre-priming", the particles are coated with a thin layer of polymer solution prior to the combination with the bulk polymer solution. In this process a small amount of polymer solution is added to the particle/solvent solution. Priming is reported to be an effective protocol to minimize the particle aggregation and enhance the particle/polymer interface.[69-71] Vu et al. applied 10 wt% of the total polymer solution to the particle solution to carry out the priming process.[71] Even distribution of MOF particles in Matrimid®-PI polymer matrix was accomplished through this priming method.[71] In this thesis we utilized a 300 W probe-sonicator and the priming method to combat dispersion challenges of ZIF-71 into PDMS matrix.

High silica zeolites such as silicalite-1 and ZSM-5 exhibited great alcohol/water separation potential as mentioned earlier and have been used in MMMs for removing dilute organic compounds from water solutions. Vane et al. prepared zeolites (ZSM-5 and silicalite1-1) incorporated PDMS MMMs to separate ethanol from water through pervaporation (Figure 1-7).[3] The maximum ethanol/water selectivity observed was 3.0 obtained from 65 wt% ZSM-5 loading MMMs. The separation performance of PDMS polymer was significantly improved through the addition of zeolites.

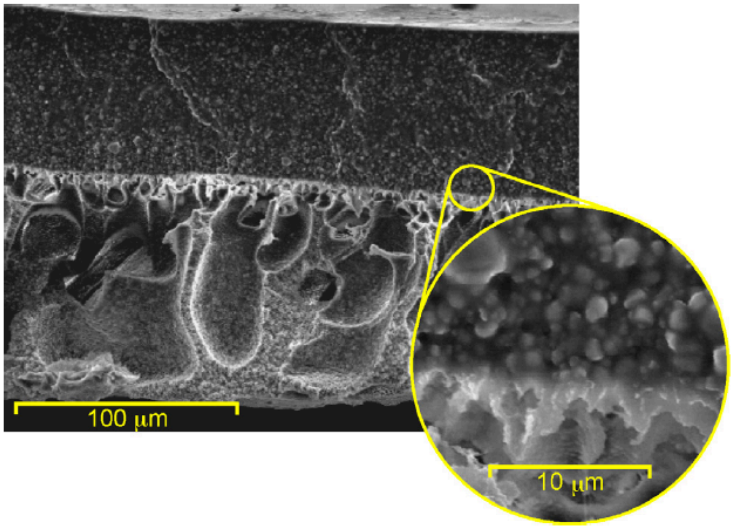

Figure 1-7. SEM cross-section view of 50 wt% zeolite loading zeolite/PDMS MMMs. Image is reproduced from Vane et al.[3]

PVA polymer separation performance can also be enhanced through the addition of zeolites. Guan et al. developed PVA MMMs with incorporated KA zeolites for ethanol/water dehydration application.[72] The inclusion of zeolites increased both the selectivity and permeances of the MMMs as compared to the pure PVA membranes. For 20 wt% KA zeolite loading membranes, the selectivity was greatly increased from 511 to 1279 at 60 °C with 80 wt% ethanol/water feed solution. In addition, the water permeance was enhanced while the ethanol permeance was reduced because of the hydrophilicity of KA zeolites.

1.4 MOF-based mixed matrix membranes for the removal of alcohols from aqueous solutions

Many MOFs (including ZIFs) have been incorporated into different polymers to form MMMs for recovering dilute alcohols from aqueous solutions through

pervaporation. Table 1-2 summarizes recent work in alcohol/water separation results for MOF-based MMMs. The current benchmark polymer material for the synthesis of MOF MMMs for alcohol/water separation is PDMS. Polyether block amide (PEBA) is another polymer used for alcohol/water separation research, yet the separation performance is inferior compared to PDMS. Figure 1-8 shows the chemical structure of PEBA.[73] PEBA membrane synthesis process is simple and straightforward. It is prepared by the solution casting method and no cross-linking is needed.[69] As shown in Table 1-2, the reported ethanol/water separation factors for different MOF-included MMMs are similar. According to Baker, in ethanol/water pervaporation the relationship between separation factor β and selectivity α is $\beta = (12\sim15)\alpha$.[33] Based on this estimate, all MOF MMMs listed in Table 1-2 have ethanol/water selectivity of less than one, indicating that the membranes are still water-selective. Among all the reported membranes, PDMS MMMs with 40 wt% loading Materials Institute Lavoisier-53 (MIL-53) (Al) zeolites demonstrated highest ethanol normalized flux (16,401 g/m^2 h, normalized to 1 μm membrane thickness).[74] MIL-53 (Al) is composed of trivalent metal ions Al and organic ligand 1,4-benzeneducarboxylic acid (BDC) with 0.85 nm pore size and hydrophobic aromatic ring walls. The hydrophobic nature of MIL-53 (Al) facilities the ethanol separation through the membrane.

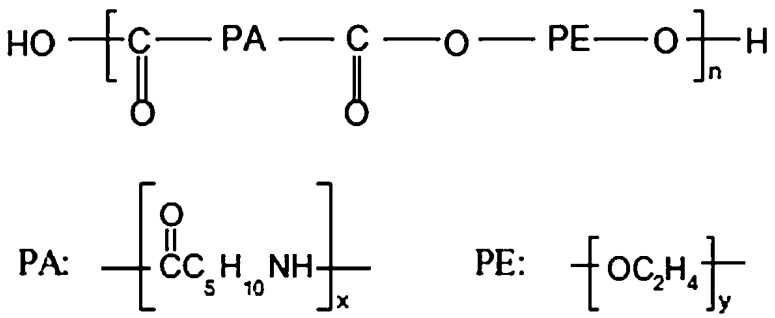

Figure 1-8. The chemical structure of polyether block amide (PEBA) polymer.

Table 1-2. Alcohol/water separation performance of MOF-based MMMs through pervaporation.

Membrane	Alcohol	MOF loading (wt%)	Feed Temp (°C)	Alcohol/water β	Notes (feed conc, thickness, flux*, etc)	Ref
MIL-53(Al)/PDMS	Ethanol	40	70	11.1	5 wt% EtOH, 3 μm, 16,401 g/m^2 h	[74]
MAF-6/PDMS	Ethanol	15	40	14.9	5 wt% EtOH, 5 μm, 6,000 g/m^2 h	[75]
ZIF-71/PDMS	Ethanol	16.7	50	α=0.64	5 wt% EtOH, 9 μm, ~1,000 g/m^2 h	[76]
ZIF-71/PDMS	Ethanol	40	50	~10 (α=0.67)	5 wt% EtOH, 2.8 μm, ~3,500 g/m^2 h	[77]
ZIF-8/PMPS	Ethanol	9.1	80	~ 12	1 wt% alchols, EtOH 7,000 Barrer, n-BuOH 4,612 g/m^2 h	[78]
	1-Butanol			40.1		
ZIF-7/PDMS	1-Butanol	20	60	66	1 wt% n-BuOH, 20(±2) μm, 1689 g/m^2 h	[79]

ZIF-71/PEBA	1-Butanol	20	40	20 (α=4.2)	1 wt% n-BuOH, 10-20 μm, n-BuOH 200,000 Barrer	[69]
$Zn(BDC)(TED)_{2.5}$ /PEBA	1-Butanol	20	40	18	1 wt% n-BuOH, 10-20 μm, n-BuOH 170,000 Barrer	[80]
ZIF-8/PDMS	1-Butanol	40	80	81.6	1.0 wt% n-BuOH, 4846.2 g/m^2 h,	[81]

* The flux listed here is normalized to 1 μm.

The 1-butanol/water separation factors with MOF included MMMs are significantly higher than the separation factors for the same membranes for ethanol/water. Based on Table 1-2, 40 wt% loading ZIF-8/PDMS membranes obtained the highest separation factor of 81.6 when tested at 80 °C with 1 wt% 1-butanol/water solution as feed. In summary, the MOF MMMs exhibit great potential for bio-butanol production.

1.5 Surface modification of zeolites and MOFs

The surface chemistry of zeolites and MOFs can be tailored to meet the need of various practical applications. For example, zeolite-polymer interface adhesion in MMMs has been improved by surface modification of zeolites with silane coupling agents in order to enhance separation performance. Proper silane coupling agents are crucial to improve the separation performance of membranes, as some silane agents may reduce both the permeability and selectivity. Li et al. modified zeolite 3A, 4A and 5A particles with (3-aminopropyl)-diethoxymethyl silane (APDEMS) for the incorporation into polyethersulfone (PES) MMMs.[82] The chemistry modification process is described in Figure 1-9. No obvious change in total pore volume and BET surface area were observed

after the modification. Better adhesion between the zeolite particles and PES polymer was proved by the SEM characterization. The gas separation experiments showed that the modification resulted in improved He, H_2, O_2 and CO_2 permeability and He/N_2, O_2/N_2, O_2/N_2 and CO_2/CH_4 selectivity.

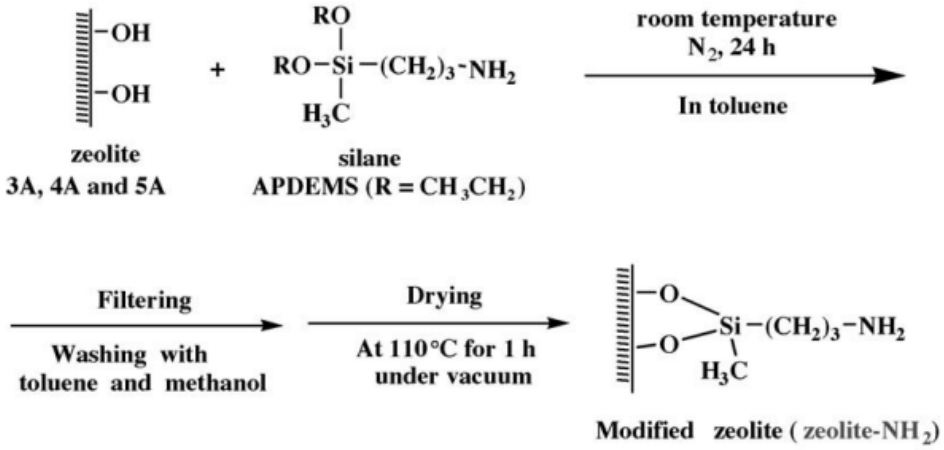

Figure 1-9. Surface modification process of zeolites with APDEMS coupling agent. Image reproduced from Li et al.[82]

The catalytic properties of zeolites can also be enhanced through surface modification. For instance, the conversion of bioethanol to propylene is studied as a method to reduce CO_2 emission. The surface modification of ZSM-5 zeolite catalysts for this conversion reaction was applied to enhance the propylene selectivity. To enhance the propylene selectivity, the number of acid sites on the outer surface of zeolites needs to be reduced to avoid undesired reactions. Takamitsu et al. were able to achieve this by covering the external surface of ZSM-5 zeolites with a thin layer of pure silica ZSM-5 zeolites.[83] The modified zeolites exhibited higher propylene yield than unmodified ones.

Post-synthetic surface modification has been studied to modify the surface chemistry of MOFs. It is a very useful method to introduce new functionality groups to MOFs. The incorporation of silica to the surface of MOF particles not only improves the stability, but also enables further modification of the particles for biomedical use. In order to form silica on the particle surfaces, the surface can be coated with poly(vinylpyrrolidone) (PVP) polymer first followed by the hydrolysis of tetraethylorthosilicate (TEOS). PVP polymer is applied to avoid particle agglomeration and facilities homogeneous growth during the silica formation on the particle surface. Taylor et al. functionalized a silica coated Mn-based nano-MOF material with Rhodamine B and cyclicarginine-glycine-aspartate (RGD) peptide.[84] Rhodamine B is able to fluoresce and be detected by optical imaging, while RGD peptide is used to target cancer cells. Enhanced targeted delivery of the Mn based MOFs to cancer cells was observed after the functionalization based on the confocal microscopic imaging characterization.

Post-synthetic surface modification has applied to not only MOF particles, but also shaped MOF materials to address their applications. Aguado et al. carried out imine synthesis with substituted imidazolate-based MOF (SIM-1) films.[85] First, the untreated SIM-1 was synthesized on different support materials (e.g., alumina beads for catalysis purpose and alumina tubes for separation applications). The C_{12} aliphatic groups were then added to the film surface through an imino-functionalization reaction. Compared to alumina-supported un-modified SIM-1, the catalytic activity of alumina supported C_{12} modified SIM-1 was about 15 times higher during the Knoevenagel reaction. Improved

surface hydrophobicity reduces the amount of water (secondary product) being adsorbed, and is hypothesized to explain the observed improved catalytic performance. SIM-1 was synthesized on tubular supports for combustion CO_2 capture. Higher CO_2 separation factor was found with C_{12} modified SIM-1 membranes for the separation of $CO_2/N_2/H_2O$, yet the CO_2 flux was reduced.[85]

Surface modification of MOFs has also been accomplished through a ligand-exchange method.[86, 87] The ligand can be partially or completely exchanged by this solvent assisted ligand exchange (SALE) method while maintaining the original topology.[88] The ligand exchange could be confined to the particle surface during the modification due to the steric effect. The SALE approach is able to introduce ligands that can be not added directly through normal synthesis routes.

Recently, SALE of ZIFs has been discovered as an effective approach to improve the particle surface hydrophobicity. Liu and coworkers successfully exchanged the 2-methylimidazole (MIM) ligands on the outer shell ZIF-8 particles with 5,6-dimethylbenzimidazole (DMBIM) ligands.[87] When they applied UV-vis Raman spectroscopy characterization with different exciting laser wavelengths on the DMBIM-ZIF-8 particles, different composition of the surface and bulk material was observed. This indicates that the ligand exchange was confined to the surface as a result of steric effects. Improved hydrothermal stability was found with the DMBIM surface-modified ZIF-8 particles. A small amount of both ZIF-8 and DMBIM-ZIF-8 particles were soaked in water at 80 °C for 24 hours. Afterwards, SEM and XRD were carried out on those particles. It was found that ZIF-8 suffered from hydrolysis and completely dissociated

into ZnO, while DMBIM-ZIF-8 maintained the crystal structure and morphology. Further, DMBIM-ZIF-8 was dispersed in polymethylphenylsiloxane (PMPS) polymer to form MMMs to separate isobutanol from water through pervaporation. The isobutanol/water selectivity was improved compared to the un-modified ZIF-8 contained PMPS MMMs without lowering the isobutanol flux.

1.6 Research objectives and structure of this dissertation

As mentioned above, MMMs are an effective strategy to improve biofuel separation performance of hydrophobic PDMS polymer membranes. In this research, we chose ZIF-71 as filler material for the synthesis of PDMS MMMs. In order to explore the optimization of membrane performance for ethanol and 1-butanol separation from aqueous solutions, we considered several factors. The factors studied in this research are described in details as follows in three research objectives.

1.5.1 Research objective 1

The compatibility between polymer matrix and filler materials is crucial to membrane performance.[89] In our work, for the first time, the compatibility of addition cure and condensation cure PDMS systems with ZIF-71 particles was explored. To obtain maximum alcohol/water separation, the effect of ZIF-71 loading on membrane separation performances was also studied. Three different ZIF-71 loadings were explored: 5, 25 and 40 wt%. The separation performances will be evaluated through pervaporation experiments of separating ethanol and 1-butanol from water solutions.

1.5.2 Research objective 2

Particle size is one of the most important parameters influencing membrane separation performances. The second part of this research aims to figure out how different size ZIF-71 particles affect the membrane separation performances. In order to obtain different size ZIF-71 particles, different particle synthesis parameters including synthesis time, synthesis temperature and reactant ratios were altered. Then the particle size effect on membrane separation was explored via pervaporation separation experiments.

1.5.3 Research objective 3

ZIF-71 surface hydrophobicity can be improved by the SALE technique as mentioned earlier in this chapter. Our objective in this section is to enhance the MMMs separation performances by enhancing ZIF-71 surface hydrophobicity. Five different imidazole ligands, which are more hydrophobic than the original ligand 4,5-dichloroimidazole, were selected. Those five imidazole ligands include: 4-methylimidazole, 4-phenylimidazole, benzimidazole, 5-methylimidazole as well as 5,6-dimethylbenzimidazole. Ligand-modified ZIFs were incorporated into PDMS at 25 wt% loading and the pervaporation separation experiments of ethanol and 1-butanol from water solutions were carried out. The effect of ZIF-71 surface modification on separation performances will be evaluated based on ethanol and 1-butanol selectivity and permeability values.

1.7 Structure of dissertation

The subsequent chapters focus on fulfilling the three objectives mentioned above. Specifically, Chapter 2 focuses on Objective 1 to study the compatibility between ZIF-71 and addition cure, condensation cure PDMS systems. The two chemicals (imidazole ligand and zinc salt) that are used to synthesis ZIF-71 are added to the two PDMS systems separately. Then the effect of particle loading on alcohol/water separation performances is discussed. Objective 2 is addressed by Chapter 3, focusing on the varying synthesis parameters to obtain various size ZIF-71 particles, and then the effect of particle size on alcohol/water separation membrane performances is demonstrated. Following Chapter 3, Chapter 4 addresses Objective 3, and aims to modify ZIF-71 particles with hydrophobic ligands to enhance alcohol separation from aqueous solutions through SALE method. The ligand exchange results are demonstrated through various characterizations and the effect of modification on membrane separation performance is discussed. Finally, Chapter 5 gives a summary of the results demonstrated in this dissertation, and some future work recommendations for membrane development for biofuel separations.

2 FREE-STANDING ZIF-71/PDMS NANOCOMPOSITE MEMBRANES FOR THE RECOVERY OF ETHANOL AND 1-BUTANOL FROM WATER THROUGH PERVAPORATION

2.1 Introduction

As described earlier in Chapter 1, PDMS polymer is the state-of-art hydrophobic material for the separation of VOCs through pervaporation. Therefore, we chose PDMS as the polymer matrix for the synthesis of MMMs. The filler material selected in this research is ZIF-71. ZIF-71 has hydrophobic structure and a window size of 0.48nm.[66] It is reported that the MMMs made with ZIF-71 particles have improved gas separations (e.g., H_2/CH_4, H_2/CO_2), biofuel separations (e.g., butanol, ethanol) and organic/organic separations (e.g., dimethyl carbonate/methanol).[66, 90] Particularly, ZIF-71 is reported to be promising filler material for biobutanol recovery through pervaporation process. Zhang et al. found that ZIF-71 has 1-butanol/water vapor sorption selectivity as high as 290.[91]

There are two main categories of PDMS synthesis: condensation cure PDMS and addition cure PDMS. In addition cure PDMS synthesis the cross-linking occurs via a hydrosilylation reaction between the vinyl-terminated PDMS and the -SiH groups of the cross-linker in the presence of platinum-based catalysts without producing by-products.[92] The reaction mechanism is shown in Figure 2-1.[93] In comparison, in condensation cure PDMS synthesis the cross-linking happens through a condensation reaction between silanol-terminated PDMS and alkoxy silane groups which is catalyzed by tin-based catalysts.[94] The detailed reaction mechanism is demonstrated in Figure 2-

2. These two types of PDMS have their unique properties and are not compatible with one another. The condensation cure PDMS is less expensive, more tear resistant than addition cure PDMS. In addition, the tin-based catalysts used in condensation cure are not liable to be inhibited while the Pt catalyst used in addition cure PDMS synthesis is easily poisoned in the presence of amine or sulfur-containing compounds.[95] The inhibition of catalysts prevents the polymer from curing completely. The condensation cure PDMS reaction releases by-products that lead to slight shrinkage of the polymer, while the addition cure PDMS system provides very little shrinkage. Certain addition cure PDMS polymers are skin safe and food safe.

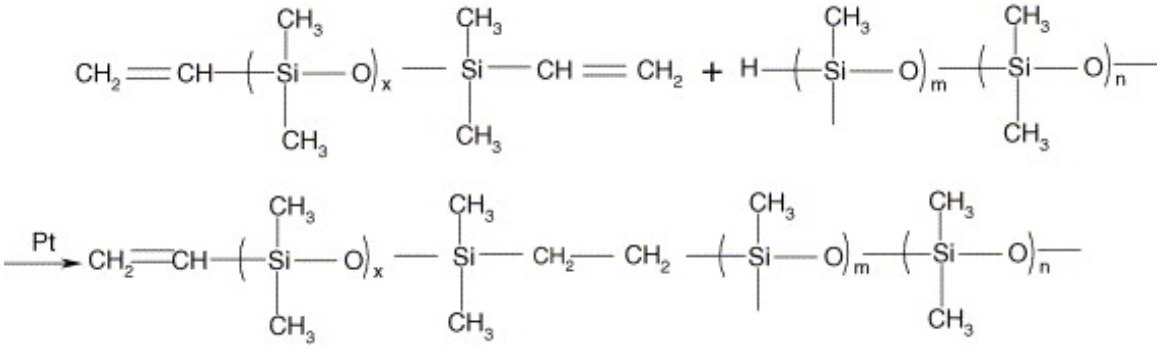

Figure 2-1. The cross-linking reaction mechanism occurred in addition cure PDMS preparation. Image reproduced from Stafie et al.[93]

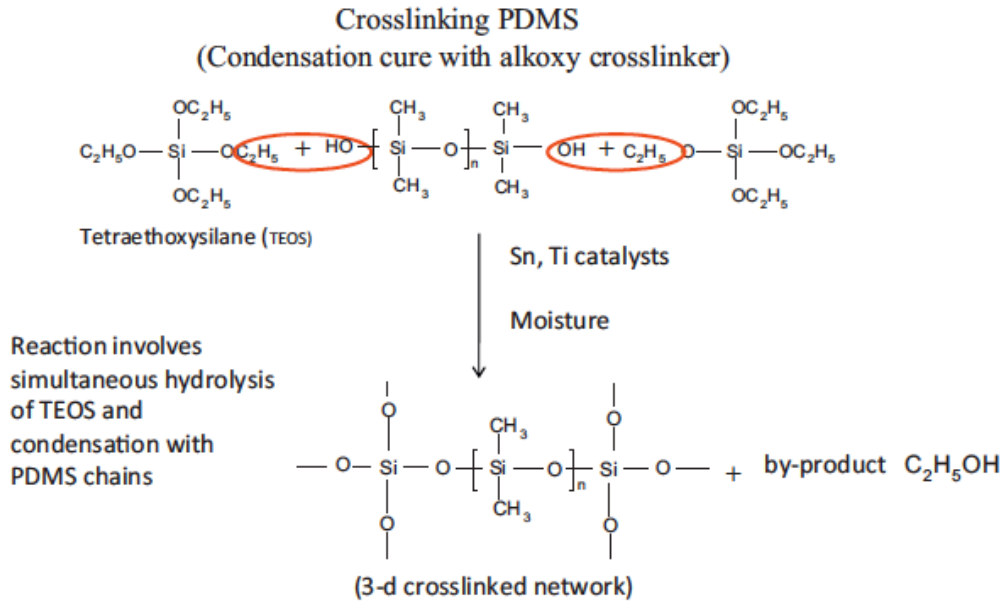

Figure 2-2. The cross-linking reaction mechanism occurred in condensation cure PDMS system. Image reproduced from Bighane et al.[96]

It is important to make sure ZIF-71 particles are compatible with the PDMS polymer to form a proper composite membrane. The motivation for the ZIF-71/PDMS compatibility test is that incomplete cross-linking was observed during the preparation of ZIF-71/addition cure PDMS MMMs. The 40 wt% ZIF-71 loading membranes did not cure properly (they were gelatinous). As a result, experiments were carried out to study the compatibility between ZIF-71 and two types of PDMS systems. To discern the influence of Zn salt and imidazole ligand on the cross-linking process, these two chemicals were added separately during the PDMS polymer synthesis.

Two recent references reported polyvinylidene fluoride (PVDF)-supported ZIF-71/PDMS MMMs for alcohol recovery of water through pervaporation.[76, 77] Both studies utilized addition cure PDMS synthesis for their MMMs, conversely here we used the condensation cure method and made unsupported membranes. Li et al. reported

ethanol/water selectivity of 0.64 from 17 wt% ZIF-71 loading ZIF-71/addition-cure PDMS composite membranes on PVDF substrates. Wee et al. reported that 40 wt% submicron-sized ZIF-71 loading addition-cure PDMS MMMs on PVDF substrates had an ethanol/water selectivity of about 0.66.[77]

2.2 Experimental

2.2.1 Materials

RTV615A (Silicone potting compound) and RTV615B (cross-linking agent) were purchased from Momentive Performance Materials. Ethanol (ACS reagent grade, ≥99.5%), n-heptane (anhydrous, 99%), tetraethyl orthosilicate (TEOS, 99.999% trace metals basis) and 2-methylimidazole (mIm) (99%) were obtained from Sigma-Aldrich. Alfa Aesar supplied zinc acetate dihydrate ($Zn(OOCCH_3)_2 \cdot 2H_2O$) (ACS, 98.0-101.0%) and toluene (ACS reagent grade, 99.5%). The 4,5-dichloroimidazole (dcIm) (>97%) was purchased from Tokyo Chemical Industry, methanol (HPLC) was purchased from LabChem Inc. and BYTAC® surface protector (FEP, white, aluminum) was supplied by Cole-Parmer. The silanol terminated polydimethylsiloxane (DMS-S45, 110,000 g/mol), titanium 2-ethylhexoxide (AKT867) and di-n-butyldiacetoxytin tech-95 (SND3160) were obtained from Gelest.

2.2.2 Synthesis of PDMS polymers and ZIF-71 particles

2.2.2.1 Addition cure PDMS synthesis

The addition cure PDMS membranes were prepared from RTV615 (Momentive Performance Materials). The component RTV615A was the vinyl terminated polymer base, which included Pt-based catalysts, while RTV615B was the cross-linker with -SiH

groups. To prepare free-standing pure PDMS films, RTV615B, RTV615A and toluene were mixed at a mass ratio of 1:10:100. The solution was heated to 50 °C while stirring until the solution became viscous. The solution was degassed under vacuum after mixing for approximately two minutes. Finally, a GARDCO® casting blade was used to cast the solution into membranes on borosilicate glass plates coated with BYTAC® (to prevent the PDMS film from sticking to the glass plate). After casting, the membranes were dried at room temperature for 48 hours and then heated at 100 °C for 15 hours under vacuum (to complete cross-linking).

The preparation of ZIF-71/PDMS nanocomposite membranes was similar to the free-standing pure PDMS membranes. RTV615A in toluene was first mixed with a probe sonicator (FS-300N, Shanghai Shengxi Ultrasonic Instrument Co., Ltd.). Then, ZIF-71 particles were dispersed into the RTV615A/toluene solution by sonicating for 1 hour with a bath sonicator (FS220, Fisher Scientific). Finally, RTV615B was added to the RTV615A/toluene/ZIF-71 solution and stirred, heated, degassed and was cast the same as the pure PDMS films.

2.2.2.2 Condensation cure PDMS synthesis

The synthesis of the condensation cure PDMS was based on Bighane et al.'s method.[96] To prepare pure PDMS films, 8 g of anhydrous heptane was added to 1 g of silanol terminated polydimethylsiloxane. To ensure the polymer was thoroughly mixed with solvent, first 3 minutes vortex mixing was applied. Next eight repeats of the two-step process of: (1) 60s of sonication with the probe sonicator at 300 W followed by (2) 90s vortex mixing were performed. After the sonication repeats were completed, 0.2 g of

TEOS was mixed into the solution with 3 minutes vortex mixing. Finally, approximately 0.012 to 0.04 g of each titanium 2-ethylhexoxide and di-n-butyldiacetoxytin tech-95 were added followed with 3 minutes vortex mixing. Then, the solution was poured into a 9 cm diameter Teflon flat-bottom evaporating dish in a humidity controlled box under 75% relative humidity to cross-link the polymer. After 21 hours, the films were removed from the humidity controlled box and dried them in two stages – first in a vacuum oven at 100 ˚C for 20 hours and second in a vacuum oven at 120 ˚C for 11 hours to remove any residual solvent and byproducts.

To synthesis ZIF-71/PDMS MMMs, the PDMS-heptane solution was first prepared by adding 8 g of n-heptane to 1 g of silanol terminated PDMS, followed by 3 minutes vortex mixing. Next, 8 repeats of the combination of 60 s of probe sonication at 300 W followed by 90 s vortex mixing were performed. Then, a ZIF-71-heptane solution was prepared. A fixed amount of ZIF-71 (varies with different loadings) was added to 6 g of n-heptane. Then the solution was mixed with probe sonication at 90 W for 3 minutes followed by 3 minutes vortex mixing. This sonication-vortex mixing was repeated for two cycles. After that, 1 g of PDMS-heptane solution was transferred to the ZIF-71-heptane solution, followed by 3 minutes probe sonication at 90 W and 3 minutes vortex mixing. The remainder of the PDMS-heptane solution was then transferred to the ZIF-71-PDMS-heptane solution. Again the solution was mixed with probe sonication at 90 W for 3 minutes followed by vortex mixing 3 minutes. The sonication-vortex mixing combination is repeated twice. After that, 8g of n-heptane was removed by evaporation while stirring. After stirring, 0.2 g of TEOS was added followed by an additional 3

minutes of stirring. Finally approximately 0.012 to 0.04 g of each titanium 2-ethylhexoxide and di-n-butyldiacetoxytin tech-95 were added to the solution, followed with 3 minutes stirring. Similar to the neat PDMS membranes, the solution was then poured into the Teflon flat dish in a humidity-controlled box (75 % RH) to cross-link the polymer. Again, after 21 hours, the films were removed from the humidity controlled box and dried in two stages – first in a vacuum oven at 100 ˚C for 20 hours and second in a vacuum oven at 120 ˚C for 11 hours.

2.2.2.3 ZIF-71 synthesis

The ZIF-71 nanoparticles were synthesized based on the method published by Lively et al. [97] The $Zn(OOCCH_3)_2 \cdot 2H_2O$ (0.1756g, 1mmol) and dcIm (4mmol, 0.4383g) each were dissolved individually in 25 mL of methanol. Then, the dcIm was added dropwise into the $Zn(OOCCH_3)_2 \cdot 2H_2O$/methanol solution. Next, the $Zn(OOCCH_3)_2 \cdot 2H_2O$/dcIm/methanol solution was stirred at room temperature for 2 hours. After completion of the stirring, the ZIF-71 nanoparticles were washed with centrifugation and sonication in methanol three times. Finally, the product was dried at 40 °C for 6 hours to remove any remaining methanol.

2.2.2.4 ZIF-71 Water stability test

In order to evaluate the stability of ZIF-71 in water, the ZIF-71 particles were dispersed in water at 25 °C and 60 °C for seven days. Then a centrifuge was used to remove the water and the particles were then dried in an oven. Finally, XRD was applied to confirm the ZIF-71 crystal structure and SEM was carried out to confirm the morphology.

2.2.2.5 ZIF-71/PDMS compatibility test

In order to investigate the compatibility of ZIF-71 with the two PDMS synthesis methods, the dcIm/PDMS and zinc acetate dihydrate/PDMS membranes were made via the same processes as ZIF-71/PDMS membranes. The amount of dcIm and zinc salt used was equivalent to the amount of dcIm or zinc salt present in a 25 wt% ZIF-71 loading PDMS membrane.

2.2.2.6 Pervaporation performance

The pervaporation performance was measured in a batch apparatus with heated-recirculating feed. The schematic of the setup used in this research is shown in Figure 2-3. The feed circulation speed was maintained at 60 mL/min. The membrane was fixed at the bottom of the feed cell with a porous stainless steel support. The feed solution had a mass of 35 g and was either of 2 wt% ethanol in water or 2 wt% 1-butanol in water. The support side of the system was connected to a vacuum pump, maintaining a pressure on the downstream side of the membrane of 4.67 Pa. The effective surface area of the membranes was 1.431×10^{-4} m^2. The thicknesses of the free-standing membranes were measured with a Marathon electronic digital micrometer (Part No. CO 030025) of ±2 μm accuracy. The average of four measurements from different parts of the membrane was taken as the thickness. Prior to collecting permeate, the feed cell and circulation lines were heated to 60 °C and the system was stabilized at this temperature for 1.5 hours to ensure the system approached steady state operation. The permeate was collected with a liquid nitrogen cold trap for two hours. The permeate was weighed and the composition was analyzed via gas chromatography (Agilent technologies 7890A GC system).

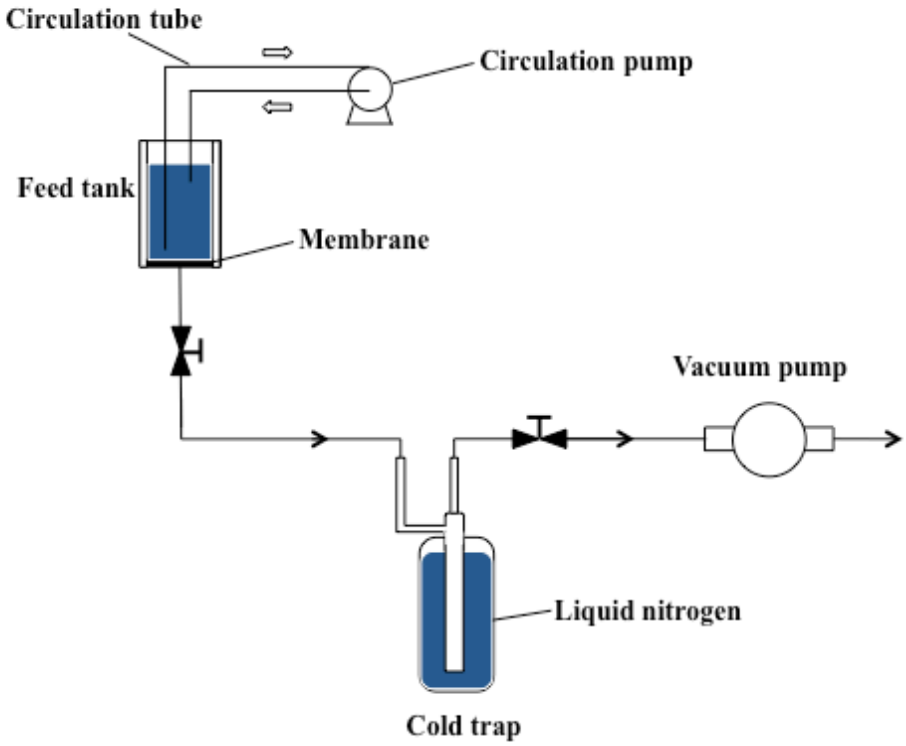

Figure 2-3. Schematic diagram of the pervaporation setup used in this research.

The composition of feed solution was essentially unchanged during the experiment because the mass transferred across the membrane was very small compared to the total mass of the feed solution (the mass of the permeate weight was a factor of 600 less than the mass of feed solution).

2.2.3 Characterization

X-ray diffraction (XRD) with powder X-ray diffractometer (Siemens D5000) was used to investigate and confirm the crystal structure of the ZIF-71 particles. The diffraction patterns were collected on a Panalytical X'pert Pro X-ray Diffractometer using Cu Kα radiation.

The morphology of the synthesized ZIF-71 particles and membranes were evaluated with scanning electron microscopy (SEM) (Philips FEI XL-30). Prior to SEM, the samples were sputter coated with gold. Dynamic light scattering (DLS, DynaPro MS/X, Protein Solutions Inc.) was applied to quantify the mean diameter of the ZIF-71 particles.

Tensile testing with a TA XT Plus Texture analyzer was performed to quantify the mechanical properties (Young's modulus, fracture stress and strain) of the membranes at a test speed of 0.5 mm/s at room temperature. For each sample type, it is reported the average of 5 samples. The membrane thicknesses vary from 100 to 300 μm depending on the ZIF-71 loadings.

2.3 Results and discussion

2.3.1 Characterization of ZIF-71 and stability test in water

Figure 2-4 shows the X-ray diffraction pattern of as-synthesized ZIF-71, ZIF-71 after immersion in water at room temperature for 7 days, and ZIF-71 after immersion in water at 60°C for seven days. In the as-synthesized ZIF-71 data, all of the reflections matched the reference diffraction pattern for ZIF-71. For both the reference pattern and the pattern of the as-synthesized ZIF-71, there was a characteristic reflection around a 2θ of 7.[66] After immersion in water for seven days at both 25 °C and 60 °C, all of the ZIF-71 reflections were still present in the XRD pattern with no peak shifting or broadening. This indicated that the ZIF-71 crystal structure was maintained. As a result, we concluded that ZIF-71 was stable in water and can be used for the pervaporation of alcohols from dilute aqueous solutions. Decomposition of ZIF-8 was reported by Liu et al. with crystal

concentration of 0.6 wt% ($W_{ZIF-8}/(W_{ZIF-8} + W_{water})$) and 0.060 wt% in water at 80 °C for 24h.[87] In fact, ZIF-8 was fully converted to ZnO when the crystal concentration is low at 0.060 wt%. The degradation of ZIF-8 in water was also observed by Zhang et al., they reported an increase in Zn^{2+} concentration and pH value in the liquid supernatant when ZIF-8 powders were dispersed in pure water solution.[98] This suggests the hydrolysis of ZIF-8 crystals in water solution. In contrast to ZIF-8, here we found ZIF-71 to be stable in water. We hypothesize this results from the hydrophobicity of dcIm (ligand used in ZIF-71) which is higher than mIm (ligand used in ZIF-8). The ligand mIm has water solubility of 780 g/L while dcIm is insoluble in water. The hydrophobic nature of dcIm ligand enhances the ZIF-71 hydrothermal stability compared to ZIF-8.

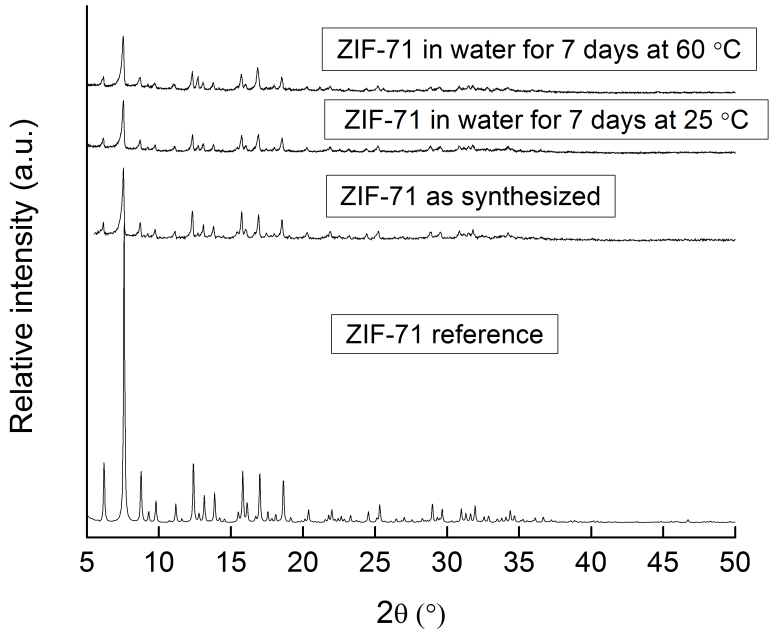

Figure 2-4. XRD patterns of ZIF-71 and ZIF-71 after immersion in water for seven days at two temperatures. The ZIF-71 reference is simulated reflection pattern obtained through Cambridge Crystallographic Data Center.

The morphology of the as-synthesized ZIF-71 particles was also checked using SEM imaging. Figure 2-5a shows that the ZIF-71 particles are cubic-shaped. DLS showed that the average size of the ZIF-71 particles was 646.2 ± 6.3 nm. The morphology of ZIF-71 particles remained the same after exposure to water, which was consistent with the XRD data. The particle diameter measured from DLS was 630.0 ± 3.7 nm after the particles were immersed in water for 6 days at 60°C. Additionally, the SEM images confirmed that ZIF-71 was stable after 7 days of immersion in water at 60°C.

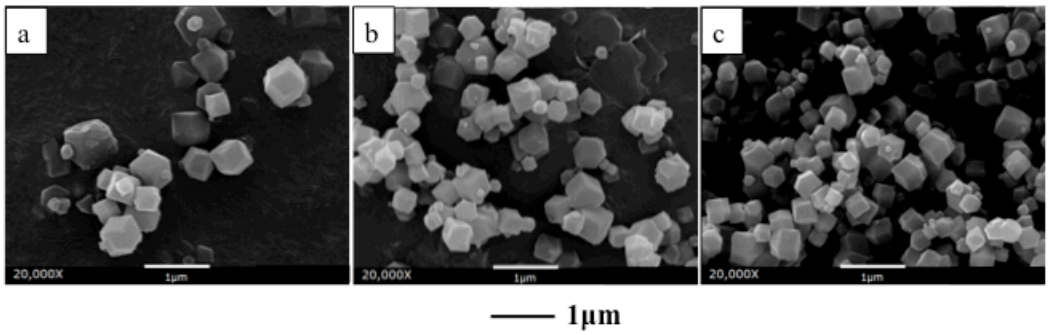

Figure 2-5. SEM images of (a) ZIF-71, (b) ZIF-71 immersed in water for seven days at 25°C, and (c) ZIF-71 immersed in water for seven days at 60 °C.

2.3.2 The effect of dcIm and zinc acetate dihydrate on the cross-linking of PDMS

An issue was observed with the cross-linking of the PDMS during synthesis of the addition cure ZIF-71/PDMS composite membranes. It was found that for the 40 wt% ZIF-71 loading PDMS composite membranes synthesized via addition cure, the membranes are much less flexible and they tear easily compared to pure PDMS membranes. It was unable to obtain a 40 wt% ZIF-71 loaded membrane with enough area to test because the membrane tore when we peeled it from the casting plate. Our hypothesis was that the imidazole linker interfered with the cross-linking process. Specifically, the platinum-based catalyst participating in the cross-linking reaction was poisoned by the imidazole linker. Previously, Yang et al. and Fu et al. observed that imidazole was chemically incompatible with Pt catalysts, which was consistent our hypothesis. Yang et al. found that imidazole-based Nafion membranes used in fuel cells could not generate current as a result of imidazole poisoning the platinum catalyst.[99] Fu et al.[100] also observed imidazole molecules poisoning the Pt catalyst in the Nafion-imidazole membrane fuel cells. They found that the doping of H_3PO_4 improved the fuel

cell performance because incorporated H_3PO_4 reacted with the imidazole to form imidazolium salts, thus suppressing the poisoning effect of the imidazole on the Pt catalyst. When Fu et al. replaced the Pt catalyst with a Pd-Co-Mo catalyst, they found the Nafion-imidazole-H_3PO_4 membrane had better performance - even though the Pd-Co-Mo catalyst had lower catalytic activity compared to Pt catalyst. These results confirmed the incompatibility between imidazole and Pt catalyst.

Some experiments were performed to test our hypothesis about ZIF-71 interfering with PDMS cross-linking. To discern the effect of ZIF-71 incorporation on the cross-linking of PDMS, the two synthesis components of ZIF-71 (the organic linker dcIm and zinc acetate dihydrate) were added separately into the PDMS casting solution during preparation of both addition cure and condensation cure PDMS films. It appeared that dcIm interfered with the cross-linking of RTV615A and RTV615B as is shown in Figure 2-6a. Typically addition cure free-standing PDMS films with no extra components are optically transparent and can be picked up off of the casting plate. Films loaded with dcIm did not form a film, but a gel. We could not quantify the mechanical properties of the dcIm/addition cure PDMS with tensile testing because of the lack of film formation. These experiments supported our hypothesis that the imidazolate linker dcIm poisoned the Pt catalyst during the addition cure formation of PDMS.

Figure 2-6. Addition cure PDMS film made with (a) 4,5-dichloroimidazole (dcIm) and (b) zinc acetate dihydrate and (c) pure PDMS. Note the white spots in (a) which are dcIm and note that a membrane film was not formed in (a), only a gel that could not be picked up in a single piece from the casting plate.

The compatibility test between 2-methylimidazole (mIm), the imidazole ligand used in ZIF-8, and addition cure PDMS was also carried out to check if the Pt poisoning effect applies to other ZIFs besides ZIF-71. Similar to the compatibility test of dcIm, equivalent to 25 wt% ZIF-8 loading was incorporated into addition cure PDMS synthesis solution. The result is shown in Figure 2-7. Same as dcIm, the PDMS did not cure and the polymer solution remained like a gel. Therefore, we conclude that ZIFs containing imidazole ligands may poison the Pt catalyst and interfere with the addition cure PDMS cross-linking process.

Figure 2-7. The 2-methylimidazole incorporated addition cure PDMS membrane. The amount of 2-methylimidazole added is equivalent to 25 wt% ZIF-8 loading.

In contrast, normal film formation was observed in zinc acetate dihydrate/addition cure PDMS membrane (Figure 2-6b), dcIm/condensation cure PDMS (Figure 2-8b) and zinc acetate dihydrate/PDMS membranes (Figure 2-8a). It is concluded that the condensation cure method was compatible with ZIF-71 incorporation while addition cure PDMS membranes were not compatible with ZIF-71. The permeation and mechanical results reported below were based on membranes formed with condensation cure PDMS synthesis.

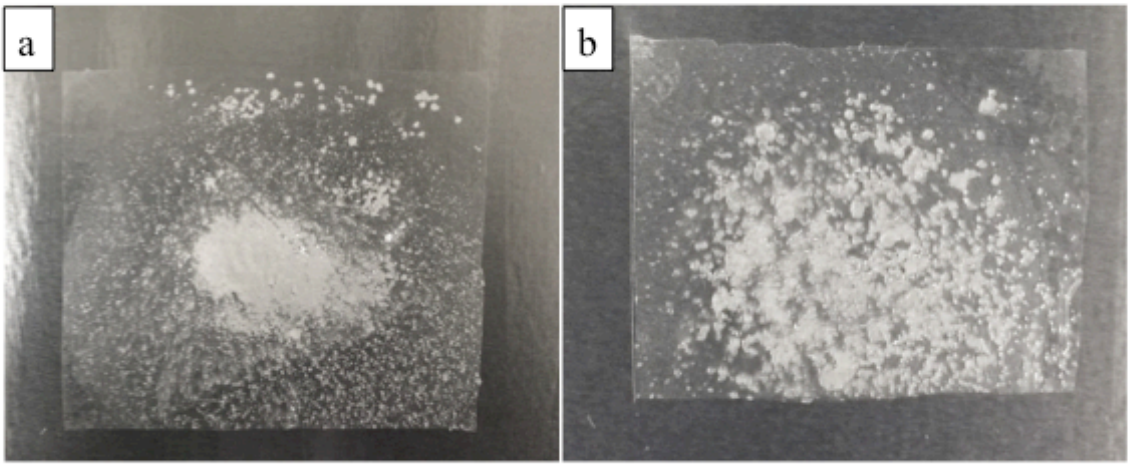

Figure 2-8. Condensation cure PDMS films made with (a) zinc acetate dihydrate and (b) 4,5-dichloroimidazole. Note the white spots in (a) and (b) which are zinc acetate dihydrate and 4,5-dichloroimidazole.

2.3.3 Characterization and pervaporation performance of the ZIF-71/PDMS nanocomposite membranes

SEM was performed to characterize pure PDMS membranes and ZIF-71/PDMS nanocomposite membranes. Figure 2-9 shows SEM images that verify the incorporation of ZIF-71 in the composite membranes. From the surface view of the membranes good film formation with no obvious defects or cracks was observed. The ZIF-71 particles appeared evenly distributed through the polymer matrix. No large aggregates in the composite membranes were observed, even in the membranes with the highest ZIF-71 loading (40 wt%).

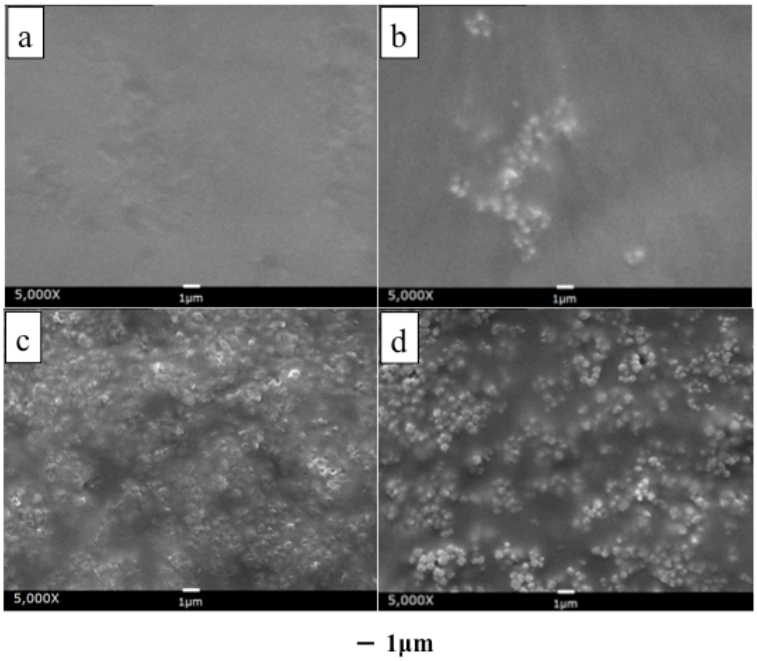

Figure 2-9. SEM images of surface view of condensation-cure PDMS-based membranes a) pure PDMS, (b) 5 wt%, (c) 25 wt% and (d) 40 wt% ZIF-71 loading nanocomposite membranes.

Figure 2-10 shows the permeability of water and 1-butanol as well as the 1-butanol/water selectivity of the various loading membranes. Permeabilities of both 1-butanol and water as well as 1-butanol/water selectivity increased with increasing ZIF-71 loading. The 40 wt% ZIF-71 membrane had the largest water permeability of 21758 ± 2497 Barrer, 1-butanol permeability of 123045 ± 17118 Barrer, and 1-butanol/water selectivity of 5.64 ± 0.15 (corresponding separation factor is 69.9±1.8). Liu et al. obtained similar results with ZIF-71/PEBA MMMs, they observed an increase in both water and 1-butanol permeabilities with higher ZIF-71 loadings.[69] In this research, the increased 1-butanol permeability might result from the hydrophobic nature of the ZIF-71

particles as well as the loose chain packing of the PDMS polymer matrix. The increased 1-butanol/water selectivity indicated that the increase in 1-butnaol permeability outweighed the increase in water permeability. This was because of the hydrophobic nature of the ZIF-71 particles that facilitates the adsorption and transport of 1-butanol molecules.

Liu et al. obtained a maximum 1-butanol/water selectivity of approximately 5 for 25 wt% ZIF-71 loading PEBA MMMs, while in our research 40 wt% ZIF-71 loading PDMS membranes achieved a higher 1-butanol/water selectivity of 5.64.[69] However, ZIF-71/PEBA MMMs had higher 1-butanol and water permeabilities compared to our ZIF-71/PDMS membranes. The highest 1-butanol permeability obtained in ZIF-71/PEBA membranes was close to 200,000 Barrer compared to 123,045 Barrer achieved in our research with ZIF-71/PDMS MMMs. Bai et al. observed a maximum 1-butanol/water selectivity of approximately 3.7 for 2 wt % ZIF-8/PDMS MMMs with a feed temperature of 60 °C.[101] Bai et al. achieved a 1-butanol permeability approximately half of the amount compared with the 40 wt% ZIF-71 loading PDMS MMMs reported here.

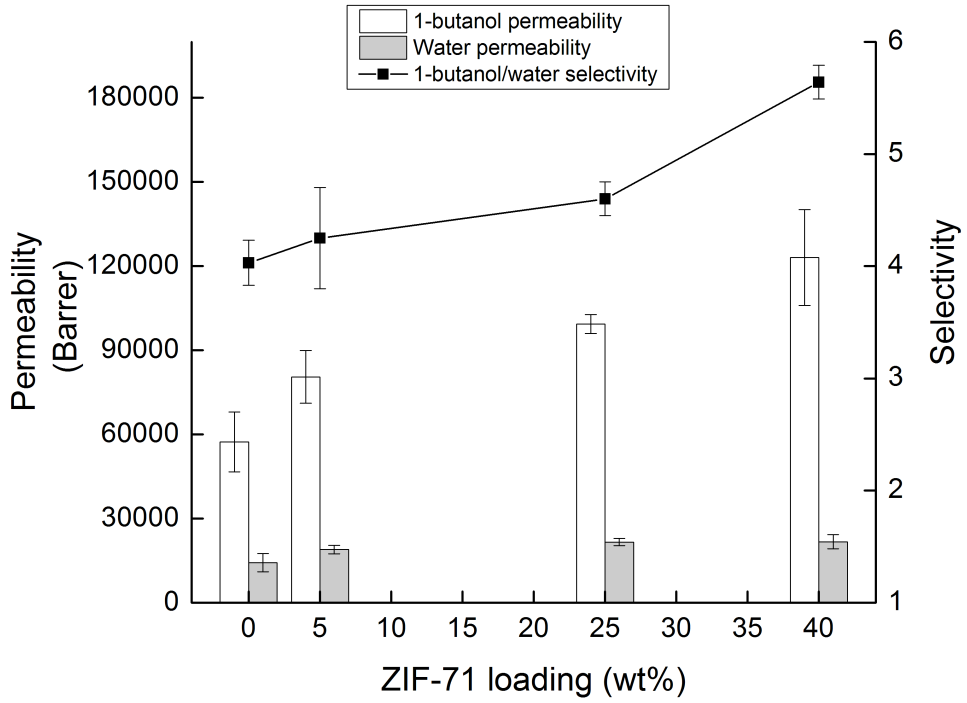

Figure 2-10. 1-butanol/water selectivity, water permeability, and 1-butanol permeability for pervaporation tests at 60 °C.

Figure 2-11 presents the ethanol and water permeability and ethanol/water selectivity of the membranes. Consistent with the separation performance observed for 1-butanol and water, these membranes had an increase in both ethanol and water permeability, and ethanol/water selectivity as the ZIF-71 loading increased. The ethanol permeability increase in 40 wt% ZIF-71 membranes is double that of pure PDMS membranes. The water permeability of these membranes increased by a factor of 1.8. The ethanol/water selectivity increased from 0.60 ± 0.05 (separation factor of 9.2 ± 0.7) for pure PDMS membranes to 0.81 ± 0.04 (separation factor of 12.4 ± 0.3) with 40 wt% ZIF-71 loading MMMs. The maximum ethanol/water selectivity achieved here (0.81) is roughly half of the value obtained from pure crystalline ZIF-71 membranes, which is 1.5.[66]

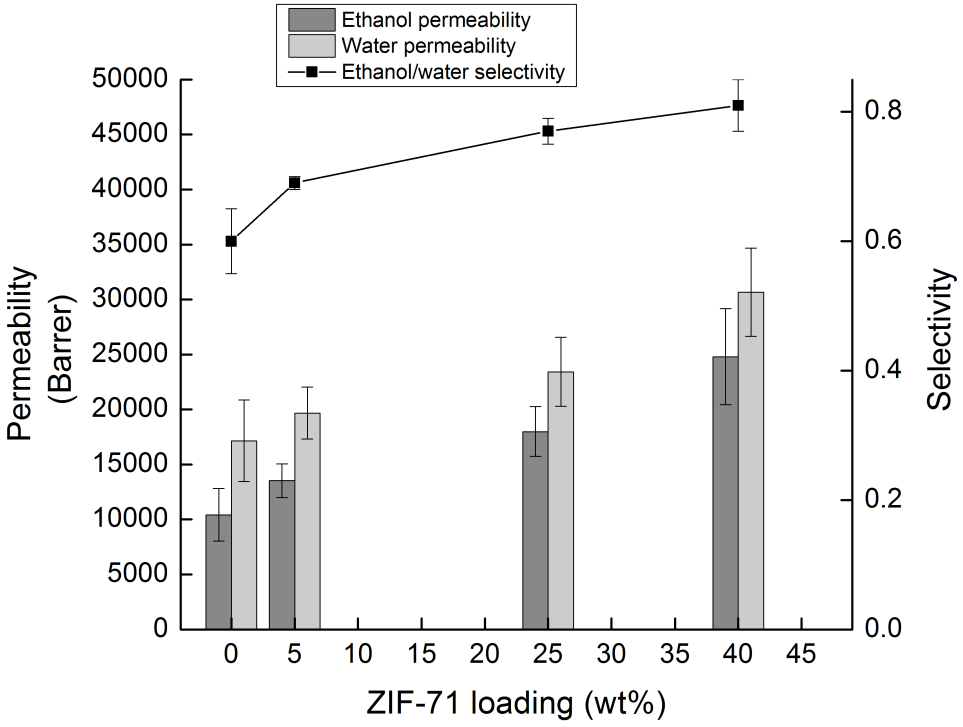

Figure 2-11. Ethanol/water selectivity, water permeability, and ethanol permeability for pervaporation tests at 60 °C.

2.3.4 Tensile test of ZIF-71/PDMS nanocomposite membranes

Table 2-1 presents the tensile test results of the pure PDMS and ZIF-71/PDMS membranes. The table clearly shows that the fracture strain decreased from 381.4 ± 32.6 to 35.6 ± 3.1 when the ZIF-71 loading increased to 40wt%. This suggests that the membrane ductility was declining with the addition of ZIF-71. This might be attributed to the low ductility of ZIF-71 particles. The Young's modulus increased significantly with higher ZIF-71 loadings, indicating that the addition of ZIF-71 stiffened the membranes. The enhanced Young's modulus might result from the ZIF-71 particles restricting PDMS

film deformation.[102] Additionally, no significant change of fracture stress was observed between all the membranes.

Table 2-1. Young's modulus, fracture stress and fracture strain of different ZIF-71 loading MMMs.

ZIF-71 loading (wt%)	Young's modulus (kPa)	Fracture stress (kg/mm^2)	Fracture strain (%)
0	10.00±0.44	0.28±0.02	381.4±32.6
5	11.57±1.89	0.24±0.05	255.9±52.5
25	41.97±1.75	0.32±0.02	242.3±56.0
40	225.75±26.14	0.21±0.03	35.6±3.1

2.4 Conclusion

In this chapter, the stability of ZIF-71 in water was evaluated. It was found that ZIF-71 is stable after seven days of exposure to water at 60°C. The imidazole organic linker dcIm impairs the cross-linking of the vinyl terminated PDMS (RTV615A) and the -SiH groups (RTV615B) by poisoning the Pt catalyst contained in RTV615A, which was used in the addition cure PDMS synthesis solution. The imidazole linker dcIm was compatible with condensation cure PDMS. The ZIF-71/condensation cure PDMS nanocomposite membranes were synthesized with four different ZIF-71 loadings: 0, 5, 25 and 40 wt%. The alcohol/water separation performances of condensation-cure PDMS membranes were enhanced through the incorporation of ZIF-71 particles. The improved separation performances can lead to the reduction of energy costs during the

pervaporation process. Overall, the membranes with 40 wt% ZIF-71 had the highest permeabilities as well as selectivities. For ethanol/water separation, 40 wt% ZIF-71 loading MMMs had the greatest observed ethanol permeability of 24809 ± 4374 Barrer, water permeability of 30661 ± 4015 Barrer and selectivity of 0.81 ± 0.04. For 1-butanol/water separation, 40 wt% ZIF-71 loading MMMs had the highest 1-butanol permeability of 123045 ± 17118 Barrer, water permeability of 21758 ± 2497 Barrer and selectivity of 5.64 ± 0.15. According to tensile testing, the fracture strain of the membranes decreased significantly with the incorporation of ZIF-71 into the PDMS. The Young's modulus increased considerably with the addition of ZIF-71 particles.

3 EFFECT OF ZIF-71 PARTICLE SIZE ON ZIF-71/PDMS COMPOSITE MEMBRANES PERFORMANCES FOR ETHANOL AND 1-BUTANOL REMOVAL FROM WATER THROUGH PERVAPORATION

3.1 Introduction

PDMS is the state-of-art polymer for separating organic compounds from water solutions through pervaporation processes. It possesses many advantages over other polymers including high selectivity, good mechanical stability and chemical stability.[33] However, the separation performances of PDMS membranes need improvement to be economically competitive with traditional distillation methods. One of the most promising techniques is to incorporate filler materials of high organophilic selectivity such as high-silica zeolites into the PDMS polymer to form MMMs.[33] Vane et al. observed a significant improvement of PDMS separation performances with the addition of high silica ZSM-5 zeolites.[3] They reported an ethanol/water selectivity of 3.0 with 65 wt% ZSM-5 zeolites incorporated into PDMS membranes.

Particle size plays a significant role in MMMs separations with variable results. It is challenging to predict the effect of particle size on MMM separation performance, and mixed results have been observed. Tantekin-Ersolmaz et al. studied the effect of zeolite particle size on the O_2, N_2 and CO_2 gas permeabilities through silicalite-1/PDMS membranes.[103] They prepared 20 wt% and 40 wt% zeolite loading MMMs with five different size silcialite-1 particles: 0.1, 0.4, 0.7, 0.8 and 8 μm. For both zeolite loadings, they observed increasing gas permeabilities with increasing particle sizes. It is obvious that MMMs made with smaller particles have significantly higher zeolite-polymer

interfacial areas. They concluded that the decrease in gas permeability might be the result of enhanced mass transfer resistance through the interfaces. Tantekin-Ersolmaz et al. also observed the highest CO_2/ N_2 and CO_2/ O_2 selectivity with 0.8 μm silicalite-1 particles.[103] Vane et al. evaluated the effect of high-silica zeolite particle size on membrane performances with zeolite/PDMS MMMs for recovering ethanol from water through pervaporation.[3] Membranes made with 2.4 μm zeolite particles had better separation performances than membranes made with submicron size zeolite particles. Another study carried out by Wang et al., however, showed that smaller silicalite-1 particles (100 and 200 nm) had better compatibility with the PDMS polymer matrix than larger particles (400 and 1000 nm).[104] The separation factor of silicalite-1/PDMS MMMs was enhanced from 8.9 to 10.5 with smaller size particles. Because the reported variable effects of particle size on MMM separation performance, in our research we investigated the role of zeolitic imidazolate framework-71 (ZIF-71) particle size in PDMS membranes.

ZIFs are an attractive filler material for the preparation of pervaporation MMMs.[69, 76, 77, 105, 106] ZIFs are a subclass of MOFs. They are composed of transition metal ions, such as Zn^{2+}, that are connected by imidazole organic linkers.[63] ZIFs have zeolitic topologies and their high thermal and chemical stability are attractive for challenging separation applications.[87] The numbering convention in ZIFs is arbitrary and loosely based on when the ZIF was discovered. ZIF-71, Zn(4,5-dichloroimidazole)$_2$, was used as the filler material for making PDMS composite membranes. ZIF-71 is hydrophobic and has the Rho topology. The pore size is 0.48 nm

and ZIF-71 displays high sorption capacity for butanol, ethanol, and other alcohols.[63, 91, 97] In addition, a number of studies have shown ZIF-71 has good performances in removing methanol (MeOH), ethanol and butanol from water solutions via pervaporation.[66, 69, 77] Work by Dong et al. shows that ZIF-71 membranes have a MeOH/water selectivity of 4.32 and ethanol/water selectivity of 1.50. Zhang et al. found that ZIF-71 has a vapor phase 1-butanol/water selectivity of 290 for a 0.25 mol% 1-butanol/water feed, which is higher than ZIF-8 and ZIF-90.[91] Those results indicate that ZIF-71 is a promising filler material for separation of alcohols from water solution.

Several synthesis techniques have been explored to control the size of ZIFs. Sánchez-Laínez et al. synthesized ZIF-11 with average size of 36 ± 6 nm with a centrifugation method.[107] Using the same reaction time, Sánchez-Laínez et al. synthesized nanoscale ZIF-11 through centrifugation synthesis technique, but only obtained micro-sized ZIF-11 through conventional synthesis. Seoane et al. found that ZIF-8 and ZIF-20 can be synthesized with ultrasound (US) method.[108] In the US method, cavitation of the solvent generates high temperature and pressure, which facilitates the synthesis of different type nano-materials. The US synthesis method achieved particles two orders of magnitude smaller with narrower size distribution than particles made with the traditional solvothermal method.

Below summarizes the literature on tailoring ZIF sizes by altering different parameters such as 1) reactant ratio: ZIF-8 is one of the most reported on ZIF structures, Bao et al. altered the reactant ratio and observed ZIF-8 particle size decreased from 350 to 190 nm when 2-methylimidazole (mIm)/Zn molar ratio increased from 10 to 20 using

$Zn(OAc)_2 \cdot 2H_2O$ as zinc salt in aqueous solution.[109] Tanaka et al. also altered reactant ratio and found that ZIF-8 particle size decreased with increasing mIm/zinc ratio.[110] 2) Zinc salt sources: Chi and coworkers reported the size control of ZIF-8 nanoparticles through different sources of zinc salts.[111] They obtained nanoparticles of diameters 88, 240 and 533 nm using zinc nitrate, zinc acetate and zinc chloride, respectively. Owing to the solubility and reactivity difference of different zinc sources, the zinc precursors with greater solubility provide more Zn^{2+} ions. As a result, the nucleation rate is enhanced which leads to smaller particles sizes.[111] 3) Synthesis temperature: ZIF-7 and ZIF-62 are much less prevalent in the literature than ZIF-8, however Gustafsson et al. studied the influence of synthesis temperature on ZIF-7 and ZIF-62 particle size.[112] They determined that the effect of temperature is different for ZIF-7 and ZIF-62, implying that the effects of changing the synthesis temperature on particle size are not predictable. The particle size of ZIF-7 decreased with increasing temperature while the particle size of ZIF-62 increased several times when the synthesis temperature increased from 85 °C to 110 °C. Tsai et al. observed a decrease in ZIF-8 particle size from 78 to 26 nm when the synthesis temperature increased from -15 to 60 °C.[113] The opposite results with different ZIFs might because the temperature has different influences on the crystal nucleation rates. If the nucleation rate increases with temperature, the final particle size will become smaller.[113] 4) Synthesis solvent: Wee et al. prepared ZIF-71 with different particle sizes (140, 290 and 430 nm) by changing the MeOH : Dimethylformamide (DMF) volume ratio. They found that the deprotonation rate of organic linkers was altered upon changing the synthesis solvent, thus the nucleation and crystal growth rate

were affected. The addition of DMF solvent into the synthesis solution enhanced the ligand deprotonation rate and the nucleation rate. Therefore, smaller particles were obtained. 5) Use of additives: research done by Nordin et al. demonstrated that the addition of different concentration trimethylamine (TEA) additive results in ZIF-8 particles of sizes ~134nm and ~288nm.[114] The presence of TEA facilities the mIm deprotonation rate and the nucleation is induced. Smaller size ZIF-8 particles were produced with higher TEA concentrations.

Several groups have reported synthesizing ZIF-71 of different particle sizes by 1) using different solvents, 2) using additives, and 3) by increasing temperature above room temperature. 1) Japip et al. reported ZIF-71 with particle size less than 100 nm.[90] They obtained the nanoparticles with a room temperature method using DMF as synthesis solvent. They also obtained ZIF-71 particles of 30, 200 and 600 nm with different MeOH : DMF volume ratios based on Wee et al.'s research. Lively et al. synthesized one micrometer diameter ZIF-71 particles at room temperature in MeOH.[97] As mentioned earlier, Wee's group obtained different size ZIF-71 particles by varying MeOH : DMF volume ratios. However, DMF has a kinetic diameter of 5.2-5.5 Å, which is larger than the window size of ZIF-71 (4.8 Å). Thus, DMF is hard to remove from the framework structure and lowers the surface area of the particles.[97] Therefore, methanol with a smaller kinetic diameter (3.6 Å) is easier to remove from the network and is a better option for ZIF-71 synthesis. 2&3) Wang et al. added formic acid into the synthesis solution (with MeOH as solvent) at room temperature, and obtained smaller size (450 nm) particles compared to synthesized without additives (800 nm).[115] They also

observed an increase in particle size (1~2 μm) when synthesis temperature was increased from room temperature to 50 and 80 °C with a solvothermal synthesis process.[115]

Although there have been several research reports on the synthesis of ZIF-71 particles with different sizes (as described above), to our knowledge, the effect of synthesis temperature, reaction ratio and reaction time on ZIF-71 size has not been systematically studied for the non-solvothermal synthesis process when MeOH is used as solvent.[77, 90, 115] Note that Wee et al. previously reported the effect of ZIF-71 particle size on ZIF-71/PDMS MMMs performances for ethanol removal from water. However, Wee et al. synthesized addition cure PDMS membranes, conversely we report results from condensation cure PDMS membranes. Based on our previous research, condensation cure PDMS is more compatible with ZIF-71 particles than addition cure PDMS.[116] In addition, we observed different particle size effect on membrane performances than Wee et al. The goals are to investigate the influence of different synthesis parameters (temperature, reaction ratio, reactant time) on ZIF-71 particle size and study the impact of ZIF-71 particle size on free-standing ZIF-71/PDMS MMMs performances for removing ethanol and 1-butanol from water through pervaporation.

3.2 Materials

For the synthesis of ZIF-71 particles, zinc acetate dihydrate ($Zn(OAC)_2 \cdot 2H_2O$) (ACS, 98.0-101.0%) was purchased from Alfa Aesar, 4,5-dichloroimidazole (dcIm) (>97%) was purchased from Tokyo Chemical Industry and MeOH (HPLC) was supplied by LabChem Inc. Gelest supplied the silanol terminated PDMS (DMS-S45, 110,000 g/mol), titanium 2-ethylhexoxide (AKT867) and di-n-butyldiacetoxytin tech-95

(SND3160) for ZIF-71/PDMS composite membrane synthesis. The n-heptane (anhydrous, 99%) and tetraethyl orthosilicate (TEOS, 99.999% trace metals basis) were purchased from Sigma-Aldrich.

3.3 Sample preparation and characterization instrumentation

X-ray diffraction (XRD) with powder X-ray diffractometer (X'pert Pro, Panalytical) was carried out to evaluate the crystal structure of ZIF-71 particles. Using scanning electron microscope (SEM) imaging (XL-30 ESEM), the morphology of both ZIF-71 particles and membranes were evaluated. Dynamic light scattering (DLS) (DynaPro MS/X, Protein Solutions Inc.) was performed to study the ZIF-71 particle size and distribution. For DLS sample preparation, a sonication bath (FS220, Fisher Scientific) was used. Gas chromatography (GC, Agilent technologies 7890A GC system) was used to analyze the composition of the permeance solution from the pervaporation experiments. For membrane synthesis, the synthesis solution was sonicated with probe sonicator (FS-300N, Shanghai Shengxi Ultrasonic Instrument Co., Ltd.) and the solution was also mixed by VWR fixed speed vortex mixer (Model No. 945302).

3.4 Preparation and characterization of different sizes of ZIF-71

The synthesis of ZIF-71 particles was based on a method presented by Lively et al.[97] MeOH was used as the synthesis solvent. The molar ratio of dcIm to $Zn(OAC)_2 \cdot 2H_2O$ was varied from 1:1 to 7:1 at room temperature. The synthesis time was altered from 0.5 to 4 hours at room temperature. To study the influence of synthesis temperature on particle size, different temperatures (-20, -10, 0, 10, 15, 30 and 35 °C)

were used with a dcIm: $Zn(OAC)_2 \cdot 2H_2O$ molar ratio of 4:1 and a reaction time of two hours.

To perform the synthesis at -20, -10, 0, 10 and 15 ºC, the beakers containing the dcIm/MeOH and $Zn(OAC)_2 \cdot 2H_2O$/MeOH solutions were placed in a bath of MeOH and dry ice or an ice water bath at the appropriate temperature. The solutions were allowed to reach a steady temperature before dropwise addition of the dcIm/MeOH solution to the $Zn(OAC)_2 \cdot 2H_2O$ /MeOH solution. The appropriate temperature was maintained for two hours of stirring by periodically adding small amounts of ice or dry ice to the water or MeOH bath. To increase the synthesis temperature to 30 and 35 ºC, the solutions were placed on a hot plate during dissolution of dcIm and $Zn(OAC)_2 \cdot 2H_2O$, and were allowed to reach steady temperature before mixing. The beakers were covered to minimize MeOH evaporation. After completion of the reaction, the particles were washed in MeOH (centrifugation and decanting of supernatant) three times and dried overnight in an oven at 40 °C.

XRD was used with CuKα radiation at 45 kV, 40 mA with a scan step size of 0.025 to confirm that the crystal structure of the synthesis products matched the published ZIF-71 pattern. The XRD samples were prepared by grinding the synthesized particles into a fine powder and pressing onto a zero background plate. To determine the particle diameter produced at each synthesis condition, the samples were analyzed by DLS. The DLS samples were prepared by dispersing 5 wt% of the synthesized particles in MeOH with a sonication bath at 250 W for 2 hours prior to analysis. SEM showed particle size

and shape and confirmed the particle diameters obtained by DLS were not influenced by aggregation.

ZIF-71 particle size distribution is presented in a box and whisker plot. The horizontal line through the box represents the median value of the data. The upper and lower whiskers represent the maximum and minimum values of the data. The small square box inside the larger box indicates the 50^{th} percentile the value. While the top of the box represents the 75^{th} percentile value and the bottom of the box represents the 25^{th} percentile value

3.5 Membrane preparation

The synthesis of condensation cure pure PDMS membranes followed the protocol mentioned earlier in chapter 2.

The ZIF-71/PDMS MMMs were made with three different ZIF-71 sizes: 152 ± 45 nm made at -20 ºC, 506 ± 28 nm made at 25 ºC and 1030 ± 385 nm made at 35 ºC. We followed a similar procedure as pure PDMS synthesis to prepare the 25 wt% loading ZIF-71/PDMS MMMs. The 25 wt% ZIF-71 loading was chosen based on the optimum ZIF loading reported previously.[69, 79, 117] The detailed ZIF-71/PDMS MMMs synthesis method is described in chapter 2. SEM characterization was carried out to investigate the membrane morphology and particle distribution in the polymer matrix. The membranes synthesized have thicknesses ranges from 140 to 390 μm.

3.6 Pervaporation test

The membrane was tested in a batch pervaporation as mentioned in chapter 2. The pervaporation setup used in our lab is shown in Figure 3-1. The test parameters (feed

concentration, test temperature, etc) are the same as in chapter 2. Permeability and selectivity data is calculated to quantify the membrane performances. The equations are listed earlier in chapter 1.

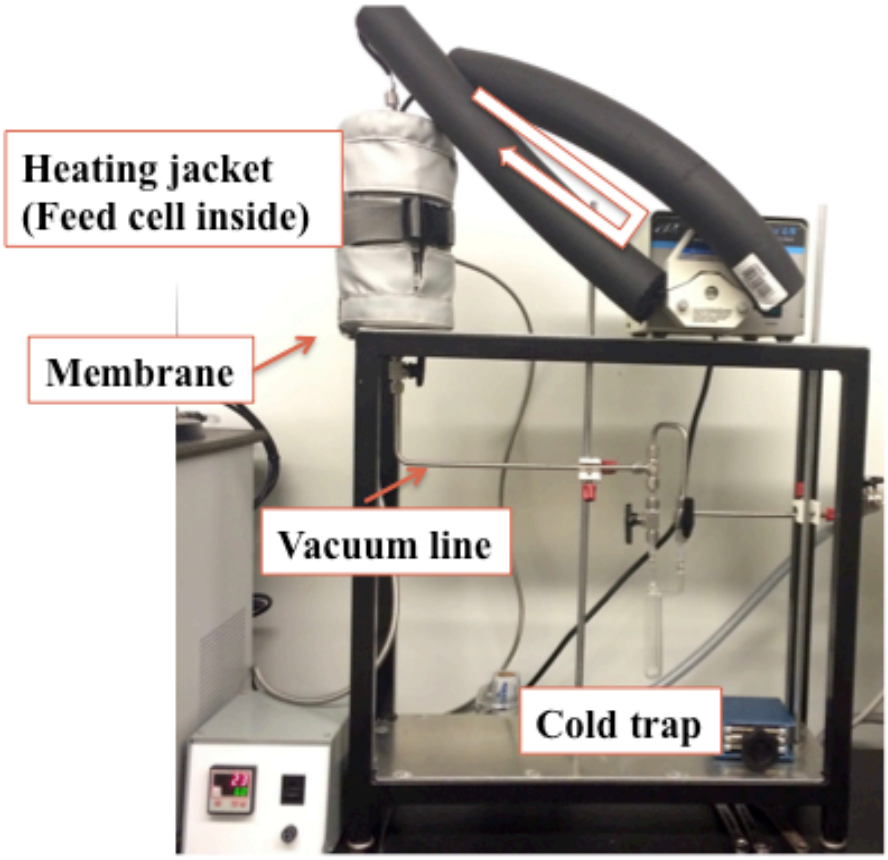

Figure 3-1. Pervaporation apparatus used for the pervaporation measurements in the lab.

3.7 Results

3.7.1 Effect of synthesis temperature on ZIF-71 particle size

Figure 3-2 shows the XRD patterns of the particles synthesized at different temperatures. This confirms that the particles all have the same crystal structure of ZIF-

71 as the reference pattern. Lower XRD peak intensity was observed with samples made at -10 and -20 ºC. This may result from the significant decrease in particle size as shown in DLS and SEM results mentioned later.

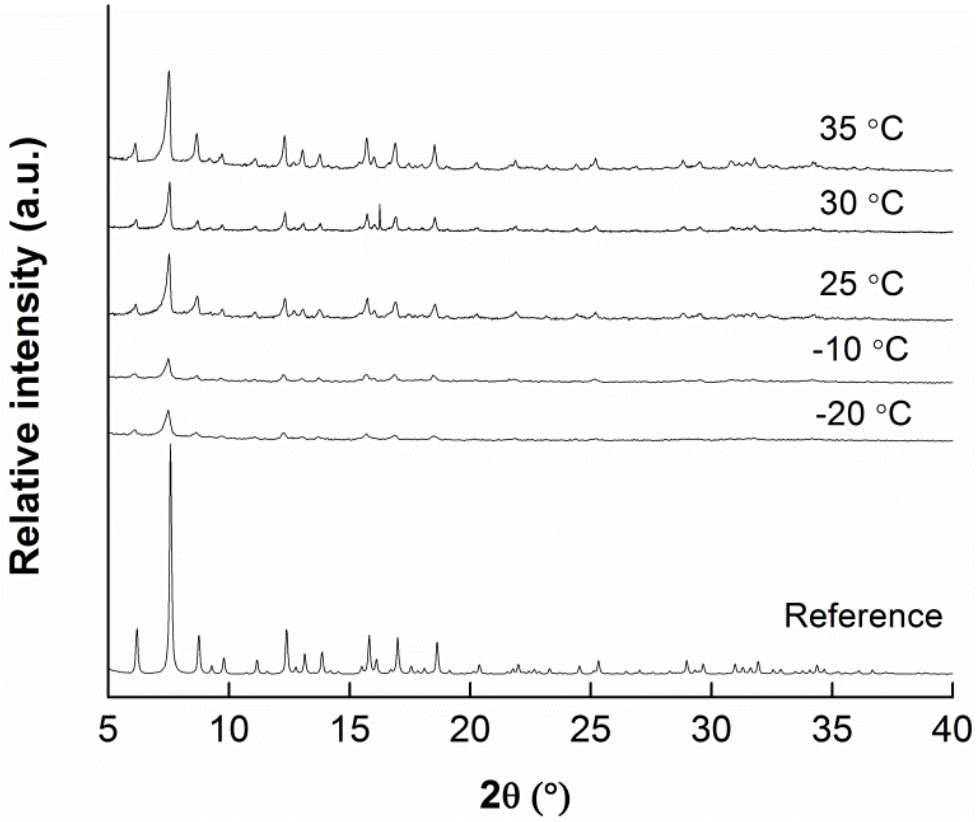

Figure 3-2. XRD patterns of ZIF-71 particles made at different temperatures. The ZIF-71 reference data is simulated reflection pattern obtained from Cambridge Crystallographic Data Center.

Figure 3-3 presents the particle size distribution measured by DLS for ZIF-71 produced at varying synthesis temperatures and a common reactant molar ratio of 4:1. Table 3-1 summarizes the particle diameter and distribution. Clearly, the mean particle diameter increases with increasing temperature. Also, the ZIF-71 particles synthesized at temperatures of 30 °C and 35 °C have a much broader size distribution than those

synthesized at lower temperatures. This is in contrast to what Gustafsson et al. reported for ZIF-7 and ZIF-8, where ZIF-7 crystal size increased from 2.4 to 4.7 μm when the synthesis temperature decreased from 110 to 85 °C at reactant ratio of (Zn:Im:bIm) equal to (1:6:9).[112] Tsai et al. observed ZIF-8 particle size decrease from 78 to 26 nm as synthesis temperature increased from -15 to 60 °C.[113] Similarly to ZIF-62, here the ZIF-71 particle diameter increases with increasing temperature.[112] Our hypothesis is temperature has the opposite effect on the nucleation rates during the synthesis of ZIF-71 and ZIF-62 compared to ZIF-7 and ZIF-8. ZIFs that have a decrease in particle size is a result of enhanced nucleation rate when synthesis temperature increases. This increase in nucleation was observed during ZIF-8 synthesis.[118] Whereas in the case of ZIF-71, the increase in particle size may be caused by the reduction of nucleation rate with increasing temperature.

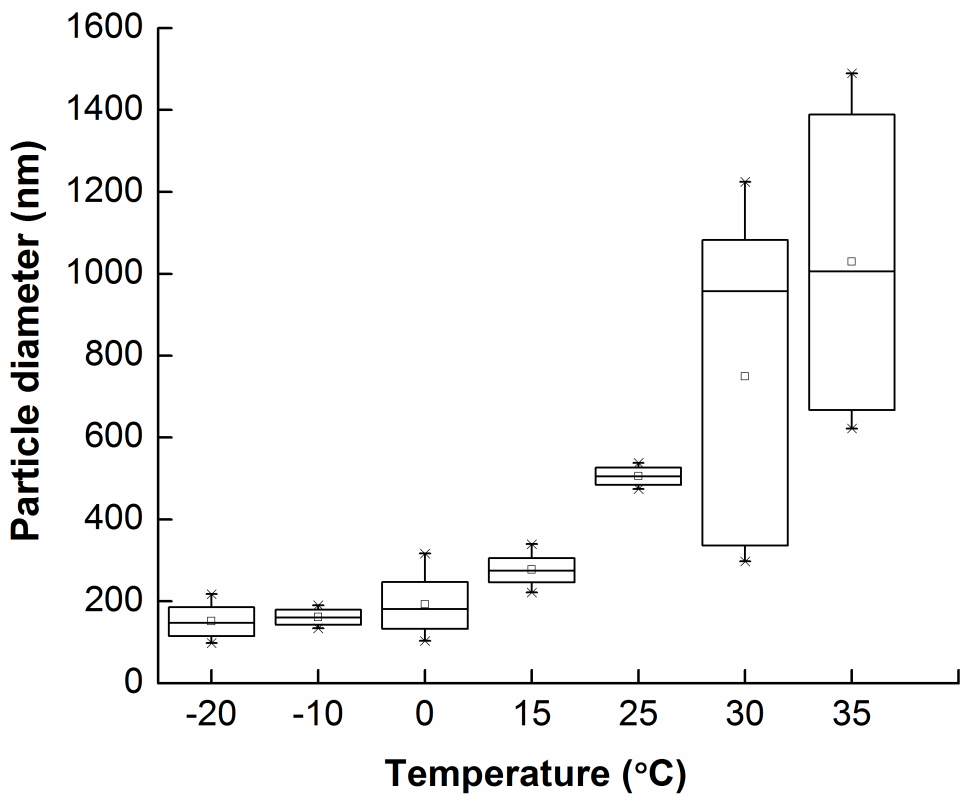

Figure 3-3. DLS data of the ZIF-71 particles made at different temperatures.

Table 3-1. Particle size distribution of ZIF-71made at different temperatures.

Temperature (°C)	-20	-10	0	15	25	30	35
Particle size (nm)	152 ± 45	161 ± 20	192 ± 72	278 ± 47	506 ± 28	749 ± 408	1030 ± 385

The formation of crystals starts from nucleation followed by the growth of the nucleus. Nucleation occurs when the solution is supersaturated and the diffusion of ions and molecules promotes the growth of crystals. We hypothesize that in the case of ZIF-

71, on one hand, increasing the temperature decreases the degree of the supersaturation which leads to the decrease in the nucleation rate. On the other hand, crystal growth from the nuclei is enhanced when temperature increases because of enhanced diffusion rate of ions to the crystal surface. Therefore, in the synthesis of ZIF-71 at 35 °C, there is less nucleation and a higher crystal growth rate which leads to the larger crystals than those synthesized at lower temperatures.

Figure 3-4 (a)-(f) present SEM images of ZIF-71 synthesized at different temperatures. These images confirm that the particle diameter dramatically increases with increased synthesis temperature. The particle diameters visually observed in Figure 3-4 are consistent with the average diameters measured by DLS. Figure 3-4 (f) shows individual particles with largest particle diameters, confirming that the large particle sizes measured in the DLS are not the result of particle agglomeration.

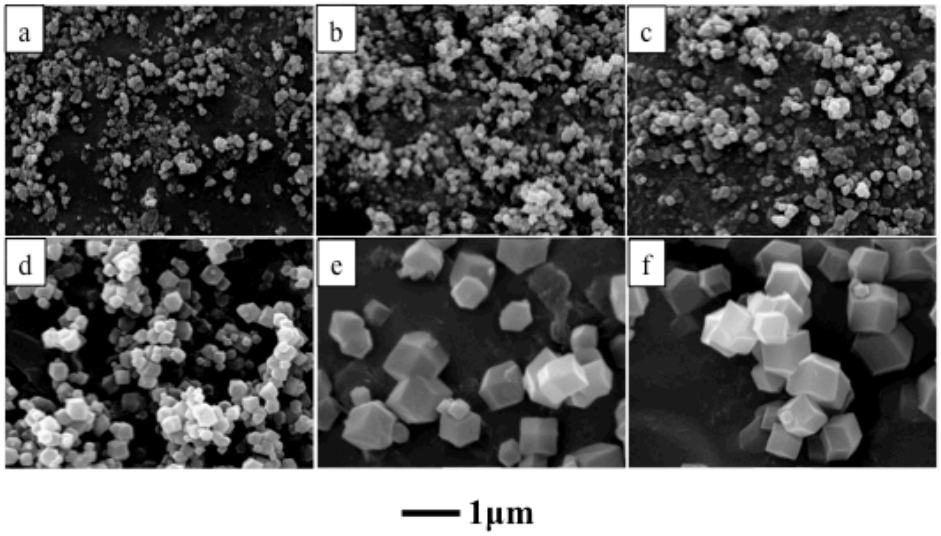

Figure 3-4. SEM of ZIF-71 particles made at (a) -20 ℃, (b) -10 ℃, (c) 0 ℃, (d) 15 ℃, (e) 25 ℃ and (f) 35 ℃.

3.7.2 Effect of dcIm/zinc ratio on ZIF-71 particle size

Figure 3-5 shows the representative XRD patterns for ZIF-71 produced with various molar ratios (from 1:1 to 7:1) of dcIm to $Zn(OAC)_2 \cdot 2H_2O$. All molar ratios (except 1:1) produced particles with the ZIF-71 crystal structure that matches the reference XRD patterns. The crystal structure of ZIF-71 is not retained in the 1:1 molar ratio sample. In this case, there is inadequate dcIm is present to produce the correct ZIF-71 crystal, because the molar ratio of imidazole to zinc in the ZIF-71 structure is 2:1. Similar results were observed with ZIF-8 synthesis. Cravillon et al. found that extra mIm is essential to synthesis ZIF-8 in methanol. They were able to acquire good results with a mIm/Zn molar ratio of 8.[119] Tanaka et al. did not obtain the sodalite structure in particles synthesized at a low mIm/Zn molar ratio of 4 in an aqueous system.[110] However, they were able to synthesize pure phase ZIF-8 when mIm/Zn ratio ranges from 40 to 100. Bao et al. also showed that ZIF-8 structure was not obtained until the mIm/Zn

molar ratio is above 5 in aqueous solution under microwave irradiation.[109] It is important to note, that the crystal growth mechanism is reported to be different in water versus organic solvents.

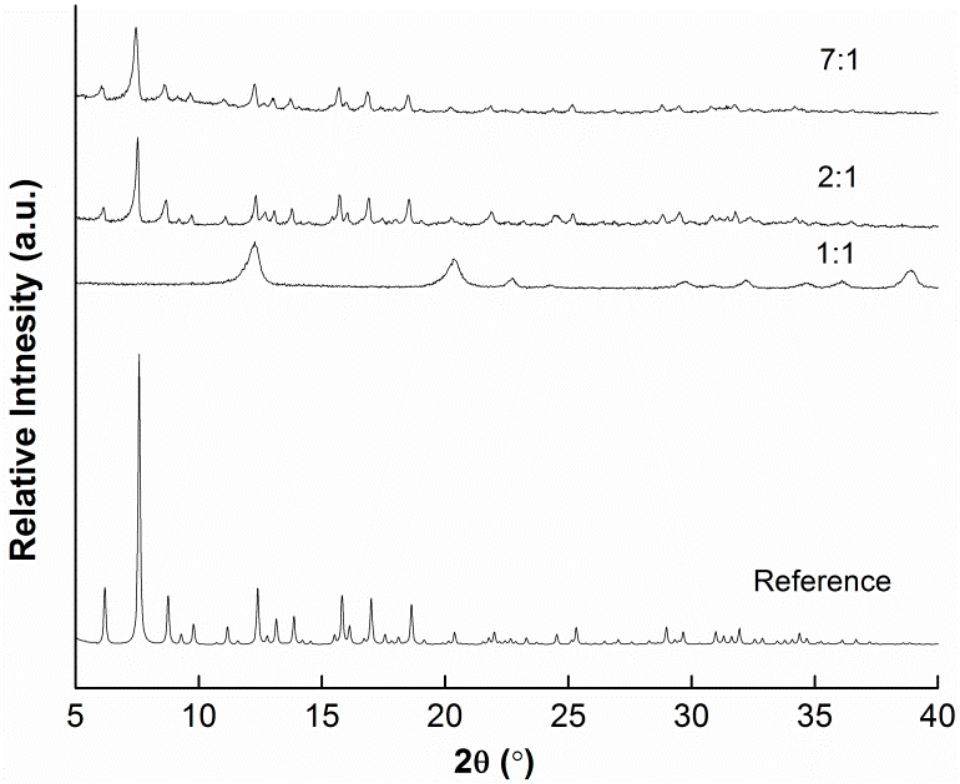

Figure 3-5. XRD pattern of ZIF-71 made at different reactant ratios.

Figure 3-6 presents the DLS results of ZIF-71 produced at different reactant molar ratios at room temperature. Small variations in the particle size distribution are evident. While changes in reactant molar ratios have proven to alter particle size significantly in ZIF-8, the particle diameter of ZIF-71 is only altered slightly by changing the reactant ratios.[109] Note that both references carried out the synthesis of ZIF-8 in aqueous solutions while here we reports methanol as solvent for ZIF-71 synthesis. We hypothesize, based on the 2:1 molar ratio of imidazole to zinc in the ZIF-71 structure,

that $Zn(OAC)_2 \cdot 2H_2O$ is the limiting reactant in the ZIF-71 formation process.[120] Increasing dcIm concentrations has no significant influence on the extent of reaction beyond a molar ratio of 2:1.

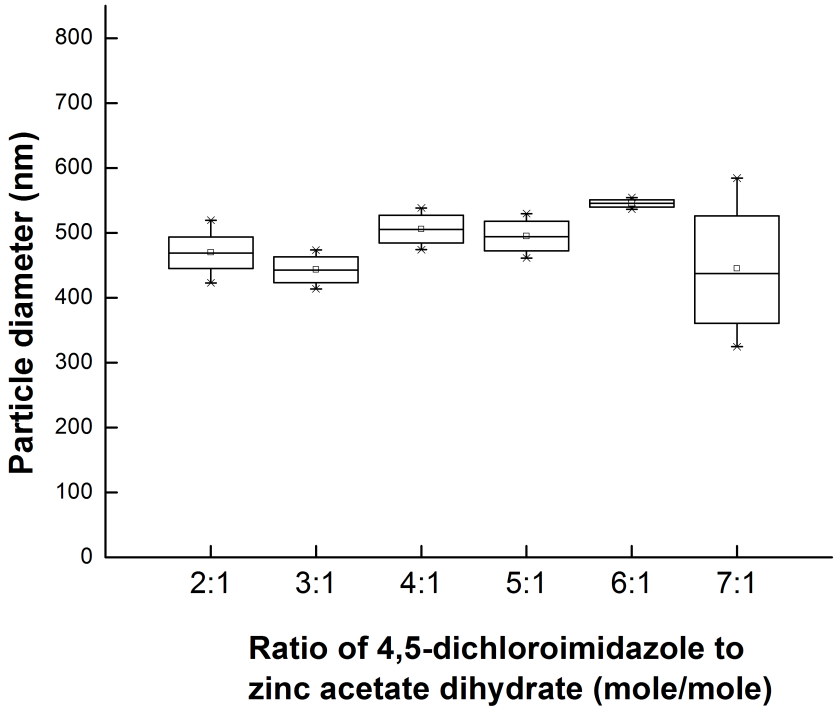

Figure 3-6. DLS results of ZIF-71 particles made at different reactant ratios.

3.7.3 Effect of synthesis time on ZIF-71 particle size

Figure 3-7 shows the particle size distribution measured with DLS for ZIF-71 produced by altering synthesis time from 0.5 to 4 hours at room temperature (25 °C). The average particle diameter is around 500 nm for samples synthesized for 1 hour or more. The particles synthesized at 0.5 and 1 hour have broader size distributions than those synthesized at longer times. We conclude that during the first one hour, the nucleation and growth occur simultaneously leads to formation of broad range of particle sizes.

After one hour, the medium of solute decreases significantly (or supersaturation depletes) and that may cease nucleation, therefore growth occurs and leads to formation of monodisperse particles.[121] We believe that the reaction is finished within two hours of beginning the synthesis and increasing synthesis time does not significantly influence the particle diameter.

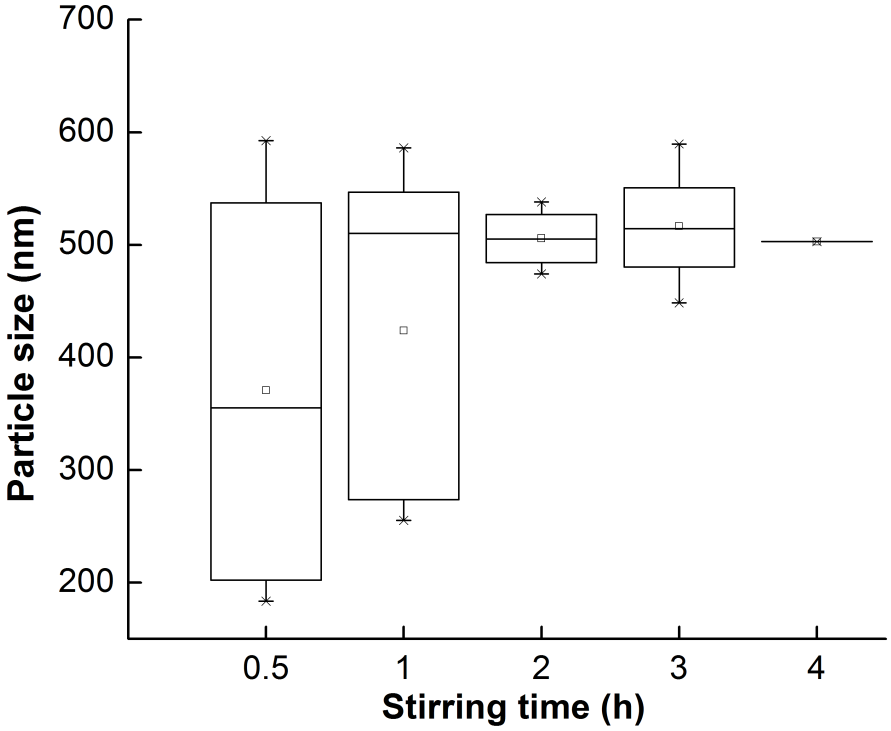

Figure 3-7. DLS results of ZIF-71 particles synthesized with different stirring time at dcIm/zinc ratio of 4:1 at room temperature.

3.7.4 Effect of ZIF-71 particle size on membrane performance

Figure 3-8 presents SEM images of the surface view of 25 wt% ZIF-71 loading MMMs made with three different particle sizes. From these SEM images, increased particle agglomeration was observed in membranes made with the smaller particle sizes (the 152 ± 45 nm diameter particles made at -20 ºC) than in the membranes made with

larger particles (the 506 ± 28 nm particles made at 25 ºC). In addition, the agglomeration size is much larger in MMMs made with -20 °C ZIF-71 particles than the membrane made with 25 °C ZIFs. The membrane made with 35 °C ZIF-71 particles has no obvious particle agglomeration and even dispersion of the particles in the polymer matrix was observed. While ZIF-71 is considered more "hydrophobic" than other ZIFs and MOFs, according to Lively et al. the ZIF-71 particle surfaces still have hydrophilic character from the –N-H group in the imidazole ligand.[97] The smaller ZIF-71 particles have a higher surface area to volume ratio than the larger particles. Therefore, because of this hydrophilic surface nature, the smaller ZIF-71 particles are thermodynamically driven to agglomerate when dispersed into the n-heptane based-casting solution. This effect is stronger for the smaller particles (~150 nm) than for the larger particles (~1000 nm) particles thus yielding less agglomeration of the larger particles in the final membranes.

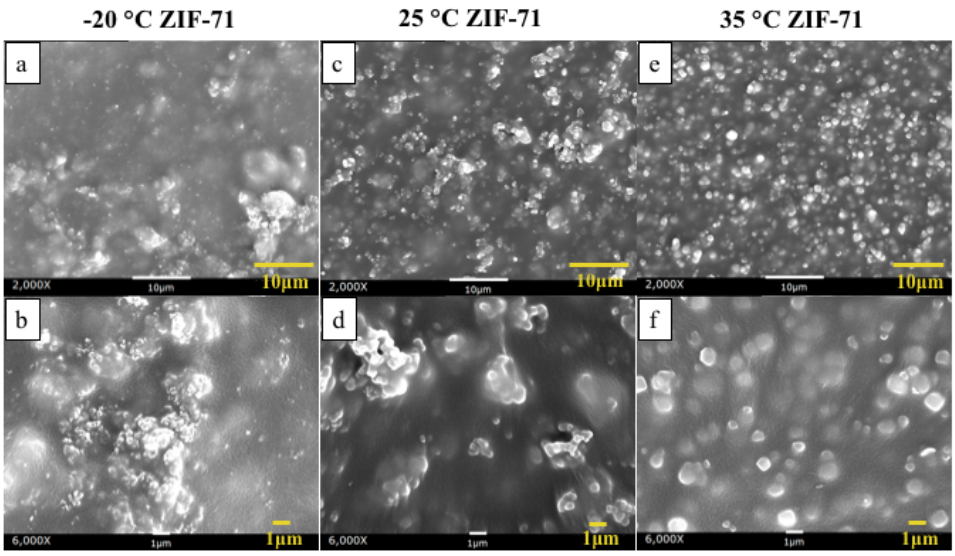

Figure 3-8. SEM image surface view of 25 wt% ZIF-71 loading PDMS MMMs. Membranes synthesized with ZIF-71 particles made at three temperatures: (a) and (b) were made at -20 °C, (c) and (d) were made at 25 °C, (e) and (f) were made at 35 °C.

Figure 3-9 and Figure 3-10 present the pervaporation performance results of the membranes for the separation of both ethanol/water and 1-butanol/water solutions. The calculated selectivity and permeability results are also listed in Table 3-2 and Table 3-3. The original flux and permeate concentration results are shown in Table 3-4. Compared with pure PDMS membranes, the incorporation of different size ZIF-71 particles significantly improved the permeability and selectivity for both ethanol/water and 1-butanol/water separations. For ethanol/water separation, both ethanol and water permeability increased with increasing ZIF-71 particle size. Compared with the MMMs made with -20 °C ZIF-71 particles, the ethanol permeability was doubled in the membranes synthesized with 35 °C particles. Meanwhile, the ethanol/water selectivity also increased from 0.67 ± 0.07 to 0.82 ± 0.10 with increasing particle sizes. In the case

of 1-butanol/water separation, the membranes made with the 25 °C and 35 °C ZIF-71 particles had higher 1-butanol and water permeability than the membranes made with -20 °C particles. Again, the 35 °C ZIF-71/PDMS membranes had the greatest 1-butanol/water selectivity 5.09 ± 0.94 over the other two.

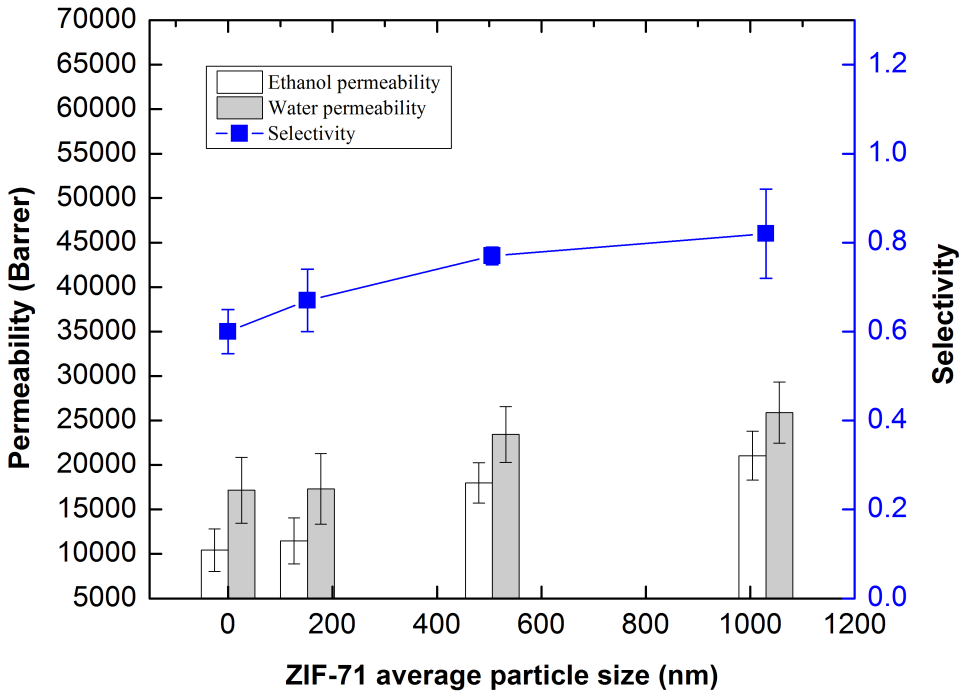

Figure 3-9. Ethanol/water pervaporation results of PDMS membranes with three different size ZIF-71 particles performed at 60 ºC with a 2 wt% ethanol/water feed mixture.

Table 3-2. Ethanol/water pervaporation results of ZIF-71/PDMS MMMs made with different particle sizes.

ZIF-71 particle size (nm)	Ethanol permeability (Barrer)	Water permeability (Barrer)	Ethanol/water selectivity
PDMS	10,428±2393	17,162±3708	0.60±0.05
152 ± 45	11,472±2600	17,305±3972	0.67±0.07
506 ± 28	17,992±2265	23,431±3139	0.77±0.02
1030 ± 385	21,042±2754	25,883±3443	0.82±0.10

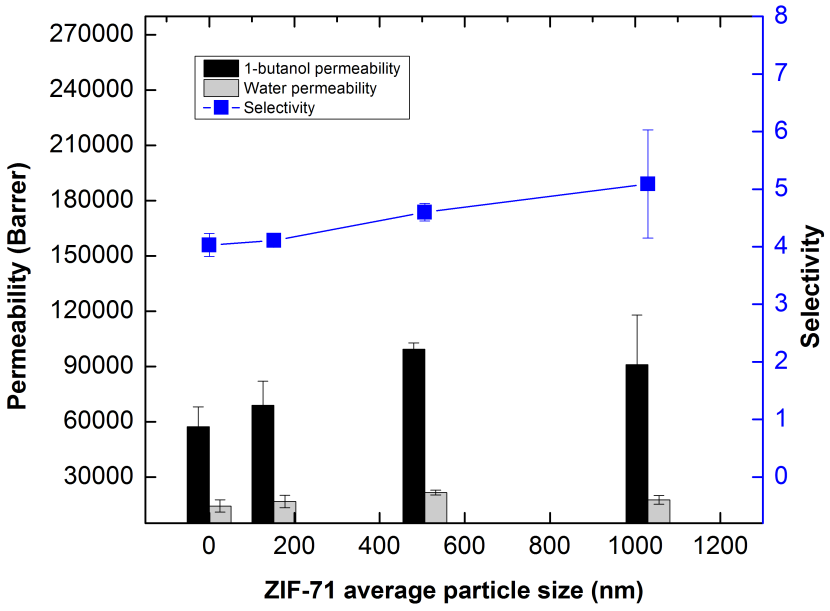

Figure 3-10. 1-Butanol/water pervaporation results of PDMS membranes made with three different size ZIF-71 particles tested at 60 ºC with a 2 wt% 1-butanol/water feed mixture.

Table 3-3. 1-Butanol/water pervaporation results of ZIF-71/PDMS MMMs made with different particle sizes.

ZIF-71 particle size (nm)	1-Butanol permeability (Barrer)	Water permeability (Barrer)	1-Butnaol/water selectivity
PDMS	57,347±10677	14,305±3275	4.03±0.20
152 ± 45	68,866±13207	16,761±3341	4.11±0.07
506 ± 28	99,359±3374	21,604±1292	4.60±0.15
1030 ± 385	90,966±27004	17,647±2337	5.09±0.94

Table 3-4. Thickness normalized flux and permeate concentration pervaporation results of ZIF-71/PDMS MMMs made with different particle sizes for 2 wt% 1-butanol/water separation at 60 ° C. All the flux results are normalized to 1 µm.

Alcohol	ZIF-71 particle size (nm)	Alcohol flux ($*10^3$ g m^{-2} h^{-1})	Water flux ($*10^3$ g m^{-2} h^{-1})	Permeate alcohol concentration (wt %)
Ethanol	PDMS	1.62±0.49	8.35±1.82	16.11±1.52
	152 ± 45	1.57±3.55	7.62±1.75	17.12±1.57
	506 ± 28	2.47±0.77	10.32±1.38	19.24±0.28
	1030 ± 385	2.47±0.75	9.63±2.48	20.25±1.79
1-Butanol	PDMS	6.07±1.28	6.14±1.41	50.47±1.21

	152 ± 45	7.47±1.43	7.20±1.44	50.96±0.42
	506 ± 28	10.78±3.66	9.28±055	53.77±0.79
	1030 ± 385	9.87±2.93	7.58±1.00	55.88±4.61

We hypothesize that the increase in permeability of membranes synthesized with larger ZIF-71 particles is the result of less tortuous pathways through the membrane that provides less transport resistance compared to membranes made with smaller particles. Similar to our results, Nordin et al. and Chi et al. also observed the increase in permeability of membranes made with larger ZIF-8 particles in gas separation.[114] The decrease in selectivity of membranes made with smaller ZIF-71 particles may be caused by particle agglomeration, which can be observed from the SEM images in Figure 3-8. Particle agglomeration may introduce defects, which can act as non-selective pathways through the membrane and decrease the membrane selectivity performance. Vane et al. observed the same behavior with zeolite/PDMS MMMs, they obtained lower ethanol/water separation with submicron size zeolites. They concluded that the agglomeration of the submicron size particles lowered the separation performance.[3]

Compare with other reported membranes, ZIF-71/PDMS MMMs synthesized in this work have good alcohol permeability and selectivity as is shown in

Membrane	T (ºC)	Feed solution	Alcohol permeability (Barrer)	Selectivity	Separation factor	Reference

ZIF-71/PEBA	40	1 wt% 1-butanol	~160,000	4.88	-	[69]
ZIF-8/PMPS	80	1 wt% 1-butanol	~18,300	-	~37.5	[78]
		1 wt% ethanol	~6,500	-	~11.5	
ZSM-5/PDMS	75	2 wt% ethanol	~21,350	~2.25	-	[33]
ZIF-71/PDMS	60	2 wt% 1-butanol	90,966	5.09	63.0	This work
		2 wt% ethanol	25,882	0.82	12.2	

. The 1-butanol/water selectivity measured in this work is higher than that of ZIF-71/PEBA and ZIF-8/PMPS membranes, and the 1-butanol permeability of the membranes in this work is in between ZIF-8/PMPS and ZIF-71/PEBA membranes. In terms of ethanol/water separation, ZIF-71/PDMS MMMs have higher ethanol permeability and selectivity than ZIF-8/PMPS membranes. The ethanol permeability is comparable with ZSM-5/PDMS membranes, while the selectivity measured with ZIF-71/PDMS MMMs is lower.[33] Overall, the ZIF-71/PDMS membranes reported here have comparable or better alcohol/water separation performances compared to other ZIF contained MMMs, except for ZSM-5/PDMS MMMs.

Table 3-5. Pervaporation performance compared with other published membrane performances.

Membrane	T (ºC)	Feed solution	Alcohol permeability (Barrer)	Selectivity	Separation factor	Reference
ZIF-71/PEBA	40	1 wt% 1-butanol	~160,000	4.88	-	[69]

ZIF-8/PMPS	80	1 wt% 1-butanol	~18,300	-	~37.5	[78]
		1 wt% ethanol	~6,500	-	~11.5	
ZSM-5/PDMS	75	2 wt% ethanol	~21,350	~2.25	-	[33]
ZIF-71/PDMS	60	2 wt% 1-butanol	90,966	5.09	63.0	This work
		2 wt% ethanol	25,882	0.82	12.2	

3.8 Conclusions

In the synthesis of ZIF-71, the molar ratio of dcIm to $Zn(OAC)_2 \cdot 2H_2O$, the synthesis time, and the synthesis temperature were altered. Synthesis temperature had significant influence on particle size – smaller particles at lower temperature and larger particles at higher temperature. An increase of only 10 ºC above room temperature results in an over 100% increase in the particle diameter of the ZIF-71 particles, as determined by DLS and SEM characterization. This small change in temperature required to alter particle size makes this MeOH-derived method more favorable than a DMF-based solvothermal method for synthesis of ZIF-71; because the DMF-based synthesis uses more expensive solvents, is more difficult to remove from the framework then MeOH, and has much greater heat requirements to achieve similarly sized ZIFs.[122] The ZIF-71 particle size did not change significantly with synthesis time; this is because the reaction appears to reach completion within two hours. Additionally, the change in reactant molar ratio has limited effect on particle diameter. ZIF-71 particles were still consistently produced at a molar ratio of 2:1. This is a lower molar ratio than that published by Lively et al. and may provide an opportunity to reduce synthesis costs (as the previously published synthesis procedure called for a molar ratio of 4:1).[97] By deriving a

correlation between the particle size and synthesis temperature, we eliminate the need for trial and error experimentation with alternative ligands, which is costly and difficult to predict.

We incorporated these ZIF-71 particles with different sizes into PDMS membranes for bio-alcohol separations through pervaporation and we found that ZIF-71 particle size had significant influence on ZIF-71/PDMS MMMs performances. We observed particle agglomeration in membranes made with nano-size ZIF-71 particles. However, the membranes made with micron-sized ZIF-71 particles had better particle dispersion in the polymer matrix and no particle aggregation was found. Membranes made with 500 nm and micron-sized ZIF-71 particles outperformed those made with 150 nm particles, and higher alcohol and water permeability as well as higher alcohol/water selectivity were observed.

4 EFFECT OF ZIF-71 LIGAND-EXCHANGE SURFACE MODIFICATION ON BIOFUEL RECOVERY THROUGH PERVAPORATION

4.1 Introduction

ZIFs are porous crystalline materials composed of tetrahedral transition metal ions (e.g. Zn, Co) bridged by imidazole organic linkers.[123, 124] ZIFs possess high surface area,[125] high porosity[126] and low density.[127] Due to these attractive properties, ZIFs are attractive in many applications such as carbon dioxide capture,[128] gas storage,[129] gas and liquid separations.[90, 130-132]

Among all ZIFs, ZIF-71 is one of the most studied materials for biofuel recovery through pervaporation separation.[69, 76, 77, 116] ZIF-71 has a RHO topology with an eight-membered-ring window size of 0.48 nm and a large cage size of 1.68 nm.[133] Owing to the hydrophobic nature of the framework, ZIF-71 demonstrated promising alcohol (e.g. 1-butanol) recovery ability from water solutions.[91] Additionally, enhanced alcohol recovery was achieved by incorporating ZIF-71 as filler materials to fabricate mixed matrix membranes (MMMs).[69, 76, 77, 116]

However, to compete with distillation separation, ZIF-71 with improved biofuel separation performances is needed. As mentioned in chapter 1, it has been reported that surface chemistry modification on ZIFs through SALE is an effective technique to enhance VOCs separation performance. By exchanging hydrophobic ligands into the ZIF material, the improved hydrophobicity facilitates the selective transport of VOCs (e.g. iso-butanol) over water.[87]

SALE is one of the most studied techniques to post modify surface chemistry of ZIFs.[87, 134] It is a useful technique to introduce new coordinative ligands or metal ions to functionalize pre-synthesized ZIFs without changing the framework crystallinity and topology. ZIFs that are not able to be synthesized directly from traditional synthesis methods can be formed through the SALE technique.[133] Liu et al. modified the surface of ZIF-8 with DMBIM via SALE reaction.[87] They successfully exchanged 9.1% (ligand exchange molar ratio) of DMBIM into ZIF-8 particles. After the introduction of the hydrophobic imidazole ligand DMBIM, the hydrothermal stability of ZIF-8 particles was improved significantly. The DMBIM modified ZIF-8 was stable in water at 80 °C for 24 hours, while the unmodified ZIF-8 had suffered complete hydrolysis. The improved hydrophobicity results from the hydrophobic property of DMBIM. The isobutanol diffusivity through the particles was also increased after the modification. Additionally, improved isobutanol recovery from water was observed when DMBIM-ZIF-8 was incorporated to PMPS membranes. Moreover, the iso-butanol/water selectivity was increased without reducing the isobutanol flux.

To the best of our knowledge, little has been done to study ligand exchange modification of ZIF-71 particles and their subsequent influence on the recovery of ethanol and 1-butanol from aqueous solutions. Our goal is to study the effect of ZIF-71 modification on ZIF alcohol (ethanol and 1-butanol) sorption capacity and ZIF/PDMS composite membrane alcohol/water separation abilities. The ZIF-71 modification was carried out by introducing new hydrophobic imidazole ligands through the SALE technique. In order to improve the hydrophobicity of ZIF-71 particles, four imidazole

ligands that are more hydrophobic than dcIm were chosen: BIM, MBIM, DMBIM and PI. The chemical structures of the ligands are listed in Figure 4-1. The hydrophobicity of these ligands based on the log D value is: BIM<MBIM<PI<DMBIM. The D value is the distribution coefficient, which is the ratio of the sum of the concentration of all forms of the compound in octanol to the concentration in water. So higher log D value indicates the compound is more hydrophobic. Both original and ligand-modified ZIF-71 particles were incorporated into PDMS polymer to form MMMs to determine their alcohol/water separation performances.

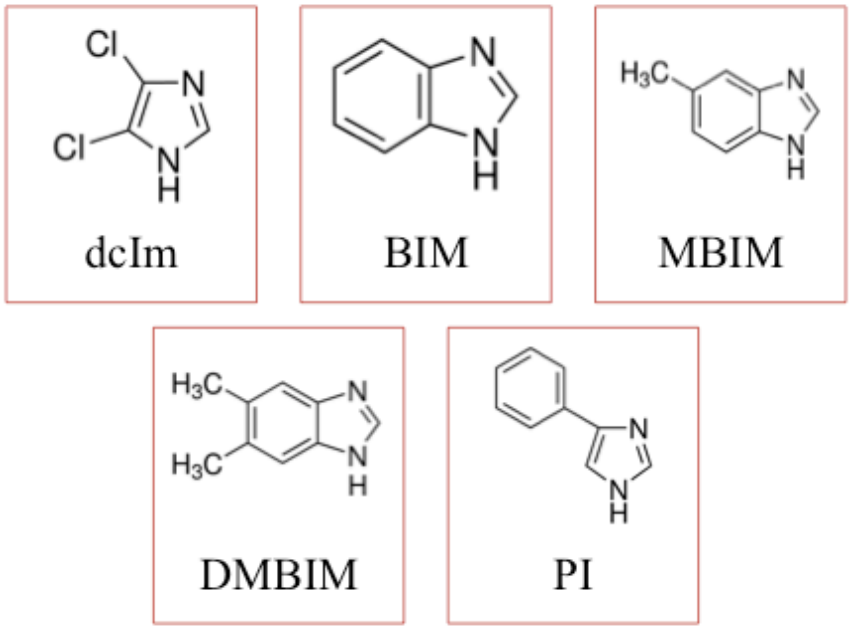

Figure 4-1. Chemical structure of dcIm and the imidazole ligands used for SALE experiments.

Table 4-1. The log D values of different ligands obtained from ChemAxon log D predictor.

Ligand	Log D pH=5	Log D pH=6	Log D pH=7	Log D pH=8
BIM	0.63	1.08	1.24	1.26
MBIM	0.99	1.42	1.71	1.77
PI	1.15	1.65	1.86	1.88
DMBIM	1.45	1.84	2.2	2.28

4.2 Materials

4,5-dichloroimidazole (dcIm) (>97%) was purchased from Tokyo Chemical Industry. Zinc acetate dihydrate ($Zn(OOCCH_3)_2 \cdot H_2O$) (ACS, 98.0-101.0%) was obtained from Alfa Aesar. Methanol (HPLC) was purchased from Honeywell. 5,6-Dimethylbenzimidazole (≥99%), 5-Methylbenzimidazole (98%), Benzimidazole (98%), 4-Phenylimidazole (97%), n-heptane (anhydrous, 99%) ethanol (ACS reagent, ≥99.5%), 1-butanol (anhydrous, 99.8%) and tetraethyl orthosilicate (TEOS, 99.999% trace metals basis) were provided by Sigma-Aldrich. Silanol terminated polydimethylsiloxane (DMS-S45, 110,000 g/mol), titanium 2-ethylhexoxide (AKT867) and di-n-butyldiacetoxytin tech-95 (SND3160) were obtained from Gelest Inc. Methanol-d_4 (D, 99.8%) and 35% (w/w) deuterium chloride (DCl, D, 99.5%) in D_2O solution were obtained from Cambridge Isotope Laboratories, Inc. All chemicals were used as received.

4.3 Synthesis of ZIF-71 particles

The room temperature ZIF-71 particles were prepared based on Lively et al's research.[97] Detailed synthesis procedures are described in chapter 2.

4.4 Ligand exchange experiments

We carried out ZIF-71 ligand exchange with four imidazole ligands: BIM, MBIM, PI and DMBIM. Methanol was used as solvent. A certain amount of ZIF-71 particles, the exchanging ligand and methanol was added to a glass container and then well sealed. The mixture was sonicated in a sonication bath for 10 minutes to make sure ZIF particles were well dispersed in methanol. The molar ratio of ZIF-71 to the new ligand equals to 1:0.75. The mass ratio of solvent methanol to ZIF-71 is 150:1.

The mixture was placed in an oven at 55 ºC for 72h to carry out the ligand exchange reaction. Followed by this, after cooling of the solution to room temperature, we centrifuged the mixture and washed the particle with methanol for three times. Afterwards, the ligand exchange particles were soaked in methanol for three days to remove any residual imidazole ligands. Fresh methanol was replaced every day. Finally, the particles were centrifuged and dried in an oven at 40 ºC overnight.

4.5 Sorption test with ethanol and 1-butanol

The alcohol (ethanol and 1-butanol) sorption test of ZIF materials was carried out to investigate the effect of SALE modification on ZIF alcohol absorption capacity.

Unmodified ZIF-71 (0.1g) is the control group. All the ligand-exchanged ZIF-71 samples were derived from 0.1 g original synthesized ZIF-71 particles. For ethanol/water sorption test, ZIF particles were soaked in 4 g of 0.5 wt% ethanol/water solution for 24

hours. For 1-butanol/water sorption experiment, ZIF samples were soaked in 4 g of 1 wt% 1-butanol/water solution for 24 hours. After the sorption test, the solutions were filtered with 0.2 μm syringe filter. Gas chromatography (GC) was applied to determine the alcohol composition of the solutions before and after the test. The amount of ethanol or 1-butanol absorbed is calculated from equation below:

$$q = \left(\frac{w_1 m_1 - w_2 m_2}{m} \right)$$

where q (g/g) is the amount of alcohol per unit mass of the ZIF-71 particles, w_1 is the weight fraction of the original alcohol solution, m_1 is the mass of the original solution, w_2 is the weight fraction of alcohol solution after sorption test, m_2 is the mass of the alcohol solution after sorption test, m is the mass of ZIF-71 materials used as adsorbent.

4.6 Membrane synthesis

Ligand modified ZIF-71 particles were incorporated into PDMS polymer to synthesis MMMs. The particle loading applied for all the membranes is 25 wt%. Detailed membrane synthesis procedures are described in chapter 2. The condensation cure PDMS system was used for all the membranes.

4.7 Characterization

XRD was carried out with powder X-ray diffractometer (Siemens D5000) to confirm the crystal structure of the ZIF-71 and modified ZIF-71 particles. The particle and membrane surface morphology were evaluated by SEM. Attenuated total reflectance Fourier transform infrared spectroscopy (ATR-FTIR, Nicolet 6700) was applied to determine if the new ligands were incorporated into ZIF-71 particles. Proton nuclear

magnetic resonance (^{1}H NMR, Varian MR400) was utilized to quantify the amount of new ligand exchanged into the ZIF-71 particles. To prepare ^{1}H NMR samples, the ZIF particles were dried at 75 °C under vacuum for 12 hours. Then about 0.01 g of particles were digested in 750 μL of methanol-d4 and 30 μL of 35% DCl in D_2O solution. The molar ratio of new ligand exchanged into the ZIF-71 particles equals to (M_{ligand} / (M_{ligand} + M_{dcIm})). Here, M_{ligand} and M_{dcIm} is the relative integration of the new ligand and dcIm obtained from ^{1}H NMR spectra. The Brunauer-Emmett-Teller (BET) surface areas, t-plot micropore volumes and pore size distributions were determined through the N_2 physisorption measurements (TriStar II 3020). The ZIF samples were activated at 100 °C for 12 hours in a vacuum oven before the measurement.

4.8 Pervaporation performances

Pervaporation tests were carried out to study the effect of ligand-exchange modification of ZIF-71 particles on alcohol (ethanol and 1-butanol)/water separation performance. The pervaporation tests were conducted in a batch setup with feed circulation rate of 1 mL/s. The feed was circulated close to the surface of the membrane to minimize concentration polarization. The effective surface area was 1.43 cm^2. We used 35g of 2 wt% ethanol/water or 1-butanol/water solution as feed. The feed solution was heated to 60 °C with a heating jacket. We allowed the system to run 1.5 hours to reach steady state before the permeate was collected. For each membrane, we collected the permeate for two hours with the assistance of liquid nitrogen. Then we analyzed the permeate composition via GC.

The selectivity and permeability was calculated to evaluate the membrane separation performance.

4.9 Results and Discussion

4.9.1 Characterizations of ligand exchange ZIF-71 particles

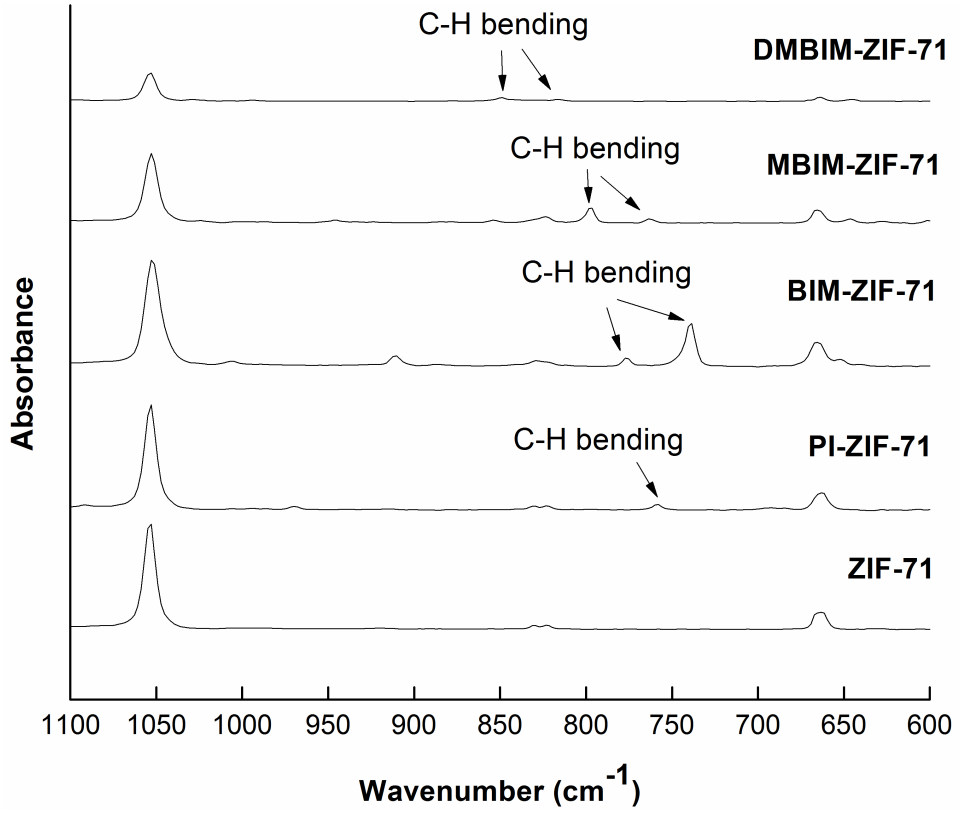

Figure 4-2. ATR-FTIR spectra of ZIF-71 and surface modified ZIF-71 materials.

The ATR-FTIR spectra confirmed the exchange of the new ligands into the ZIF-71 particles. As shown in Figure 4-2, some new peaks showed up in the range of 675-900 cm^{-1} for the SALE modified ZIF-71 samples compared to unmodified ZIF-71 sample. These peaks correspond to the out-of-plane C-H bending, which is the used to distinguish aromatic compounds. This indicates the successful incorporation of the new ligands into

the particles. Therefore we conclude that ZIF-71 particles were successfully modified with the four ligands applied here.

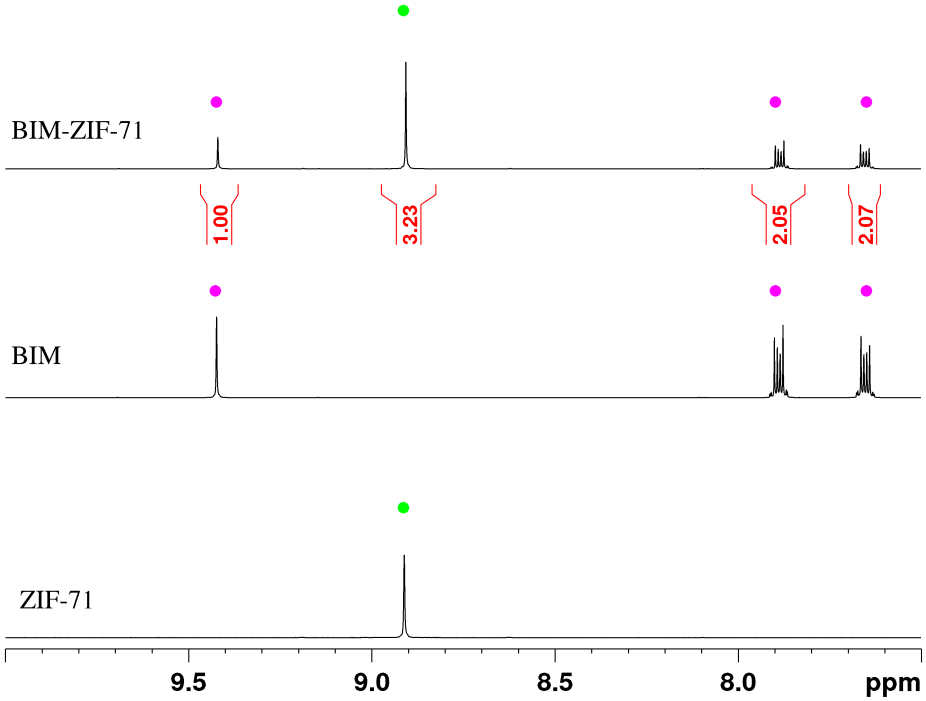

Figure 4-3. The ^{1}H NMR spectra of ZIF-71, benzimidazole and benzimidazole-ZIF-71. Green and red dots indicate BIM and dcIm, respectively.

In order to quantify the amount of ligand exchanged into ZIF-71 particles, ^{1}H NMR characterization was performed. Take benzimidazole modified ZIF-71 particles as an example, in Figure 4-3, the peaks labeled with green dots indicate BIM and the peak labeled with red dot indicates dcIm. The numbers under the peaks represent relative integration. Therefore, the BIM ligand exchange molar ratio is (1/(1+3.23)), equals to 23.64%. Same as BIM, the ligand exchange molar ratio of MBIM, DMBIM, PI was also calculated and the results are listed below in Table 4-2. Interestingly, the amount of PI exchanged into the ZIF material is significantly lower than the other three ligands. This is

probably owing to the steric effect of PI. If we look at the structure of BIM, MBIM and DMBIM, the imidazole ring and the phenyl ring are in the same plane. However, the phenyl ring in PI has free rotation around the carbon-carbon single bond, which makes it significantly bulkier than the other three ligands. As a result, the steric effect lowered the amount of PI exchanged into the ZIF material. Regarding the other three ligands, the amount exchanged is BIM < MBIM < DMBIM. The ligand exchange ratio of these three increased when the pK_a value increased based on Table 4-2. This might because ligands with higher pK_a values (more basic) yield stronger bonds with the zinc metal centers and are easier to be exchanged into the framework.[133]

Table 4-2. The ligand exchange molar ratio of surface modified ZIF-71 particles.

Ligand	Ligand exchange molar ratio (%)	pK_a
BIM	23.64	12.56
MBIM	25.82	13.15
DMBIM	27.68	13.46
PI	7.04	13.3

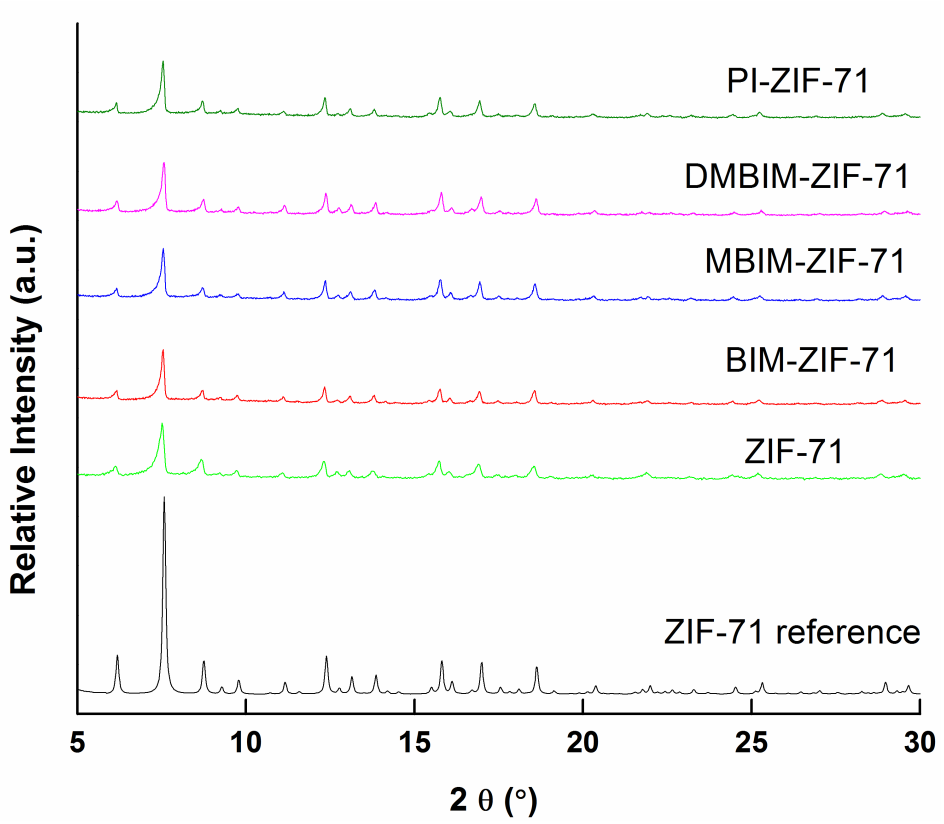

Figure 4-4. XRD patterns of un-modified ZIF-71 and surface modified ZIF-71 particles. The ZIF-71 reference is simulated reflection pattern obtained through Cambridge Crystallographic Data Center (CCDC).

To compare the crystal structure of ZIF-71 particles before and after the SALE treatment, XRD characterization was carried out. As shown in Figure 4-4, all the peaks of ZIF-71 after ligand exchange reaction seemed to be the same compared to unmodified ZIF-71 particles. No new peaks were observed. In order to further understand the crystal structure of the particles, unit cell parameter was calculated with HighScore Plus software based on the XRD patterns. The results are shown in Table 4-3. The modified ZIF-71 exhibited 0.08-0.42% smaller unit cell parameters compared to the original ZIF-71. The shrinkage of the framework after the modification is possibly caused by the

stronger Zn-ligand bond after the SLAE modification. The Zn-ligand bond length is smaller if the bond is stronger, which might attributes to smaller unit cell parameters.

Table 4-3. Unit cell parameters of the as-synthesized and modified ZIF-71 particles calculated with HighScore Plus software based on the XRD patterns.

Sample	Unit cell parameter (Å)	Change as respect to as synthesized particles (%)
ZIF-71	28.730	_
BIM-ZIF-71	28.706	-0.08
MBIM-ZIF-71	28.671	-0.21
DMBIM-ZIF-71	28.608	-0.42
PI-ZIF-71	28.684	-0.16

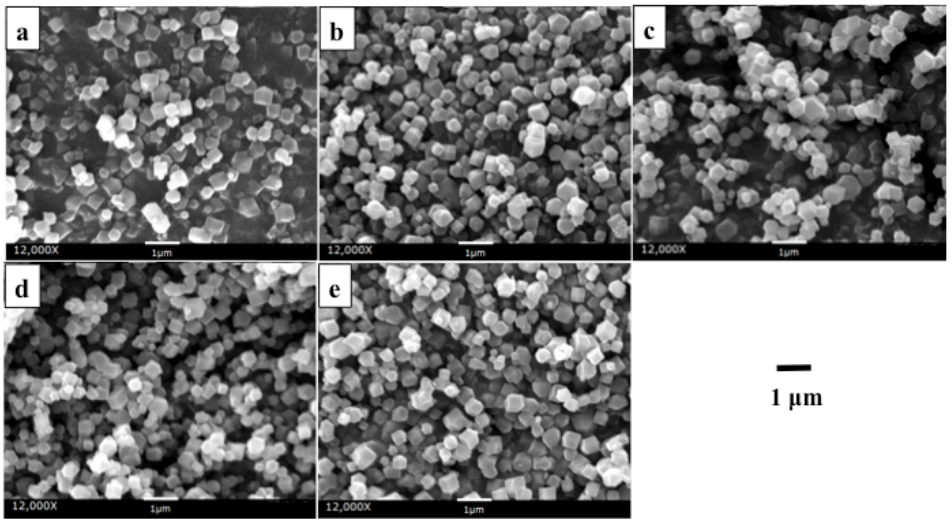

Figure 4-5. SEM images of un-modified (a) ZIF-71and modified ZIF-71 particles with (b) BIM, (c) MBIM, (d) DMBIM and (e) PI.

The morphology of the ZIF-71 particles before and after surface modification were evaluated with SEM imaging. The particle diameter of the as synthesized ZIF-71 is about 500 nm based on the SEM shown in Figure 4-5. It is obvious that the particle size

and morphology maintained after the SALE modification. No defects were observed on the particle surface. Similar results were observed by Liu et al. with the DMBIM surface modified ZIF-8 particles.[87]

The nitrogen adsorption isotherms of as-synthesized and modified ZIF-71 particles were measured at 77 K. The BET surface area, t-plot micropore volume and pore size distribution (DFT model) were then determined.

Typical I isotherm with no obvious hysteresis was observed with all the measurements shown in Figure 4-6 indicating the microporous structure of the as-synthesized and SALE modified ZIF-71 materials. The maximum quantity of N_2 absorbed was lowered after the ZIF-71 SALE modification in comparison to the as-synthesized ZIF-71. The amount of nitrogen absorbed was: ZIF-71 > BIM-ZIF-71 > PI-ZIF-71 > MBIM-ZIF-71 > DMBIM-ZIF-71. Both the BET surface area and micropore volume decreased after the SALE modification of ZIF-71 as is shown in Table 4-4. The decrease in BET surface area as well as micropore volume after SALE modification was likely owing to the weight gain from the new ligand as well as the shrinkage of the structure as shown earlier from the lattice parameters.

Table 4-4. BET surface area and micorpore volume of as-synthesized and modified ZIF-71 particles.

Sample	BET surface area (m^2/g)	t-plot micropore volume (cm^3 (STP)/g)
ZIF-71	996.4	0.332
BIM-ZIF-71	989.6	0.325

MIBIM-ZIF-71	928.9	0.303
DMBIM-ZIF-71	856.0	0.276
PI-ZIF-71	969.6	0.309

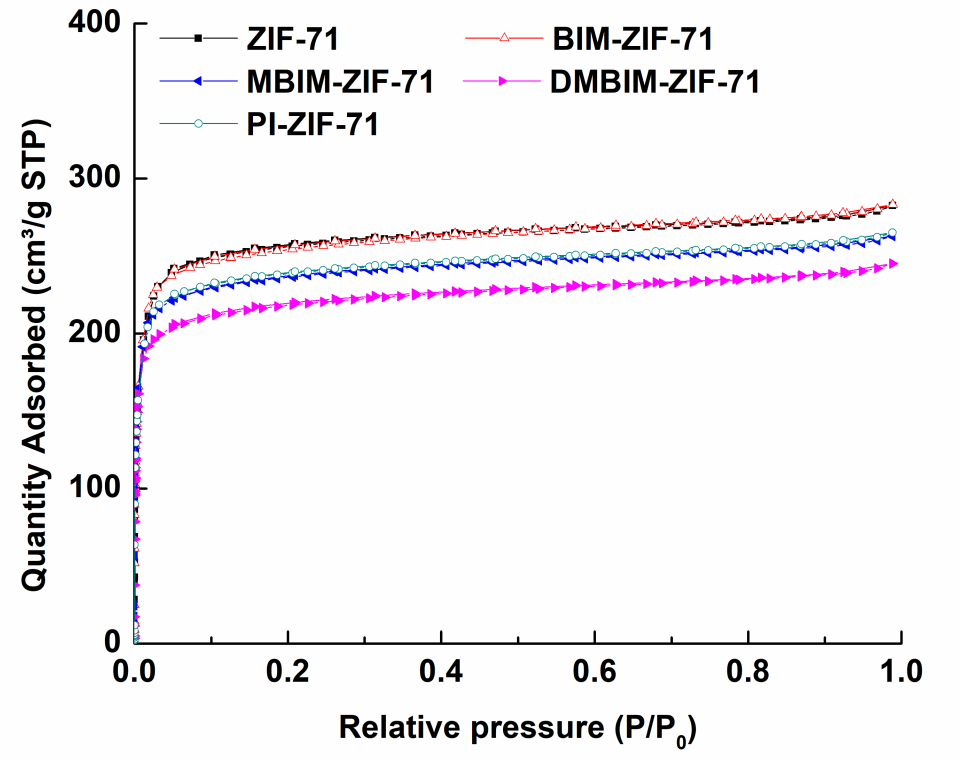

Figure 4-6. The N_2 adsorption isotherms (77K) of as-synthesized and modified ZIF-71 particles.

The DFT model was applied to determine the pore size distribution of these ZIF materials, and the results are shown in Figure 4-7. ZIF-71 showed major pore size distribution centered at ~13 Å. DMBIM-ZIF-71 demonstrated major pore size distribution centered at ~11.2 Å, which was significantly lower than original ZIF-71. ZIF-71 modified with the other three ligands overall showed slightly smaller main pore size as respect to original ZIF-71. The shift of the primary pore size to smaller values

after SALE modification of ZIF-71 indicates that the new ligands, BIM, MBIM, DMBIM and PI, had reduced the average pore size. This is reasonable since these four ligands have larger molecular size compared to dcIm.

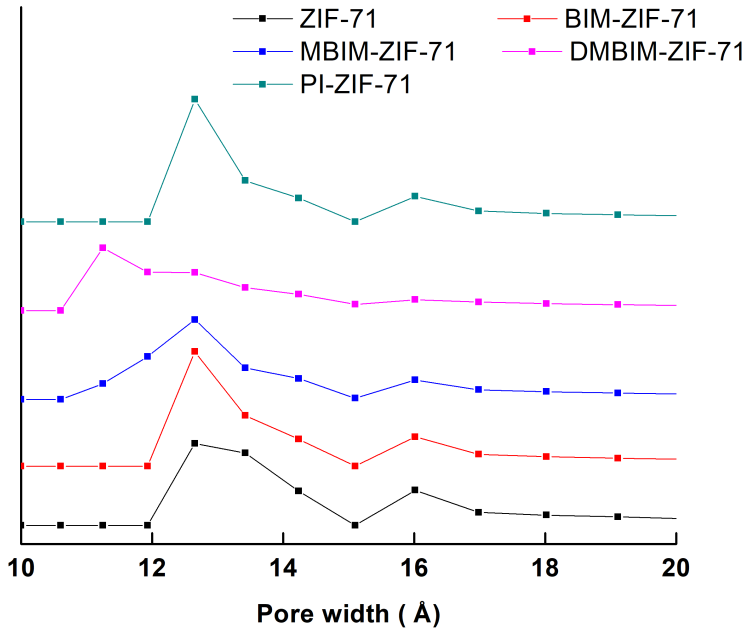

Figure 4-7. Pore size distribution based on the density functional theory (DFT) of as-synthesized and modified ZIF-71 particles.

4.9.2Alcohol sorption test with ZIF materials

The alcohol sorption capacity of different ligand modified ZIF-71 materials was measured. The alcohol/water concentration after the sorption test is shown below in Table 4-5 and Table 4-7. In order to determine the statistical significance of the mean concentration value of different ligand modified ZIFs, the independent student T test was applied to those results. The T test results are listed in Table 4-6 and Table 4-8. A student t-test is a statistical method that's used to determine if the means from two sets of data

differ significantly when the sample follows normal distribution. The significance level of 0.05 is often used as the threshold, so a p value below 0.05 indicates the mean values are statistically different.

As shown in Table 4-6, for ethanol sorption, all the p values calculated are below 0.05 besides the BIM-ZIF-71 and PI-ZIF-71 data set. This indicates that the ethanol adsorption amount is approximately equal for BIM and PI modified ZIF-71 particles, yet different compared to other ligand modified ZIF-71 materials. For 1-butanol sorption test, all the p values listed in Table 4-8 are less than 0.05, indicating the 1-butanol concentrations after the sorption test are statistically different.

Table 4-5. Ethanol/water concentration after the sorption test.

Sample	Ethanol concentration after sorption test (wt%)								Average (wt%)
ZIF-71	0.4910	0.4904	0.4919	0.4891	0.4869	0.4890	0.4918	0.4863	0.4897±0.0021
BIM-ZIF-71	0.4740	0.4710	0.4753	0.4731	0.4791	0.4745	0.4791	0.4802	0.4758±0.0033
MBIM-ZIF-71	0.4703	0.4650	0.4682	0.4683	0.4680	0.4662	0.4700	0.4700	0.4683±0.0019
PI-ZIF-71	0.4769	0.4756	0.4764	0.4767	0.4690	0.4773	0.4711	0.4783	0.4752±0.0002
DMBIM-ZIF-71	0.4661	0.4670	0.4654	0.4707	0.4656	0.4635	0.4654	0.4673	0.4664±0.0021

Table 4-6. Student T test ethanol/water sorption results.

Ethanol sorption	Sig. (1-tailed)
ZIF-71 BIM-ZIF-71	1.9E-07
BIM-ZIF-71 MBIM-ZIF-71	7.7E-05
MBIM-ZIF-71 PI-ZIF-71	0.00015
MBIM-ZIF-71 DMBIM-ZIF-71	0.041
PI-ZIF-71 BIM-ZIF-71	0.36

Table 4-7. 1-Butanol/water concentration after the sorption test.

Sample	1-Butanol concentration after sorption test (wt%)								Average (wt%)
ZIF-71	0.4936	0.4911	0.4964	0.4909	0.4899	0.4919	0.4929	0.4916	0.4923±0.0020
BIM-ZIF-71	0.5429	0.5437	0.5446	0.5449	0.5425	0.5436	0.5384	0.5428	0.5429±0.0002
MBIM-ZIF-71	0.5524	0.5573	0.5552	0.5417	0.5545	0.5561	0.5548	0.5535	0.5532±0.0049
PI-ZIF-71	0.5141	0.5180	0.5225	0.5201	0.5142	0.5190	0.5214	0.5224	0.5190±0.0034
DMBIM-ZIF-71	0.5858	0.5855	0.5830	0.5825	0.5838	0.5824	0.5835	0.5843	0.5839±0.0013

Table 4-8. Student T test 1-butanol/water sorption results.

1-Butanol sorption	Sig. (1-tailed)
ZIF-71 BIM-ZIF-71	1.7E-17
BIM-ZIF-71 MBIM-ZIF-71	0.00017
ZIF-71 PI-ZIF-71	2.1E-10
MBIM-ZIF-71 DMBIM-ZIF-71	7.0E-08

The amount of ethanol and 1-butanol absorbed per unit mass of ZIF materials were calculated based the equation introduced earlier in this chapter. The results are shown below in both Figure 4-8 and Table 4-9.

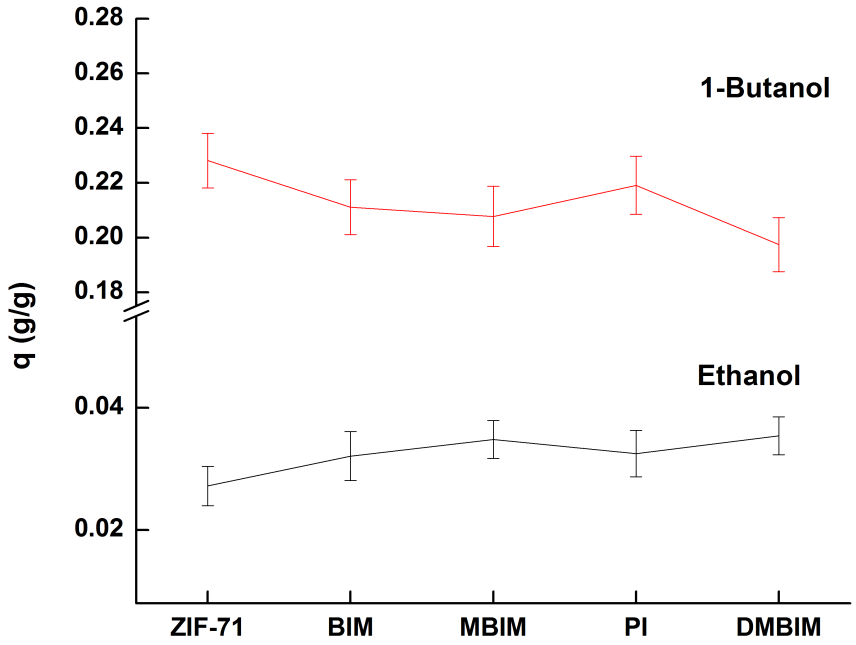

Figure 4-8. Ethanol and 1-butanol sorption test results of unmodified and ligand modified ZIF-71 materials.

Table 4-9. The amount of ethanol or 1-butanol absorbed with different ZIF materials.

Sample	ZIF-71	BIM-ZIF-71	PI-ZIF-71	MBIM-ZIF-71	DMBIM-ZIF-71
q (ethanol)	0.0272±0.0032	0.0321±0.0040	0.0325±0.0038	0.0348±0.0031	0.0354±0.0031
q (1-butanol)	0.2281±0.0100	0.2111±0.0100	0.2191±0.01058	0.2077±0.0110	0.1974±0.0099

For ethanol sorption test, the amount of ethanol absorbed into ZIF materials was: DMBIM-ZIF-71 > MBIM-ZIF-71 > PI-ZIF-71 ≈ BIM-ZIF-71 > ZIF-71. This indicates enhanced hydrophobicity of ligand modified ZIFs by the introduction of hydrophobic new ligands. The ZIFs modified with the most hydrophobic PI-ZIF-71 and BIM-ZIF-71 have similar ethanol sorption capacity based on the statistical significance study earlier. The ZIF-71 materials modified with the most hydrophobic ligand DMBIM showed the highest ethanol sorption capacity.

However, different results were obtained for 1-butanol adsorption test. Surprisingly, the equilibrium adsorption amount of 1-butanol of the modified ZIFs was less compared to the original ones. This observation is in good agreement with the literature. Liu et al. also showed that after the SALE modification of ZIF-8 with DMBIM ligand, the equilibrium adsorption capacity of isobutanol decreased.[87] The reason is probably that ZIF-71 pore size decreased after the ligand modification. Smaller pore size hinders the absorption of 1-butanol molecule into ZIF material, hence less 1-butanol was absorbed into the material. Furthermore, as is shown earlier DMBIM-ZIF-71 showed the smallest pore size, here DMBIM-ZIF-71 showed the least 1-butanol absorption. We didn't observe this problem with ethanol absorption, probably due to the fact that ethanol has a smaller kinetic diameter of 4.5 Å than 1-butanol 5.0 Å.[135]

4.9.3 Characterization of original and modified ZIF-71/PDMS MMMs with SEM imaging

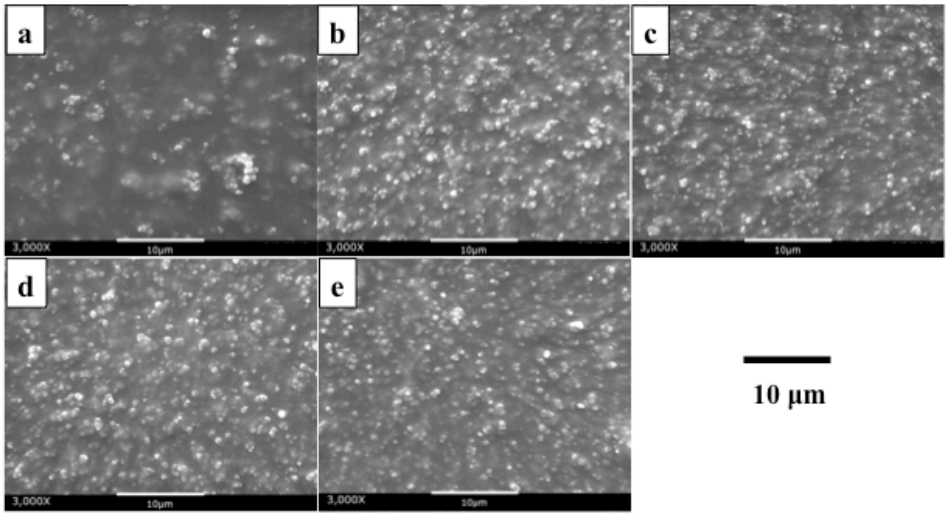

Figure 4-9. SEM images of PDMS MMMs made with (a) unmodified ZIF-71 particles and modified ZIF-71 particles with (b) BIM, (c) MBIM, (d) DMBIM and (e) PI.

SEM imaging were used to characterize the surface morphology of ZIF/PDMS MMMs. Compared to un-modified ZIF-71/PDMS MMMs, the surface modified ZIF-71/PDMS MMMs showed better particle dispersion in the polymer matrix. Some particle agglomerations were evident in the unmodified ZIF-71 membranes, while membranes made with modified ZIF-71 particles exhibit even particle distribution in the polymer matrix. This might be a result of improved particle surface hydrophobicity, which enhanced the compatibility between ZIF-71 and PDMS polymer matrix.[136]

4.9.4 Pervaporation results of ZIF/PDMS MMMs for the removal of 1-butanol and ethanol from water solutions

To study the effect of ZIF-71 SALE surface modification on ethanol and 1-butanol recovery from water, both modified and unmodified ZIF particles were

incorporated into PDMS polymer to form MMMs. The particle loading used for all the membranes is 25 wt%. The separation of both ethanol and 1-butanol from water were tested with the membranes through pervaporation.

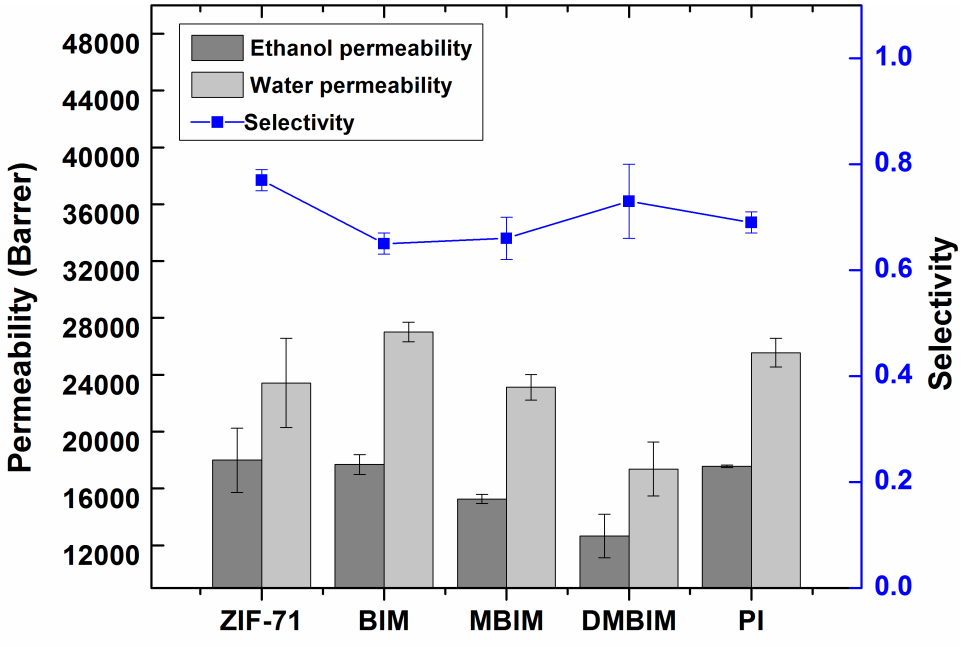

Figure 4-10. The effect of SALE modification of ZIF-71 particles on ethanol/water separation permeability and selectivity through pervaporation at 60 ℃ with 2 wt% ethanol/water feed solution.

Beyond our expectation, the surface modification did not improve the ethanol/water separations as shown in Figure 4-10. The ethanol permeability was declined with all the surface modified ZIF-71/PDMS MMMs. Interestingly, the permeability of ethanol decreased successively when ZIF-71 is modified with BIM, MBIM and DMBIM. In pervaporation, permeability $P_i = D_i \bullet K_i$, where D_i (cm^2/s) represents diffusion coefficient of component i and K_i (cm^3(STP)/cm^3 cmHg) represents sorption coefficient of component i. Our hypothesis is that the ethanol diffusion

coefficient was lowered as the ZIF-71 pore windows after SALE reaction are narrowed compared to unmodified ZIF-71, since the ligands applied to SALE modification of ZIF-71 are larger than the original dcIm ligand. Although the ethanol sorption coefficient is benefited from the hydrophobicity of the new ligands, the decrease in ethanol diffusion coefficient is more evident which results in decreased ethanol permeability. Same trend was also observed for water permeability with BIM, MBIM and DMBIM modified ZIF-71 particles. As to PI modified ZIF-71, the ethanol permeability is lower while the water permeability was similar compared to original ZIF-71/PDMS MMMs.

The ethanol/water selectivity shown in Figure 4-10 was also lowered by the presence of new ligands compared to unmodified ZIF-71/PDMS MMMs. Interestingly, if compare the selectivity of membranes made with BIM, MBIM and DMBIM modified ZIF-71 particles, the opposite trend appeared compared to ethanol or water permeability. The ethanol/water selectivity increased successively with BIM, MBIM and DMBIM modified ZIF membranes. The equation of membrane selectivity is $\alpha = (\frac{D_i}{D_j})(\frac{K_i}{K_j})$, where $\frac{D_i}{D_j}$ is the mobility selectivity and $\frac{K_i}{K_j}$ is the solubility selectivity of components i and j. Since the kinetic diameter of water (0.268 nm) is smaller than ethanol (0.45 nm), the blocking effect of new ligand on water mobility is less compared to ethanol. As a result, the mobility selectivity of ethanol to water is suppressed. The solubility selectivity, however, is enhanced by cause of hydrophobicity of these three ligands. The constant increase of ethanol/water selectivity in BIM, MBIM and DMBIM modified ZIF-71 MMMs is associated with the increasing hydrophobicity of the three ligands.

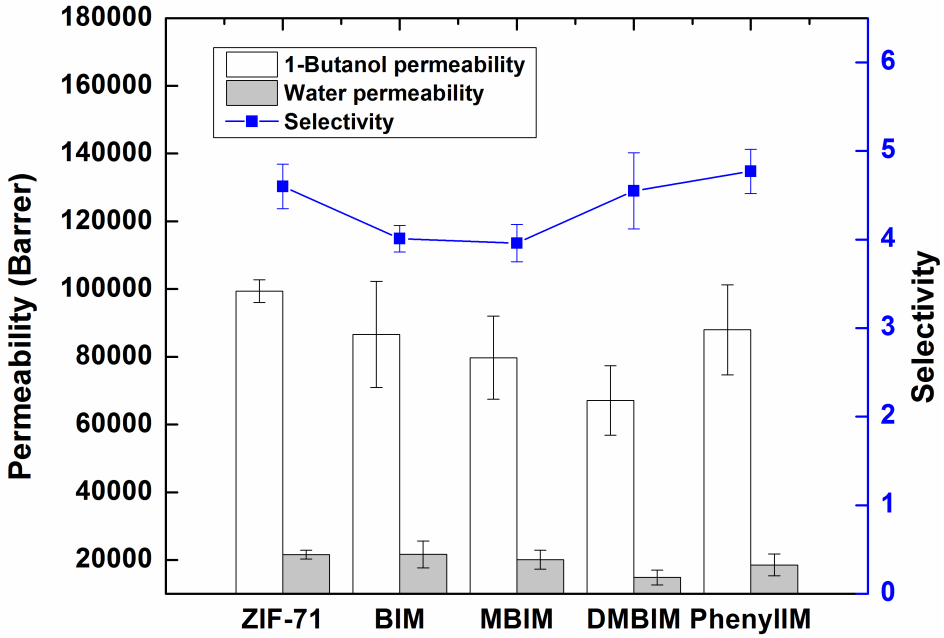

Figure 4-11. The effect of SALE modification of ZIF-71 particles on 1-butanol/water separation permeability and selectivity through pervaporation at 60 ℃ with 2 wt% 1-butanol/water feed solution.

Similar to ethanol/water separation, no enhancement in 1-butanol/water separation was seen with modified ZIF-71/PDMS MMMs as is shown in Figure 4-11. Same as ethanol/water separation, both 1-butanol and water permeability were decreased successively with BIM, MBIM and DMBIM modified ZIF MMMs. The 1-butanol/water selectivity follows the opposite trend compared to permeability, which increased successively with BIM, MBIM and DMBIM modified MMMs. As to PI modified MMMs, both 1-butanol and water permeability were slightly lower than unmodified ZIF MMMs. No obvious change in 1-butanol/water selectivity was observed when PI modified ZIF MMMs is compared to unmodified membranes. The decrease in 1-butanol

and water permeability is possibly caused by the decrease in pore size after the ligand exchange modification.

4.10 Conclusions

We attempted to modify ZIF-71 particles with four different ligands: BIM, MBIM, DMBIM and PI through SALE reaction. The ligand exchange molar ratio was 23.66%, 25.82%, 27.68% and 7.04% for BIM, MBIM, DMBIM and PI, respectively. The unite cell parameters decreased after the modification. Based on the SEM characterization of the ligand exchanged ZIF materials, the surface morphology maintained. The BET surface area and micropore volume were also lowered with the modified ZIF materials compared to pure ZIF-71 based on the N_2 adsorption test. Different ligand modified ZIF-71 materials were mixed with PDMS polymer as MMMs (25 wt% particle loading) to separate ethanol and 1-butanol from water via pervaporation. Compared to unmodified ZIF-71/PDMS MMMs, the surface modification on ZIF-71 particles did not improve the alcohol recovery from water. Reduced ethanol and 1-butanol permeability were obtained from all the ligand modified ZIF/PDMS membranes. Meanwhile, the ethanol/water as well as 1-butanol/water selectivity were lower than unmodified membranes. The ZIF-71 pore size is narrowed from the new ligand exchanged into the crystal structure, as the new ligands are larger in size than the original ligand dcIm. As a result, the alcohol diffusion through ZIFs are slowed down which causes the decrease in permeability. The membranes modified with BIM, MBIM and DMBIM demonstrated a constant decrease in alcohol and water permeability, while constant increase in alcohol/water selectivity.

5 SUMMARY AND RECOMMENDATIONS

5.1 Summary

This dissertation presented the synthesis, modification and characterization of free-standing ZIF-71/PDMS MMMs for recovering ethanol and 1-butanol from water solutions through pervaporation. The effect of various synthesis parameters on membrane performance were studied systematically. These parameters include: different PDMS systems, ZIF-71 loading, ZIF-71 particle size and ZIF-71 ligand modification. The membranes we synthesized demonstrated better alcohol separation performances compared to other reported ZIF-71/PDMS MMMs.

The first objective of this research is to study the compatibility between ZIF-71 and PDMS polymer, and the effect of ZIF-71 loading on membrane performances. For the first time, the compatibility between ZIF-71 and two PDMS systems were explored. As is shown in chapter 2, addition cure PDMS system was not compatible with ZIF-71, for the Pt based catalyst was poisoned by the imidazole ligand existed in ZIF-71. The addition cure PDMS polymer did not cure properly when ZIF-71 was present. On the contrary, the condensation cure PDMS system was compatible with ZIF-71 particles. Condensation cure PDMS system utilizes tin-based catalysts and no curing issue was observed in our research. As a result, we concluded condensation cure PDMS system is applicable in this research for the synthesis of ZIF-71/PDMS MMMs.

ZIF-71 hydrothermal stability test was carried out in chapter 2. ZIF-71 particles were soaked in water for seven days at both room temperature and 60 °C, since the membranes were tested at 60 °C with dilute alcohol/water solutions as feed. Retained

crystallinity and morphology were observed from XRD and SEM results. The ZIF-71 particle size was also maintained confirmed by the DLS results. Therefore ZIF-71 is stable under the testing conditions applied in this research.

The effect of ZIF-71 loading on membrane separation performance was also studied in chapter 2. In this chapter, MMMs with three ZIF-71 loadings were made: 5, 25 and 40 wt%. Improved alcohol permeabilities as well as alcohol/water selectivities were demonstrated when ZIF-71 was added. The highest selectivities achieved were 0.81 ± 0.04 for ethanol/water separation and 5.64 ± 0.15 for 1-butanol/water separation with the 40 wt% ZIF-71 loading MMMs. Increased stiffness and reduced ductility of the MMMs was observed with the incorporation of ZIF-71 particles based on the tensile testing results.

The second objective, which is to study the effect of particle size on membrane separation performance, was addressed in chapter 3. Firstly ZIF-71 particles of various sizes ranging from 150 nm to 1 μm were synthesized through varying synthesis temperatures from -20 to 35 °C. Temperature was found to have significant influence on ZIF-71 particle size, higher synthesis temperature produces larger size particles. Synthesis time and reactant ratio had little effect on ZIF-71 particle size. Three different size ZIF-71 particles were incorporated into condensation cure PDMS system: 152 ± 45 nm, 506 ± 28 nm and 1030 ± 385 nm. Particle agglomeration was observed with membranes made with 152 nm and 506 nm ZIF-71 particles. Membranes made with 1030 nm ZIF-71 particles had uniform particle distribution in the polymer matrix and no particle agglomeration was observed. All the 25 wt% ZIF-71 loading membranes have

enhanced alcohol separation performances compared to pure PDMS membranes. Both the alcohol permeability and alcohol selectivity increased with increasing particle size. The increase in alcohol and water permeabilities observed with larger ZIF-71 particles might because of less transport resistance through the membranes. Membranes made with smaller particles provide more tortuous pathways and more transport resistance, and thus lower alcohol and water permeabilities. The decrease in alcohol selectivity with nano-size ZIF-71/PDMS membranes might due to the particle agglomeration.

SALE modification is an effective post-synthetic technique to control the surface chemistry of ZIF materials. Chapter 4 addresses objective 3 to study the effect of ligand exchange effect on membranes separation performances. ZIF-71 particles were modified successfully by BIM, MBIM, DIBIM and PI ligands through SALE reaction for the first time. Improved hydrophobicity of modified ZIF-71 materials was confirmed through the ethanol/water sorption test results. The amount of ethanol absorbed into the ZIF material was enhanced continuously with increasing hydrophobicity of the exchanged ligands. The amount of 1-butanol absorbed, however, was lower than the un-modified ZIFs. Possible reason is that the new ligand exchanged into the ZIF material is larger than the original dcIm and the pore size was lowered. This pore narrowing effect prevented the absorption of 1-butanol into the pores and decreased the absorption ability.

The effect of ligand exchange modification of ZIF-71 materials on membrane separation performance was also studied in chapter 4. No membrane separation improvement was found with the ligand modified ZIF-71/PDMS MMMs. The alcohol or water permeability was lowered for both ethanol/water and 1-butanol/water separation

compared to un-modified ZIF membranes. Also the alcohol/water selectivity decreased compared to the unmodified membranes. Our hypothesis is that although the hydrophobicity of ZIF-71 was enhanced through the modification, the diffusion of different components was affected. Since water (kinetic diameter of 0.268 nm) is much smaller than both ethanol (kinetic diameter of 0.45 nm) and 1-butanol (kinetic diameter of 0.5 nm), the diffusion of alcohols was lowered more significantly than water. So, the alcohol/water diffusion selectivity decreased after the ligand exchange modification. As a result, the alcohol selectivity was lowered.

5.2 Recommendations

5.2.1 Synthesis of ZIF-71/PDMS MMMs with ZIF-71 loadings higher than 40 wt%

Our work presented in chapter 2 has shown that the alcohol separation performance was enhanced with increasing ZIF-71 loading. The highest ZIF-71 loading carried out in this research was 40 wt%. According to the literature, Vane et al. has reported 65 wt% zeolite loading PDMS membranes with ethanol/water selectivity of 3.[3] In order to further improve the membrane separation performances, we believe membranes with higher ZIF loadings are worth to try. ZIF-71 loadings such as 60 wt% and 70 wt% are recommended.

5.2.2 Study the effect of concentration polarization on the membrane performances

In this research all the pervaporation tests carried out utilized a feed circulation line (circulation rate 1mL/s) to reduce concentration polarization near the membrane surface. We noticed that when the feed was not circulated, the flux was significantly lowered. In order to obtain the best alcohol/water separation, it could be useful to study

the effect of concentration polarization on the membrane separation performances. Different feed circulation rates are suggested to apply to the pervaporation experiments to determine the optimum feed circulation rate.

5.2.3 Further study into the transport diffusivity of alcohols with the surface modified ZIF-71 materials

The influence of ZIF-71 surface modification with hydrophobic ligands through SALE technique has been studied in this research. In our work we proposed that the diffusion of alcohols are lowered due to the size of the new ligands larger than the original dcIm in our discussion. Further experiments are needed to calculate the exact transport diffusivity of ethanol and 1-butanol through the modified ZIF-71 materials. Also combine the alcohol transport diffusivity study with the adsorption study, one can predict the pervaporation separation performances easier than testing the membranes.

REFERENCES

[1] A. Singh, S.I. Olsen, P.S. Nigam, A viable technology to generate third-generation biofuel, Journal of Chemical Technology & Biotechnology 86 (2011) 1349-1353.

[2] J. Singh, S. Cu, Commercialization potential of microalgae for biofuels production, Renewable & Sustainable Energy Reviews 14 (2010) 2596-2610.

[3] L.M. Vane, V.V. Namboodiri, T.C. Bowen, Hydrophobic zeolite–silicone rubber mixed matrix membranes for ethanol–water separation: Effect of zeolite and silicone component selection on pervaporation performance, Journal of Membrane Science 308 (2008) 230-241.

[4] U.S.G.A. Office, Biofuels: Challenges to the Transportation, Sale, and Use of Intermediate Ethanol Blends, in: G.A. Office (Ed.), 2011.

[5] S.J. Birrell, D.L. Karlen, A. Wirt, Development of Sustainable Corn Stover Harvest Strategies for Cellulosic Ethanol Production, BioEnergy Research 7 (2014) 509-516.

[6] A. Demirbas, Biofuels sources, biofuel policy, biofuel economy and global biofuel projections, Energy Conversion and Management 49 (2008) 2106-2116.

[7] J.S. Rowbotham, H.C. Greenwell, M. Adcock, The future of alcohol-based biofuels: will we see the death of ethanol and birth of butanol?, Biofuels 5 (2014) 365-368.

[8] X. Yan, D.K.Y. Tan, O.R. Inderwildi, J.A.C. Smith, D.A. King, Life cycle energy and greenhouse gas analysis for agave-derived bioethanol, Energy & Environmental Science 4 (2011) 3110-3121.

[9] H.I. Velásquez-Arredondo, S. De Oliveira Junior, P. Benjumea, Exergy efficiency analysis of chemical and biochemical stages involved in liquid biofuels production processes, Energy 41 (2012) 138-145.

[10] Q. Kang, B. Van der Bruggen, R. Dewil, J. Baeyens, T. Tan, Hybrid operation of the bio-ethanol fermentation, Separation and Purification Technology 149 (2015) 322-330.

[11] E. Gnansounou, A. Dauriat, Technoeconomic Analysis of Lignocellulosic Ethanol, Biofuels, Academic Press, Amsterdam, 2011, pp. 123-148.

[12] Y. Huang, R.W. Baker, L.M. Vane, Low-Energy Distillation-Membrane Separation Process, Industrial & Engineering Chemistry Research 49 (2010) 3760-3768.

[13] R.D. Offeman, C.N. Ludvik, Poisoning of mixed matrix membranes by fermentation components in pervaporation of ethanol, Journal of Membrane Science 367 (2011) 288-295.

[14] X. Feng, R.Y.M. Huang, Liquid Separation by Membrane Pervaporation: A Review, Industrial & Engineering Chemistry Research 36 (1997) 1048-1066.

[15] L.M. Vane, A review of pervaporation for product recovery from biomass fermentation processes, Journal of Chemical Technology & Biotechnology 80 (2005) 603-629.

[16] P. Shao, R.Y.M. Huang, Polymeric membrane pervaporation, Journal of Membrane Science 287 (2007) 162-179.

[17] P. Garg, R.P. Singh, V. Choudhary, Pervaporation separation of organic azeotrope using poly(dimethyl siloxane)/clay nanocomposite membranes, Separation and Purification Technology 80 (2011) 435-444.

[18] B. Smitha, D. Suhanya, S. Sridhar, M. Ramakrishna, Separation of organic–organic mixtures by pervaporation—a review, Journal of Membrane Science 241 (2004) 1-21.

[19] W. Kujawski, J. Kujawa, E. Wierzbowska, S. Cerneaux, M. Bryjak, J. Kujawski, Influence of hydrophobization conditions and ceramic membranes pore size on their properties in vacuum membrane distillation of water–organic solvent mixtures, Journal of Membrane Science 499 (2016) 442-451.

[20] R.W. Baker, J.G. Wijmans, Y. Huang, Permeability, permeance and selectivity: A preferred way of reporting pervaporation performance data, Journal of Membrane Science 348 (2010) 346-352.

[21] A. Yadav, M.L. Lind, X. Ma, Y.S. Lin, Nanocomposite Silicalite-1/Polydimethylsiloxane Membranes for Pervaporation of Ethanol from Dilute Aqueous Solutions, Industrial & Engineering Chemistry Research 52 (2013) 5207-5212.

[22] G. Liu, W. Wei, H. Wu, X. Dong, M. Jiang, W. Jin, Pervaporation performance of PDMS/ceramic composite membrane in acetone butanol ethanol (ABE) fermentation–PV coupled process, Journal of Membrane Science 373 (2011) 121-129.

[23] D. Cai, T. Zhang, J. Zheng, Z. Chang, Z. Wang, P.-y. Qin, T.-w. Tan, Biobutanol from sweet sorghum bagasse hydrolysate by a hybrid pervaporation process, Bioresource Technology 145 (2013) 97-102.

[24] C. Servel, D. Roizard, E. Favre, D. Horbez, Improved Energy Efficiency of a Hybrid Pervaporation/Distillation Process for Acetic Acid Production: Identification of Target Membrane Performances by Simulation, Industrial & Engineering Chemistry Research 53 (2014) 7768-7779.

[25] M. Omidali, A. Raisi, A. Aroujalian, Separation and purification of isobutanol from dilute aqueous solutions by a hybrid hydrophobic/hydrophilic pervaporation process, Chemical Engineering and Processing: Process Intensification 77 (2014) 22-29.

[26] P. Schaetzel, C. Vauclair, Q.T. Nguyen, R. Bouzerar, A simplified solution–diffusion theory in pervaporation: the total solvent volume fraction model, Journal of Membrane Science 244 (2004) 117-127.

[27] L.Y. Ng, A.W. Mohammad, C.P. Leo, N. Hilal, Polymeric membranes incorporated with metal/metal oxide nanoparticles: A comprehensive review, Desalination 308 (2013) 15-33.

[28] L.M. Robeson, The upper bound revisited, Journal of Membrane Science 320 (2008) 390-400.

[29] H.K. Yuan, J. Ren, X.H. Ma, Z.L. Xu, Dehydration of ethyl acetate aqueous solution by pervaporation using PVA/PAN hollow fiber composite membrane, Desalination 280 (2011) 252-258.

[30] X. Qiao, T.S. Chung, W.F. Guo, T. Matsuura, M.M. Teoh, Dehydration of isopropanol and its comparison with dehydration of butanol isomers from thermodynamic and molecular aspects, Journal of Membrane Science 252 (2005) 37-49.

[31] G. Jyoti, A. Keshav, J. Anandkumar, Review on Pervaporation: Theory, Membrane Performance, and Application to Intensification of Esterification Reaction, Journal of Engineering 2015 (2015) 24.

[32] G. Liu, W. Wei, W. Jin, Pervaporation Membranes for Biobutanol Production, ACS Sustainable Chemistry & Engineering 2 (2014) 546-560.

[33] R.W. Baker, Pervaporation, Membrane Technology and Applications, Chichester, UK: John Wiley & Sons, Ltd2012, pp. 379-416.

[34] S. Claes, P. Vandezande, S. Mullens, R. Leysen, K. De Sitter, A. Andersson, F.H.J. Maurer, H. Van den Rul, R. Peeters, M.K. Van Bael, High flux composite PTMSP-silica nanohybrid membranes for the pervaporation of ethanol/water mixtures, Journal of Membrane Science 351 (2010) 160-167.

[35] S. Ulutan, T. Nakagawa, Separability of ethanol and water mixtures through PTMSP–silica membranes in pervaporation, Journal of Membrane Science 143 (1998) 275-284.

[36] A.G. Fadeev, Y.A. Selinskaya, S.S. Kelley, M.M. Meagher, E.G. Litvinova, V.S. Khotimsky, V.V. Volkov, Extraction of butanol from aqueous solutions by pervaporation through poly(1-trimethylsilyl-1-propyne), Journal of Membrane Science 186 (2001) 205-217.

[37] I.L. Borisov, A.O. Malakhov, V.S. Khotimsky, E.G. Litvinova, E.S. Finkelshtein, N.V. Ushakov, V.V. Volkov, Novel PTMSP-based membranes containing elastomeric

fillers: Enhanced 1-butanol/water pervaporation selectivity and permeability, Journal of Membrane Science 466 (2014) 322-330.

[38] J.E. Zuliani, S. Tong, D.W. Kirk, C.Q. Jia, Isolating the effect of pore size distribution on electrochemical double-layer capacitance using activated fluid coke, Journal of Power Sources 300 (2015) 190-198.

[39] S. Sommer, T. Melin, Influence of operation parameters on the separation of mixtures by pervaporation and vapor permeation with inorganic membranes. Part 1: Dehydration of solvents, Chemical Engineering Science 60 (2005) 4509-4523.

[40] H. Zhou, Y. Li, G. Zhu, J. Liu, W. Yang, Microwave-assisted hydrothermal synthesis of a&b-oriented zeolite T membranes and their pervaporation properties, Separation and Purification Technology 65 (2009) 164-172.

[41] Y.S. Lin, M.C. Duke, Recent progress in polycrystalline zeolite membrane research, Current Opinion in Chemical Engineering 2 (2013) 209-216.

[42] J. Zah, H.M. Krieg, J.C. Breytenbach, Single gas permeation through compositionally different zeolite NaA membranes: Observations on the intercrystalline porosity in an unconventional, semicrystalline layer, Journal of Membrane Science 287 (2007) 300-310.

[43] N. Kosinov, C. Auffret, G.J. Borghuis, V.G.P. Sripathi, E.J.M. Hensen, Influence of the Si/Al ratio on the separation properties of SSZ-13 zeolite membranes, Journal of Membrane Science 484 (2015) 140-145.

[44] H. Bissett, J. Zah, H.M. Krieg, Manufacture and optimization of tubular ceramic membrane supports, Powder Technology 181 (2008) 57-66.

[45] J.C. Wang, D. Tian, L.N. Han, L.P. Chang, W.R. Bao, In situ synthesized Cu-ZSM-5/cordierite for reduction of NO, Transactions of Nonferrous Metals Society of China 21 (2011) 353-358.

[46] A. Huang, Y.S. Lin, W. Yang, Synthesis and properties of A-type zeolite membranes by secondary growth method with vacuum seeding, Journal of Membrane Science 245 (2004) 41-51.

[47] W.S. Ling, T.C. Thian, S. Bhatia, Synthesis, characterization and pervaporation properties of microwave synthesized zeolite A membrane, Desalination 277 (2011) 383-389.

[48] T.C. Bowen, R.D. Noble, J.L. Falconer, Fundamentals and applications of pervaporation through zeolite membranes, Journal of Membrane Science 245 (2004) 1-33.

[49] M. Kondo, M. Komori, H. Kita, K.-i. Okamoto, Tubular-type pervaporation module with zeolite NaA membrane, Journal of Membrane Science 133 (1997) 133-141.

[50] X. Lin, X. Chen, H. Kita, K. Okamoto, Synthesis of silicalite tubular membranes by in situ crystallization, AIChE Journal 49 (2003) 237-247.

[51] H. Matsuda, H. Yanagishita, H. Negishi, D. Kitamoto, T. Ikegami, K. Haraya, T. Nakane, Y. Idemoto, N. Koura, T. Sano, Improvement of ethanol selectivity of silicalite membrane in pervaporation by silicone rubber coating, Journal of Membrane Science 210 (2002) 433-437.

[52] H. Furukawa, K.E. Cordova, M. O'Keeffe, O.M. Yaghi, The Chemistry and Applications of Metal-Organic Frameworks, Science 341 (2013).

[53] H.C. Zhou, J.R. Long, O.M. Yaghi, Introduction to Metal–Organic Frameworks, Chemical Reviews 112 (2012) 673-674.

[54] J. Yang, A. Grzech, F.M. Mulder, T.J. Dingemans, Methyl modified MOF-5: a water stable hydrogen storage material, Chemical Communications 47 (2011) 5244-5246.

[55] F. Martínez, R. Sanz, G. Orcajo, D. Briones, V. Yángüez, Amino-impregnated MOF materials for CO2 capture at post-combustion conditions, Chemical Engineering Science 142 (2016) 55-61.

[56] Y.Y. Xiong, J.Q. Li, C.S. Yan, H.Y. Gao, J.P. Zhou, L.L. Gong, M.B. Luo, L. Zhang, P.P. Meng, F. Luo, MOF catalysis of FeII-to-FeIII reaction for an ultrafast and one-step generation of the Fe2O3@MOF composite and uranium(vi) reduction by iron(ii) under ambient conditions, Chemical Communications 52 (2016) 9538-9541.

[57] I. Luz, F.X. Llabrés i Xamena, A. Corma, Bridging homogeneous and heterogeneous catalysis with MOFs: Cu-MOFs as solid catalysts for three-component coupling and cyclization reactions for the synthesis of propargylamines, indoles and imidazopyridines, Journal of Catalysis 285 (2012) 285-291.

[58] S. Vaesen, V. Guillerm, Q. Yang, A.D. Wiersum, B. Marszalek, B. Gil, A. Vimont, M. Daturi, T. Devic, P.L. Llewellyn, C. Serre, G. Maurin, G. De Weireld, A robust amino-functionalized titanium(iv) based MOF for improved separation of acid gases, Chemical Communications 49 (2013) 10082-10084.

[59] H. Jin, A. Wollbrink, R. Yao, Y. Li, J. Caro, W. Yang, A novel CAU-10-H MOF membrane for hydrogen separation under hydrothermal conditions, Journal of Membrane Science 513 (2016) 40-46.

[60] A. Kasik, Y.S. Lin, Organic solvent pervaporation properties of MOF-5 membranes, Separation and Purification Technology 121 (2014) 38-45.

[61] Y. Zhang, N. Wang, S. Ji, R. Zhang, C. Zhao, J.-R. Li, Metal–organic framework/poly(vinyl alcohol) nanohybrid membrane for the pervaporation of toluene/n-heptane mixtures, Journal of Membrane Science 489 (2015) 144-152.

[62] M. Miyamoto, K. Hori, T. Goshima, N. Takaya, Y. Oumi, S. Uemiya, An Organoselective Zirconium-Based Metal–Organic-Framework UiO-66 Membrane for Pervaporation, European Journal of Inorganic Chemistry 2017 (2017) 2094-2099.

[63] Schweinefu, S. Springer, I.A. Baburin, T. Hikov, K. Huber, S. Leoni, M. Wiebcke, Zeolitic imidazolate framework-71 nanocrystals and a novel SOD-type polymorph: solution mediated phase transformations, phase selection via coordination modulation and a density functional theory derived energy landscape, Dalton Transactions 43 (2014) 3528-3536.

[64] K.S. Park, Z. Ni, A.P. Côté, J.Y. Choi, R. Huang, F.J. Uribe-Romo, H.K. Chae, M. O'Keeffe, O.M. Yaghi, Exceptional chemical and thermal stability of zeolitic imidazolate frameworks, Proceedings of the National Academy of Sciences 103 (2006) 10186-10191.

[65] Y. Hu, Z. Liu, J. Xu, Y. Huang, Y. Song, Evidence of Pressure Enhanced CO2 Storage in ZIF-8 Probed by FTIR Spectroscopy, Journal of the American Chemical Society 135 (2013) 9287-9290.

[66] X. Dong, Y.S. Lin, Synthesis of an organophilic ZIF-71 membrane for pervaporation solvent separation, Chemical Communications 49 (2013) 1196-1198.

[67] Y. Pan, T. Li, G. Lestari, Z. Lai, Effective separation of propylene/propane binary mixtures by ZIF-8 membranes, Journal of Membrane Science 390–391 (2012) 93-98.

[68] T. Khosravi, S. Mosleh, O. Bakhtiari, T. Mohammadi, Mixed matrix membranes of Matrimid 5218 loaded with zeolite 4A for pervaporation separation of water–isopropanol mixtures, Chemical Engineering Research and Design 90 (2012) 2353-2363.

[69] S. Liu, G. Liu, X. Zhao, W. Jin, Hydrophobic-ZIF-71 filled PEBA mixed matrix membranes for recovery of biobutanol via pervaporation, Journal of Membrane Science 446 (2013) 181-188.

[70] Z. Jia, G. Wu, Metal-organic frameworks based mixed matrix membranes for pervaporation, Microporous and Mesoporous Materials 235 (2016) 151-159.

[71] D.Q. Vu, W.J. Koros, S.J. Miller, Mixed matrix membranes using carbon molecular sieves: II. Modeling permeation behavior, Journal of Membrane Science 211 (2003) 335-348.

[72] H.M. Guan, T.S. Chung, Z. Huang, M.L. Chng, S. Kulprathipanja, Poly(vinyl alcohol) multilayer mixed matrix membranes for the dehydration of ethanol–water mixture, Journal of Membrane Science 268 (2006) 113-122.

[73] T. Khosravi, M. Omidkhah, Preparation of CO2-philic polymeric membranes by blending poly(ether-b-amide-6) and PEG/PPG-containing copolymer, RSC Advances 5 (2015) 12849-12859.

[74] G. Zhang, J. Li, N. Wang, H. Fan, R. Zhang, G. Zhang, S. Ji, Enhanced flux of polydimethylsiloxane membrane for ethanol permselective pervaporation via incorporation of MIL-53 particles, Journal of Membrane Science 492 (2015) 322-330.

[75] Q. Li, L. Cheng, J. Shen, J. Shi, G. Chen, J. Zhao, J. Duan, G. Liu, W. Jin, Improved ethanol recovery through mixed-matrix membrane with hydrophobic MAF-6 as filler, Separation and Purification Technology 178 (2017) 105-112.

[76] Y. Li, L.H. Wee, J.A. Martens, I.F.J. Vankelecom, ZIF-71 as a potential filler to prepare pervaporation membranes for bio-alcohol recovery, Journal of Materials Chemistry A 2 (2014) 10034-10040.

[77] L.H. Wee, Y. Li, K. Zhang, P. Davit, S. Bordiga, J. Jiang, I.F.J. Vankelecom, J.A. Martens, Submicrometer-Sized ZIF-71 Filled Organophilic Membranes for Improved Bioethanol Recovery: Mechanistic Insights by Monte Carlo Simulation and FTIR Spectroscopy, Advanced Functional Materials 25 (2015) 516-525.

[78] X.L. Liu, Y.S. Li, G.Q. Zhu, Y.J. Ban, L.Y. Xu, W.S. Yang, An Organophilic Pervaporation Membrane Derived from Metal–Organic Framework Nanoparticles for Efficient Recovery of Bio-Alcohols, Angewandte Chemie International Edition 50 (2011) 10636-10639.

[79] X. Wang, J. Chen, M. Fang, T. Wang, L. Yu, J. Li, ZIF-7/PDMS mixed matrix membranes for pervaporation recovery of butanol from aqueous solution, Separation and Purification Technology 163 (2016) 39-47.

[80] S. Liu, G. Liu, J. Shen, W. Jin, Fabrication of MOFs/PEBA mixed matrix membranes and their application in bio-butanol production, Separation and Purification Technology 133 (2014) 40-47.

[81] H. Fan, Q. Shi, H. Yan, S. Ji, J. Dong, G. Zhang, Simultaneous Spray Self-Assembly of Highly Loaded ZIF-8–PDMS Nanohybrid Membranes Exhibiting Exceptionally High Biobutanol-Permselective Pervaporation, Angewandte Chemie International Edition 53 (2014) 5578-5582.

[82] Y. Li, H.M. Guan, T.S. Chung, S. Kulprathipanja, Effects of novel silane modification of zeolite surface on polymer chain rigidification and partial pore blockage in polyethersulfone (PES)–zeolite A mixed matrix membranes, Journal of Membrane Science 275 (2006) 17-28.

[83] Y. Takamitsu, K. Yamamoto, S. Yoshida, H. Ogawa, T. Sano, Effect of crystal size and surface modification of ZSM-5 zeolites on conversion of ethanol to propylene, Journal of Porous Materials 21 (2014) 433-440.

[84] K.M.L. Taylor, W.J. Rieter, W. Lin, Manganese-Based Nanoscale Metal−Organic Frameworks for Magnetic Resonance Imaging, Journal of the American Chemical Society 130 (2008) 14358-14359.

[85] S. Aguado, J. Canivet, D. Farrusseng, Engineering structured MOF at nano and macroscales for catalysis and separation, Journal of Materials Chemistry 21 (2011) 7582-7588.

[86] N. Yanai, S. Granick, Directional Self-Assembly of a Colloidal Metal–Organic Framework, Angewandte Chemie International Edition 51 (2012) 5638-5641.

[87] X. Liu, Y. Li, Y. Ban, Y. Peng, H. Jin, H. Bux, L. Xu, J. Caro, W. Yang, Improvement of hydrothermal stability of zeolitic imidazolate frameworks, Chemical Communications 49 (2013) 9140-9142.

[88] H. Fei, J.F. Cahill, K.A. Prather, S.M. Cohen, Tandem Postsynthetic Metal Ion and Ligand Exchange in Zeolitic Imidazolate Frameworks, Inorganic Chemistry 52 (2013) 4011-4016.

[89] R. Lin, L. Ge, H. Diao, V. Rudolph, Z. Zhu, Ionic Liquids as the MOFs/Polymer Interfacial Binder for Efficient Membrane Separation, ACS Applied Materials & Interfaces 8 (2016) 32041-32049.

[90] S. Japip, H. Wang, Y. Xiao, T. Shung Chung, Highly permeable zeolitic imidazolate framework (ZIF)-71 nano-particles enhanced polyimide membranes for gas separation., Journal of Membrane Science 467 (2014) 162-174.

[91] K. Zhang, R.P. Lively, M.E. Dose, A.J. Brown, C. Zhang, J. Chung, S. Nair, W.J. Koros, R.R. Chance, Alcohol and water adsorption in zeolitic imidazolate frameworks, Chemical Communications 49 (2013) 3245-3247.

[92] A.C.C. Esteves, J. Brokken-Zijp, J. Laven, H.P. Huinink, N.J.W. Reuvers, M.P. Van, G. de With, Influence of cross-linker concentration on the cross-linking of PDMS and the network structures formed, Polymer 50 (2009) 3955-3966.

[93] N. Stafie, D. Stamatialis, M. Wessling, Effect of PDMS cross-linking degree on the permeation performance of PAN/PDMS composite nanofiltration membranes, Separation and purification technology 45 (2006) 220 - 231.

[94] D. Damiron, N. Okhay, S.A. Akhrass, P. Cassagnau, E. Drockenmuller, Crosslinked PDMS elastomers and coatings from the thermal curing of vinyl-functionalized PDMS

and a diazide aliphatic crosslinker, Journal of Polymer Science Part A: Polymer Chemistry 50 (2012) 98-107.

[95] R.D. Jaeger, M. Gleria, Silicon-based Inorganic Polymers, Nova Science Publishers, Inc., New York, UNITED STATES, 2008.

[96] N. Bighane, W.J. Koros, Novel silica membranes for high temperature gas separations, Journal of Membrane Science 371 (2011) 254-262.

[97] R.P. Lively, M.E. Dose, J.A. Thompson, B.A. McCool, R.R. Chance, W.J. Koros, Ethanol and water adsorption in methanol-derived ZIF-71, Chemical Communications 47 (2011) 8667-8669.

[98] H. Zhang, D. Liu, Y. Yao, B. Zhang, Y.S. Lin, Stability of ZIF-8 membranes and crystalline powders in water at room temperature, Journal of Membrane Science 485 (2015) 103-111.

[99] C. Yang, P. Costamagna, S. Srinivasan, J. Benziger, A.B. Bocarsly, Approaches and technical challenges to high temperature operation of proton exchange membrane fuel cells, Journal of Power Sources 103 (2001) 1-9.

[100] Y.Z. Fu, A. Manthiram, Nafion-imidazole-H3PO4 composite membranes for proton exchange membrane fuel cells, Journal of The Electrochemical Society 154 (2007) B8-B12.

[101] Y. Bai, L. Dong, C. Zhang, J. Gu, Y. Sun, L. Zhang, H. Chen, ZIF-8 Filled Polydimethylsiloxane Membranes for Pervaporative Separation of n-Butanol from Aqueous Solution, Separation Science and Technology 48 (2013) 2531-2539.

[102] Y. Feng, E. Shamsaei, C.H.J. Davies, H. Wang, Inorganic particle enhanced polymer hollow fiber membranes with high mechanical properties, Materials Chemistry and Physics 167 (2015) 209-218.

[103] Ş.B. Tantekin-Ersolmaz, Ç. Atalay-Oral, M. Tatlıer, A. Erdem-Şenatalar, B. Schoeman, J. Sterte, Effect of zeolite particle size on the performance of polymer–zeolite mixed matrix membranes, Journal of Membrane Science 175 (2000) 285-288.

[104] N. Wang, J. Liu, J. Li, J. Gao, S. Ji, J.-R. Li, Tuning properties of silicalite-1 for enhanced ethanol/water pervaporation separation in its PDMS hybrid membrane, Microporous and Mesoporous Materials 201 (2015) 35-42.

[105] X. Liu, H. Jin, Y. Li, H. Bux, Z. Hu, Y. Ban, W. Yang, Metal–organic framework ZIF-8 nanocomposite membrane for efficient recovery of furfural via pervaporation and vapor permeation, Journal of Membrane Science 428 (2013) 498-506.

[106] A. Kudasheva, S. Sorribas, B. Zornoza, C. Téllez, J. Coronas, Pervaporation of water/ethanol mixtures through polyimide based mixed matrix membranes containing ZIF-8, ordered mesoporous silica and ZIF-8-silica core-shell spheres, Journal of Chemical Technology & Biotechnology 90 (2015) 669-677.

[107] J. Sanchez-Lainez, B. Zornoza, A. Mayoral, A. Berenguer-Murcia, D. Cazorla-Amoros, C. Tellez, J. Coronas, Beyond the H2/CO2 upper bound: one-step crystallization and separation of nano-sized ZIF-11 by centrifugation and its application in mixed matrix membranes, Journal of Materials Chemistry A 3 (2015) 6549-6556.

[108] B. Seoane, J.M. Zamaro, C. Tellez, J. Coronas, Sonocrystallization of zeolitic imidazolate frameworks (ZIF-7, ZIF-8, ZIF-11 and ZIF-20), Crystal Engineering Communications 14 (2012) 3103-3107.

[109] Q. Bao, Y. Lou, T. Xing, J. Chen, Rapid synthesis of zeolitic imidazolate framework-8 (ZIF-8) in aqueous solution via microwave irradiation, Inorganic Chemistry Communications 37 (2013) 170-173.

[110] S. Tanaka, T. Shimada, K. Fujita, Y. Miyake, K. Kida, K. Yogo, J.F.M. Denayer, M. Sugita, T. Takewaki, Seeding-free aqueous synthesis of zeolitic imidazolate framework-8 membranes: How to trigger preferential heterogeneous nucleation and membrane growth in aqueous rapid reaction solution, Journal of Membrane Science 472 (2014) 29-38.

[111] W.S. Chi, S. Hwang, S.-J. Lee, S. Park, Y.-S. Bae, D.Y. Ryu, J.H. Kim, J. Kim, Mixed matrix membranes consisting of SEBS block copolymers and size-controlled ZIF-8 nanoparticles for CO2 capture, Journal of Membrane Science 495 (2015) 479-488.

[112] M. Gustafsson, X. Zou, Crystal formation and size control of zeolitic imidazolate frameworks with mixed imidazolate linkers, Journal of Porous Materials 20 (2013) 55-63.

[113] C.W. Tsai, E.H.G. Langner, The effect of synthesis temperature on the particle size of nano-ZIF-8, Microporous and Mesoporous Materials 221 (2016) 8-13.

[114] N.A.H.M. Nordin, A.F. Ismail, A. Mustafa, P.S. Goh, D. Rana, T. Matsuura, Aqueous room temperature synthesis of zeolitic imidazole framework 8 (ZIF-8) with various concentrations of triethylamine, RSC Advances 4 (2014) 33292-33300.

[115] Y.H. Wang, Q. Shi, H. Xu, J.X. Dong, The synthesis and tribological properties of small- and large-sized crystals of zeolitic imidazolate framework-71, RSC Advances 6 (2016) 18052-18059.

[116] H. Yin, C.Y. Lau, M. Rozowski, C. Howard, Y. Xu, T. Lai, M.E. Dose, R.P. Lively, M.L. Lind, Free-standing ZIF-71/PDMS nanocomposite membranes for the

recovery of ethanol and 1-butanol from water through pervaporation, Journal of Membrane Science 529 (2017) 286-292.

[117] Y. Ying, Y. Xiao, J. Ma, X. Guo, H. Huang, Q. Yang, D. Liu, C. Zhong, Recovery of acetone from aqueous solution by ZIF-7/PDMS mixed matrix membranes, RSC Advances 5 (2015) 28394-28400.

[118] P.Y. Moh, M. Brenda, M.W. Anderson, M.P. Attfield, Crystallisation of solvothermally synthesised ZIF-8 investigated at the bulk, single crystal and surface level, Crystal Engineering Communications 15 (2013) 9672-9678.

[119] J. Cravillon, S. Münzer, S.-J. Lohmeier, A. Feldhoff, K. Huber, M. Wiebcke, Rapid Room-Temperature Synthesis and Characterization of Nanocrystals of a Prototypical Zeolitic Imidazolate Framework, Chemistry of Materials 21 (2009) 1410-1412.

[120] I. Khay, G. Chaplais, H. Nouali, G. Ortiz, C. Marichal, J. Patarin, Assessment of the energetic performances of various ZIFs with SOD or RHO topology using high pressure water intrusion-extrusion experiments, Dalton Transactions 45 (2016) 4392-4400.

[121] P.G. Vekilov, Nucleation, Crystal Growth & Design 10 (2010) 5007-5019.

[122] C. Wang, W. Tian, Y. Wei, X. Li, Q. Zhang, C. Huang, Study on the association between residential exposure to N, N-dimethylformamide and hospitalization for respiratory disease, Atmospheric Environment 77 (2013) 166-171.

[123] B. Wang, A.P. Cote, H. Furukawa, M. O/'Keeffe, O.M. Yaghi, Colossal cages in zeolitic imidazolate frameworks as selective carbon dioxide reservoirs, Nature 453 (2008) 207-211.

[124] S. Bhattacharjee, M.S. Jang, H.J. Kwon, W.S. Ahn, Zeolitic Imidazolate Frameworks: Synthesis, Functionalization, and Catalytic/Adsorption Applications, Catalysis Surveys from Asia 18 (2014) 101-127.

[125] J.Q. Jiang, C.X. Yang, X.P. Yan, Postsynthetic ligand exchange for the synthesis of benzotriazole-containing zeolitic imidazolate framework, Chemical Communications 51 (2015) 6540-6543.

[126] Z. Shi, Y. Yu, C. Fu, L. Wang, X. Li, Water-based synthesis of zeolitic imidazolate framework-8 for CO2 capture, RSC Advances 7 (2017) 29227-29232.

[127] R.J. Verploegh, S. Nair, D.S. Sholl, Temperature and Loading-Dependent Diffusion of Light Hydrocarbons in ZIF-8 as Predicted Through Fully Flexible Molecular Simulations, Journal of the American Chemical Society 137 (2015) 15760-15771.

[128] A. Phan, C.J. Doonan, F.J. Uribe-Romo, C.B. Knobler, M. O'Keeffe, O.M. Yaghi, Synthesis, Structure, and Carbon Dioxide Capture Properties of Zeolitic Imidazolate Frameworks, Accounts of Chemical Research 43 (2010) 58-67.

[129] L. Mu, B. Liu, H. Liu, Y. Yang, C. Sun, G. Chen, A novel method to improve the gas storage capacity of ZIF-8, Journal of Materials Chemistry 22 (2012) 12246-12252.

[130] C. Zhang, K. Zhang, L. Xu, Y. Labreche, B. Kraftschik, W.J. Koros, Highly scalable ZIF-based mixed-matrix hollow fiber membranes for advanced hydrocarbon separations, AIChE Journal 60 (2014) 2625-2635.

[131] S. Fazlifard, T. Mohammadi, O. Bakhtiari, Chitosan/ZIF-8 Mixed-Matrix Membranes for Pervaporation Dehydration of Isopropanol, Chemical Engineering & Technology 40 (2017) 648-655.

[132] G. Liu, Z. Jiang, K. Cao, S. Nair, X. Cheng, J. Zhao, H. Gomaa, H. Wu, F. Pan, Pervaporation performance comparison of hybrid membranes filled with two-dimensional ZIF-L nanosheets and zero-dimensional ZIF-8 nanoparticles, Journal of Membrane Science 523 (2017) 185-196.

[133] O. Karagiaridi, W. Bury, A.A. Sarjeant, C.L. Stern, O.K. Farha, J.T. Hupp, Synthesis and characterization of isostructural cadmium zeolitic imidazolate frameworks via solvent-assisted linker exchange, Chemical Science 3 (2012) 3256-3260.

[134] M.B. Lalonde, J.E. Mondloch, P. Deria, A.A. Sarjeant, S.S. Al-Juaid, O.I. Osman, O.K. Farha, J.T. Hupp, Selective Solvent-Assisted Linker Exchange (SALE) in a Series of Zeolitic Imidazolate Frameworks, Inorganic Chemistry 54 (2015) 7142-7144.

[135] T. Borjigin, F. Sun, J. Zhang, K. Cai, H. Ren, G. Zhu, A microporous metal-organic framework with high stability for GC separation of alcohols from water, Chemical Communications 48 (2012) 7613-7615.

[136] J. Yuan, Q. Li, J. Shen, K. Huang, G. Liu, J. Zhao, J. Duan, W. Jin, Hydrophobic-functionalized ZIF-8 nanoparticles incorporated PDMS membranes for high-selective separation of propane/nitrogen, Asia-Pacific Journal of Chemical Engineering 12 (2017) 110-120.

APPENDIX A

LIST OF SYMBOLS

W_i = mass of permeate component i (g)

J_i = flux of component i (g m^{-2} h^{-1})

A = effective membrane area (m^2)

t = test time (h)

P_i = permeability of component i (Barrer)

P_j = permeability of component j (Barrer)

J_i = molar flux of component i (cm^3 (STP) cm^{-2} s^{-1})

l = membrane thickness (cm)

γ_{io} = activity coefficient of component i in feed solution

x_{io} = molar fraction of component i in feed solution

P_{io}^{sat} = saturated vapor pressure of component i in feed solution (cmHg)

p_{il} = partial pressure of component i in the permeate (cmHg)

α_{ij} = selectivity of component i over j

β = separation factor

Y_{Alchol} = alcohol weight fraction in permeate

Y_{Water} = water weight fraction in permeate

$X_{Alcohol}$ = alcohol weight fraction in feed

X_{Water} = water weight fraction in feed

q = the amount of alcohol absorbed per unit mass of absorbents (g/g)

w_1 = alcohol weight fraction in the feed

m_1 = mass of feed solution (g)

w_2 = alcohol weight fraction of feed solution after sorption test

m_2 = mass of feed solution after sorption test (g)

m = mass of absorbents (g)

D_i = diffusion coefficient of component i (cm^2/s)

K_i = sorption coefficient of component i (cm^3(STP)/cm^3 cmHg)

D_j = diffusion coefficient of component j (cm^2/s)

K_j = sorption coefficient of component j (cm^3(STP)/cm^3 cmHg)

APPENDIX B

ACTIVITY COEFFICIENT DATA USED IN PERMEABILITY CALCULATION

The ethanol and water activity coefficient values shown below used in ethanol/water solution are obtained from the Dortmund Data Bank (DDB). The link is: http://www.ddbst.com/

The 1-butanol and water activity coefficient values are calculated from Aspen Plus software.

Activity coefficient values used in the permeability calculation with UNIFAC model.

Component	Activity coefficient γ
Ethanol	6.653
Water (EtOH/water solution)	1.029
1-Butanol	30.5
Water (1-butanol/water solution)	1.0

APPENDIX C

PREPARATION OF CONDENSATION CURE PDMS MEMBRANES

1. Prepare a 20 mL scintillation vial. Add 1 g of the silanol terminated PDMS and 8 g of n-heptane to the vial.
2. Mix the solution for 3 minutes with the help of a vortex mixer.
3. Then mix the polymer with the solvent with a probe sonicator at 300 W for 60s. Make sure to insert the probe tip half way into the solution to achieve good mixing results. Then close the vial and mix the solution with a vortex mixer for 90s. If the solution is still very hot, keeping vortexing the solution until it cools down before the next sonication-vortex cycle.
4. Repeat the 60s sonication and the 90s vortex mixing for 7 more times (total 8 cycles).
5. Add 0.2 g of TEOS solution into the PDMS/n-heptane solution and vortex the solution for 3 minutes.
6. Finally add 0.012 to 0.04g of each titanium 2-ethylhexoxide and di-n-butyldiacetoxytin tech-95 catalysts to the solution and again vortex it for 3 minutes.
7. Pour the solution into a 9 cm diameter flat-bottomed Teflon evaporating dish. Transfer the Teflon dish to a closed box with 75 RH%. Leave the membrane in the humidity controlled box for 21 hours. To create the 75 RH% enviroment, we placed a beaker filled with saturated sodium chloride solution into a sealed box at room temperature. A Teflon dish is used so the membrane is easily peeled off from the substrate.

8. Remove the Teflon dish and transfer it to a vacuum oven. Dry the membrane at 100 ºC for 20h and then 120 ºC for 11h.
9. Then peel the membrane off from the Teflon dish and cut with a scissor into desired shape.

APPENDIX D

ALCOHOL/WATER PERVAPORATION TEST

1. Prepare 35 g of 2 wt% ethanol/water (or 1-butanol/water) solution as feed solution.
2. Cut a piece of membrane with a scissor based on the size of the porous stainless steel support.
3. Place the membrane with the porous stainless support at the bottom side of the stainless steel pervaporation cell (shown in Figure 2-3) with the membrane facing the feed and seal it with o-rings.
4. Insert the feed circulation tubing into the feed cell and seal the top part of the pervaporation cell. Pump in the feed solution with the help of a Masterflex® peristaltic pump. Then keep the pump speed at 1 ml/s throughout the test.
5. A custom-made heating jacket is applied to the pervaporation feed cell control the feed temperature. Turn on the heating jacket and set the temperature at 60 ºC.
6. Turn on the vacuum that connects to the downstream side of the membrane. Run the setup for 1.5 hours to allow the setup to reach steady state before collecting any permeate.
7. After 1.5 hours, apply liquid nitrogen to the cold trap to condense and collect the permeate. Refill the liquid nitrogen every 30~40 minutes to maintain the cold atmosphere around the cold trap.
8. After the test is done, record the test time t, turn off the vacuum and close the valves connecting to the cold trap. Weigh the cold trap with the permeate as M_1. Then add a certain amount of water into the cold trap to dilute the permeate (the permeate is too little and cannot be collected and measured), measure the weight of cold trap+permeate+water as M_2.

9. Dry the cold trap and measure the weight of the empty cold trap as M_3.
10. Analyze the diluted permeate sample with GC. Calculate the diluted permeate alcohol concentration as C_2 based on the calibration curve.
11. Calculate the permeate alcohol concentration C_1 with the equation $C_1 = C_2 (M_2 - M_3)/(M_1 - M_3)$.
12. The mass of permeate component i W_i can be calculated based on the mass and concentration of permeate. Then the flux, permeability and selectivity are calculated according to the equations shown in equation 1.1, 1.2 and 1.3.

APPENDIX E

PROTON NUCLEAR MAGNETIC RESONANCE

1. Proton nuclear magnetic resonance (^{1}H NMR) (Varian MR400) was applied to the SALE modified ZIF-71 particles to quantify the amount of new ligand exchanged into the ZIF material.
2. Dry the ZIF powder at 75 ºC for 12 hours in a vacuum oven before the sample preparation.
3. Measure 0.01 g of the ZIF material or the new ligand (BIM, MBIM, DMBIM and PI) into a glass vial.
4. Add 75 μL of methanol-d_4 solution and then 30 μL of 35% DCl in D_2O solution to the ZIF material. Mix the solution with a vortex mixer. The solution becomes clear after the addition of DCl/D_2O solution.
5. Then transfer the solution to NMR tubes.
6. Run the sample at room temperature.